The Potential of DNA-tagged Magnetic Silica Microparticle Tracers for Surface Water Tracer Hydrology

Using tracer injection experiments in the laboratory environment

F.E.C. van Rhijn

Delft University of Technology

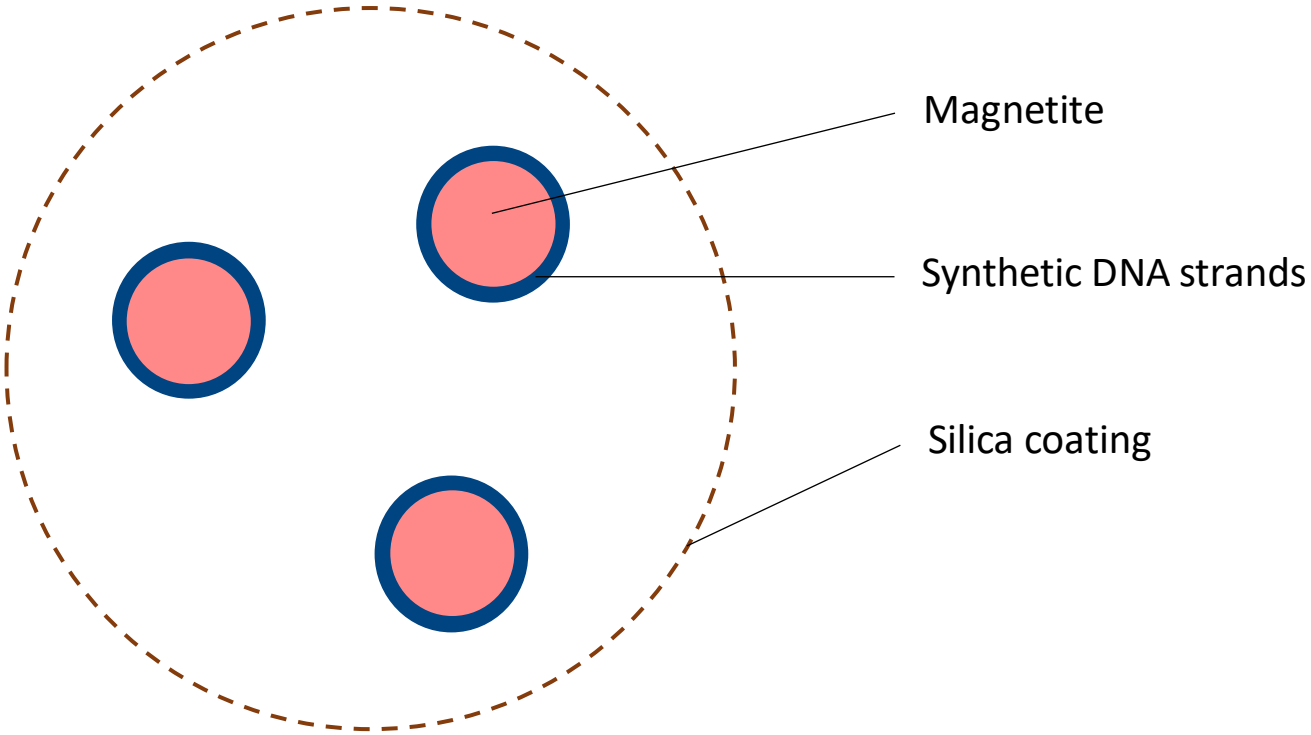

TU Delft Delft University of Technology

Challenge the future

The Potential of DNA-tagged Magnetic Silica Microparticle Tracers for Surface Water Tracer Hydrology

Using tracer injection experiments in the laboratory environment

by

F.E.C. van Rhijn

A thesis submitted to the Delft University of Technology in partial fulfillment of the requirements for the degree of Master of Science in Civil Engineering

Student number:	4744446	
Project duration:	August 31, 2020 – July 9, 2021	
Thesis committee:	Dr. Thom Bogaard,	TU Delft, chair
	Dr. Jam Willem Foppen,	IHE-Delft and TU Delft
	Yuchen Tang, MSc	TU Delft
	Dr. Ing. Kim Maren Lompe,	TU Delft

An electronic version of this thesis is available at `http://repository.tudelft.nl/`.

TU Delft

Preface

For the last 10 months, I worked with joy on my master thesis here presented before you. It was a time in which I got the opportunity to learn a lot. Besides gaining new knowledge about surface water tracing and tracers, I developed laboratory skills, got the opportunity to present at a conference and had a lot of interesting discussions with knowledgeable people.

Firstly I would like to thank my Coco Tang for introducing me into the topic, the fun hours in the laboratory and helpful brainstorming sessions. I also would like to thank Armand Middeldorp from the laboratory staff at the Waterlab of Civil engineering for helping to find creative solutions in difficult times. Furthermore, I would like to thank my supervisors. Thom Bogaard for his enthusiasm, which kept me going in difficult times, and his unlimited availability. And Jan Willem Foppen for his critical views and making time for bi-weekly meetings. I would also like to thank Kim Lompe for her outside perspective and critical questions that always opened up new insights. Last, but not least, I would like to thank my close friends and family for their support during the last 10 months.

I hope you will enjoy reading my report just as much as I did doing the research!

Fay van Rhijn

Delft, Juli 2021

Summary

Surface water tracing experiments help to identify the flow paths of in-stream mass transport. This provides useful information for developing mitigation measures for contamination, and thereby for solving environmental problems. Salts, fluorescent dyes and isotopes are commonly used tracer substances. However, it is well known these tracers have several drawbacks, including, for example, a finite number of unique tracers with similar transport properties, which limits the possibility to repeat an experiment due to system memory. Additionally, it is difficult to perform multi-tracer experiments, due to a lack of specificity. Lastly, the detection limit becomes an important constraint when using a tracer in larger water bodies or over longer travel distances, due to the vast dilution. The recently developed silica encapsulated synthetic DNA nanoparticle with a superparamagnetic core (SiDNAMag), can theoretically overcome the aforementioned limitations of existing tracers. SiDNAMag particles can be recovered from a sample by magnetic separation. This limits the influence of water quality on the qPCR analysis and provides an easy method for up-concentration of samples. However, with the presence of natural colloids, particulate matter, and river bed sediments, SiDNAMag particles are likely to undergo complex interaction processes in addition to dispersion and advection. Moreover, little is known about the possible SiDNAMag tracer sinks during transport.

The focus of this work is to identify the transport behaviour of the SiDNAMag tracer in terms of breakthrough curves (BTC) and hydrodynamic dispersion as well as to study the interactions with the natural environment, specifically water quality and sediments. This was investigated by comparing SiDNAMag particles to NaCl, a widely used solute tracer, and silica microparticles. To do so, open channel injection experiments using SiDNAMag particles were performed in the laboratory in different river water types and with the presence of sediments at the channel bottom. The resulting BTCs were interpreted with a 1D advection and dispersion model with transient storage (OTIS), to determine the hydrodynamic dispersion coefficient. Mass recovery was calculated by integrating the BTC.

The results show that SiDNAMag particles have a reproducible but different transport behaviour than NaCl solutes. The SiDNAMag particles arrive, peak and return to background concentrations earlier than NaCl solutes. Furthermore, the interpretation of the data with a 1D advection and dispersion model showed that the dispersion coefficient for SiDNAMag was lower (0.34E-3 m^2/s – 0.88E-3 m^2/s) than that of NaCl (0.81E-3 m^2/s – 2.31E-3 m^2/s). Literature on solutes and colloids in the aquatic environment supports the possible difference in the transport behaviour of solutes and colloids. No relation between the transport behaviour and presence of bottom-sediments was found. The mass recoveries for SiDNAMag experiments were between 36% and 131%, which could be partly explained by the bottom-sediments which detained between 0.16% and 16.94% of the SiDNAMag mass during the experiments. No relationship was found between the three natural water types and the observed mass losses. Additionally, the silica microparticle injection experiment showed the same BTC characteristics for silica microparticles as SiDNAMag though without mass loss, indicating mass loss occurred in the lab analysis. Due to the uncertainties in the lab analysis, no accurate mass recovery for the SiDNAMag tracer could be calculated. Furthermore, the observed scatter in the measurement data could be explained by the uncertainties in lab analysis as well as possible differences in transport behaviour of solutes and colloids.

In conclusion, the results of the laboratory experiments with the SiDNAMag particle show that it is a promising hydrological tracer in surface water tracing experiments to trace colloids. Thereby it can be a valuable tool to gain information on the movement of microparticles, like microplastics and pathogens, in the natural environment. The next step towards achieving this goal is performing a field experiment, for which upscaling of the SiDNAMag tracer production is required.

Glossary

BTC = Breakthrough Curve. This is a curve of concentration against time

Cq = cycle number in the qPCR analysis

D3 = 1000 times diluted from the original concentration (D0); in the same way is D4 10000 times diluted

Hydrodynamic dispersion = The total of mechanical dispersion and molecular diffusion. In this report it is referred to by dispersion. The dispersion coefficient (D) is also referring the total of dispersion occurring in a system

NTC = No Temple Control, a control sample in the qPCR analysis

OTIS = One-dimensional Transport with Inflow and Storage

qPCR = quantitative polymerase chain reaction. Which is a technique to quantify DNA in a sample

SiDNAMag = Silica encapsulated synthetic-DNA-tagged microparticles with a superparamagnetic core or magnetite

Contents

1

Introduction

Water travels via infinite flow paths through the environment. Rivers are the highways of these flow paths. To gain a better understanding of hydrological processes such as hydrodynamic dispersion and flow velocities, it is crucial to be able to trace the flow of water in rivers. Furthermore, tracing can investigate in-stream mass transport, which contributes to identifying water contamination pathways. Characterising hydrological processes and in-stream mass transport contributes to developing mitigation measures for contamination and thereby for solving environmental problems [1] [2] [3] [4]. In addition developing such measures provides key information for water resource management [5] [6].

Commonly used tracer substances include salts, fluorescent dyes and isotopes [7]. Well known drawbacks of these tracers are a finite number of unique tracers with similar transport properties, which limits the possibility to repeat an experiment due to system memory, and it is difficult to perform multi-tracer experiments, due to lack of specificity [8] [9] [10]. Moreover, there is a growing concern about the environmental impacts of tracers [11] [12]. When using a tracer in larger water bodies or for longer travel distances the detection limit becomes an important constraint, because of the vast dilution [9]. Also, the ubiquity of natural tracers in water bodies requires high tracer injection concentrations to limit environmental background noise [1]. To progress in hydrological science, and gain crucial information for decision making a new tracer with fewer limitations is required.

Silica encapsulated synthetic DNA with a superparamagnetic core (acronym: SiDNAMag), is a recently developed particle, which can theoretically overcome the limitations of existing tracers. Its potential is related to the presence of DNA strands. Unlimited variability in DNA sequences ensures every particle can be unique. The DNA is encapsulated with silica giving all particles the same appearance and thereby theoretically identical transport behaviour in the environment. Other advantages are that the tracer is environmentally friendly and there is an absence of background noise [1] [13] [3]. DNA concentration can be determined by Quantitative Polymerase Chain Reaction (qPCR), which can amplify DNA exponentially. This technique provides an extremely low detection limit for DNA particles, theoretically making it possible to identify one DNA molecule [14]. SiDNAMag particles can be recovered from a sample by magnetic separation [15]. This limits the influence of water quality on the qPCR analysis and provides an easy method for up-concentration of samples. Also, the synthesis and usage of DNA tracers is simple and cost-effective [1].

However, with the presence of natural colloids, particulate matter and river bed sediments, SiDNAMag particles are likely to undergo complex interaction processes in addition to dispersion and advection. Moreover, little is known about the possible SiDNAMag tracer mass loss during transport. Studies have shown that DNA-tracers undergo significant mass losses compared to conservative solute tracers [13] [16] [14]. The focus of this work is to identify the transport behaviour of the SiDNAMag tracer in terms of a breakthrough curve (BTC) and hydrodynamic dispersion and its interactions with the natural environment, specifically water quality and sediments.

The main questions of this research are:

What is the transport behaviour of SiDNAMag tracers compared to a conventional solute tracer and what is its potential as a tracer in surface water hydrology?

In order to answer the main questions, two sub-questions have to be answered.

1. How does the SiDNAMag particle perform compared to a solute and particle tracer in laboratory experiments in terms of breakthrough behaviour, and mass recovery, in different river water types?

2. What is the influence of channel-bottom sediments on the transport behaviour of the SiDNAMag tracer, in terms of breakthrough behaviour, and mass recovery, in different river water types?

To answer these research questions the SiDNAMag particles were compared to NaCl, a widely used solute tracer, and silica microparticles in terms of breakthrough curves and mass recoveries. Hereto, open channel injection experiments using SiDNAMag particles were performed in the laboratory. Possible mass loss was examined by performing injection experiments in different river water types with the presence of artificial sediments at the channel bottom. The resulting BTCs were interpreted with a 1D advection and dispersion model with transient storage (OTIS), to determine the hydrodynamic dispersion coefficient [17]. Conclusions provide a perspective on the potential of the SiDNAMag particle as a hydrological tracer in surface waters.

An introduction and critical literature review on tracers are presented in Chapter 2. Chapter 3 describes the methodology of the research. Next chapter 4 shows the results. A discussion is provided in chapter 5. Finally, conclusions and recommendations can be found in chapter 6.

2

Literature review

Section 2.1 provides an introduction on tracers, breakthrough curves (BTCs) and injection experiments. Previous research on DNA microparticles is discussed in section 2.2. Section 2.3 will discuss known differences in transport behaviour and model practices between solutes and colloids in surface waters.

2.1. Background on tracers

Substances used for tracing the flow of water are called tracers. It is important a tracer can be followed in the natural environment. A tracer can be used to gain information about flow paths, travel times, separate origins of water, water velocity, etc [7]. There are two groups of tracers: artificial and environmental tracers. Environmental tracers are naturally occurring in the environment, like isotopes. Artificial tracers are added to the environment by humans, commonly used substances are salts and fluorescent dyes. Besides being artificial or not, tracers can be conservative or non-conservative. A conservative tracer will not interact with its surroundings chemically or biologically, while the non-conservative tracer will [18]. Thus the total concentration of non-conservative tracers will be changed by in-stream processes.

In a tracer injection experiment, a tracer is injected into a stream or river and tracer concentrations are sampled at one or more downstream locations. Such an experiment can have multiple goals linked to a better understanding of river processes. The data gathered with injection experiments is plotted against time, to form a breakthrough curve (BTC). BTCs are often used in hydrology because they give good and reproducible results and are easy to carry out [5]. The y axis typically plots the relative concentration, which is the measured concentration over initial concentration (C/C_0). A BTC can be used to interpret processes in rivers see figure 2.1. If the BTC data is fitted with a mathematical model, transport parameters of the tracer in the stream can be characterised.

Two important processes in rivers, and for this research, are advection and hydrodynamic dispersion. Advection transports the tracer downstream, with the water itself, and occurs at the average water velocity. Hydrodynamic dispersion accounts for the spreading of the tracer in the water due to mixing processes in the river. It consists of two processes: molecular diffusion and mechanical dispersion [19]. The total of hydrodynamic dispersion allows some molecules to move faster or slower than the average water velocity [18]. Hydrodynamic dispersion is caused by the mass concentration gradient [20]. Throughout this report hydrodynamic dispersion is referred to as dispersion.

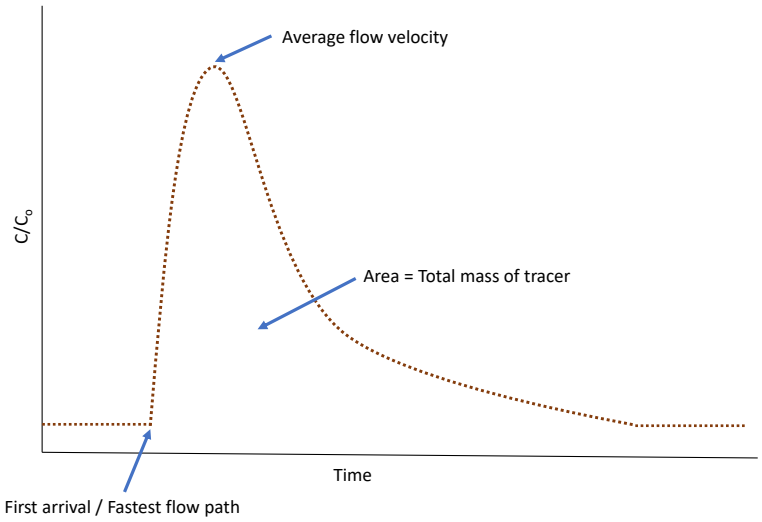

Figure 2.1 – A typical breakthrough curve of a tracer injection experiment. A BTC gives information about the tracer, some examples that were used for this research are given.

2.2. Previous research using DNA tracers

The field of DNA tracer research is relatively new. The first hydrological experiments were performed in 1999 and more attention and research for the topic came around 2010 till now. Several DNA based tracers have been developed.

- A particle with Silica core and Silica outside (SiDNASi) developed by ETH (Zurich, Switzerland) [21] [22].
- A particle with an outside of polylactic acid (PLA) developed by Cornell University (Ithaca, United States) [16] [3].
- NTNU (Trondheim, Norway) synthesised a particle-based on the Paunescu protocol [22]and Puddu protocol [15]. Their particle has a core of Iron (SiDNAFe) or Magnetite (SiDNAMag). The outside of the particle is from silica.
- The Institute of Environmental Science Research Ltd (ESR) (New Zealand) developed a particle with alginate-chitosan encapsulated DNA. [23].

In late 1990, new techniques with synthetic DNA molecules were developed by Aleström (1995) [24]. The first experiments with this technique were carried out by Sabir et al. [2] [4]. They focused on groundwater applications and were able to determine the presence or absence of synthetic DNA tracers. More experiments have been performed, the majority from 2010 onward. This review highlights the ones focusing on surface water applications.

In 2010, Foppen et al. performed 2 field experiments with naked single-stranded DNA (ssDNA) concluding that the tracer in combination with qPCR has a potential for spatially distributed surface water groundwater interaction tracer experiments and that there is a potential for quantitative use of the DNA tracer in natural streams [13]. They showed that the DNA tracer did not reduce to values below the detection limit, as the NaCl tracer did, increasing the possible spatial coverage of the tracer. Furthermore, they concluded the DNA tracer was not conservative due to the mass loss in the experiment. They highlight 3 likely options for the tracer sinks: (1) binding of DNA to particulate matter, (2) DNA sorption or attachment to the bedding of the stream, and (3) decay of the DNA. In 2012 Sharma et al. performed lab and field experiments, with ssDNA encapsulated with PLA and an iron oxide core [3]. The encapsulation improved the protection of the tracer against decay or sorption. Their experiments confirmed that it was possible to detect and quantify the tracer. Furthermore, they performed a multi-tracing experiment in which they showed it was possible to distinguish among the different tracers and that the tracers have identical transport characteristics in overland flow. In 2013, Foppen et al. performed a field experiment with naked ssDNA [25]. These experiments again showed a large loss of tracer mass. Performed batch experiments pointed out that there was no decay but an initial mass loss of 40-97%. This loss was mainly attributed to adsorption, attachment and biological uptake. They concluded that

at this point the tracer could determine advective and dispersive transport but not asses conservative solute mass exchange processes related to transient storage or hyporheic exchange. In 2015 Dahlke et al. conducted an experiment in a valley glacier with free and DNA encapsulated with polymer microspheres [16]. They showed mass recoveries of 1% to 66%. Furthermore, they found a higher mass recovery for encapsulated DNA than for the free DNA. They attributed the mass loss of both tracers to sorption to suspended particles and sediment storage since microbial activity and photochemical degradation are unlikely in a glacier. Despite the mass loss, the advection and dispersion were very similar to uranine. In 2020 Pang et al. compared free and encapsulated DNA and found that encapsulation of the DNA strands gives concentrations and mass recoveries of 1–3 orders of magnitude greater than for free DNA [23].

Thus compared to conventional tracers DNA tracers show mass losses. However, despite the mass losses, it is shown that the tracer can provide information on advective and dispersive transport.

2.3. Differences in transport behaviour between colloid and solute

Colloids represent a subset of particulates that range in size from 1 nm to 1 μm [26]. Solutes are substances that can be dissolved in water to create a solution.

Several field experiments in the subsurface concluded that the average transport velocity of colloids is larger than that of water molecules and molecular-scale conservative tracers. Luhmann et al. (2012) performed experiments in a karst aquifer and showed that sediments peak earlier than uranine, chloride and deuterium [27]. Also Goeppert et al. (2019) observe this difference between sediments and uranine in karst conduits [28]. They concluded that the mean velocity of the tracer particles increases with increasing particle size and that dispersion decreases with increasing particle size. Furthermore, they concluded larger particles were mainly transported by fast-flowing conduits, while solutes also enter low-flow zones. Goldscheider et al. (2008) compared turbidity from natural mud to uranine in an unsaturated karst zone and also observed an earlier arrival and higher peak in the BTC for the turbidity tracer and concluded this was due to higher mean velocities of the mud particles [29]. Auckenthaler et al. (2020) compared uranine to bacteriophages and microspheres in a karst aquifer [30] and Goppert et al (2008) compared uranine to microspheres of 1um and 5um in a cave stream [31]. Both concluded that the average transport velocity of colloids is higher than for solutes. Goppert et al. (2008) showed that the difference between colloids and solutes is larger in low flow conditions. The review article by W. Zhang et al. (2012) on colloid transport in fractured media also concludes that colloids transport faster than conservative solutes tracers [26]. They attribute the earlier breakthrough to a combination of large apertures, high porosity and small pore throats of the rock matrix surrounding the fractures. They summarise this as the size exclusion effect, charge exclusion effect and Taylor dispersion. Other literature confirms the finding that breakthrough of colloids can occur earlier than for solutes if Tayler dispersion or size exclusion of colloids yield enhanced advection for colloids [32] [33] [34] [35] [36]. This indicates that particle velocity increased while particle dispersion decreased [37]. In summary, colloids move faster in subsurface water transport than solutes, which can be attributed to the size exclusion effect and Taylor dispersion.

Research on particles and solutes in rivers is less consistent in its conclusion. McCluskey et al. (2021) performed an experiment in a surface stream that showed that their dsDNA tracer is having an earlier and sharper BTC than uranine, see figure 2.2 [38]. And suggest that the naked DNA tracer disperses into fewer flow paths, and thus travel in the flow paths with faster flow velocities. However, Sharma et al. (2012) performed an experiment in a short stream reach and concluded that the PLA covered DNA tracer moves similar to a dye tracer [3], with one possible exception at their furthest sampling point (61 m) where the DNA tracer peaked earlier than the dye tracer. Rossi et al. (1889) compared bacteriophages with dye tracers in a river and concluded that colloids and solutes travel at about the same velocity [39]. Thus literature is inconsistent on the differences and similarities of particle and solute transport behaviour.

Many studies with solutes or colloids model their BTC results. This section highlights the current practices of modelling colloids and solutes in literature. The critical review of I.L. Molnar et al. (2015) concludes that in the subsurface continuum-based numerical models solve the dispersion equation for solute transport in porous media are used. Indicating the observed difference between colloids and solutes is not taken into account [40]. C.V. Chrysikopoulos et al. (2015) argue that the fitted dispersion coefficients based on solute tracer data in porous medium should not be used to analyse colloid experimental data [41]. They say it is incorrect because this assumes that the solutes and colloids experience the same dispersive flux in the same flow field conditions, which many studies have proven to be incorrect. Therefore, they calibrate the dispersion

coefficient and solute or colloid particle velocity in each experiment with the model ColloidFit. In surface water studies with nanoparticles, the models include hydrodynamics of the river and often a specific part on aggregation, adsorption and sedimentation, since nanoparticles undergo these processes [42] [43] [44] [45]. Furthermore, review papers on nanoparticles (sediments, nitrogen and phosphorus, several engineered nanoparticles and carbon nanotubes), did not mention a difference in modelling method for the nanoparticles compared to solute tracers [46] [47] [48] [49]. In the review paper on phosphorus nanoparticles a distinction between particulate phosphorus and dissolved phosphorus is made, but they do not mention a difference in modelling strategy [47]. Merritt et al (2003) looked at the size distribution of particles but only use this to understand differences in settling behaviours [49]. In conclusion, there is a known difference between solutes and colloids in the subsurface and a debatable existence of this difference in surface waters. The current practice of modelling solutes or colloids in surface waters does not take this possible difference in transport behaviour into account.

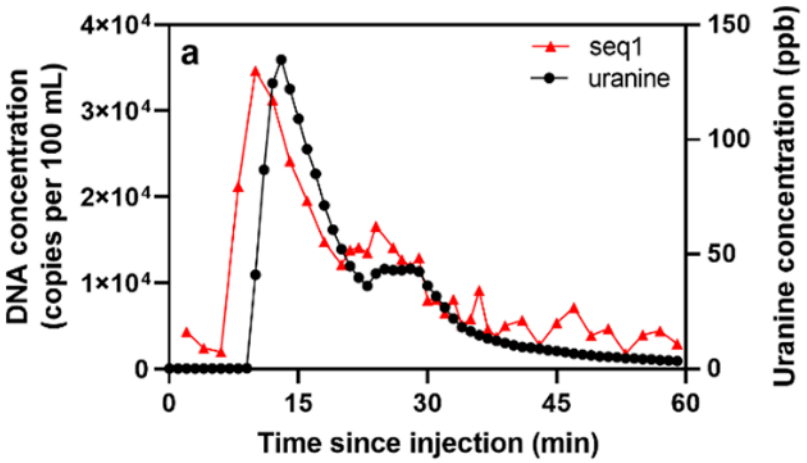

Figure 2.2 – BTC of naked DNA tracer (seq1) and Uranine from the paper of McCluskey et al. (2021) [38]

3

Methodology

The primary goal of this research was to investigate to what extent the SiDNAMag particle is comparable to NaCl as tracer, with attention to mass recovery and transport behaviour (section 3.2.2). This goal was investigated with a specific attention to the influence of bottom-sediments (subsection 3.2.3) and different river water types (subsection 3.2.4). However, extra experiments were performed for developing the laboratory setup (section 3.2.1), determining the influence of magnetic separation in sample analysis (section 3.3). The last section 3.4 of this chapter provides the methodology for modelling using OTIS and how to obtain a value for the dispersion coefficient.

3.1. Description of the SiDNAMag particle

This research investigates a new DNA based tracer: Silica encapsulated synthetic DNA with a superparamagnetic core (SiDNAMag). Figure 3.1 shows a schematic representation. This particle was synthesised in Norway by NTNU. The particle contained double stranded DNA (dsDNA) which was manufactured by Biolegio (Nijmegen, Netherlands). The particle had a size in the range of a few 100 nano-meters [50]. Appendix C provides an overview of the DNA and primer sequences.

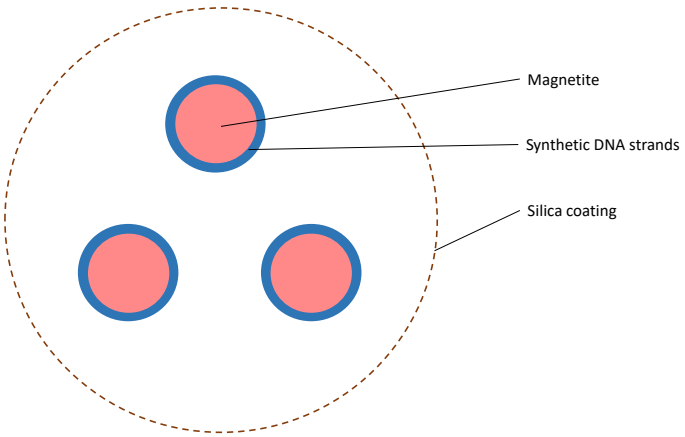

Figure 3.1 – Schematic of the SiDNAMag particle. The exact amount of magnetite particles and DNA strands inside the particle was unknown

Because of the magnetite in the core of the particle the particle comes with magnetic properties. This provides the possibility to subtract the particle from a water sample with a magnet. Appendix A.4 provides the protocol for magnetic separation.

The zeta potential of the SiDNAMag particle in Meuse, Merkske, Strijbeek, Tap and Milli-Q water was calculated using the Smoluchowski equation from the measured electrophoretic mobility by a NanoSizer (Nano Series, Malvern Instrument Ltd., Worcestershire, United Kingdom). The zeta potential is a reflection of particle surface charge and indicated the possibility of interaction of the SiDNAMag particle with ions or particulate matter present in the water. Also, the hydrodynamic radius of the SiDNAMag particle in all water types was measured using Dynamic Light Scattering with a NanoSizer (Nano Series, Malvern Instrument Ltd., Worcestershire, United Kingdom).
The samples for both measurements were prepared by filtering the natural water types with a 0.45um glass fibre filter. Then the SiDNAMag original solution was diluted 100 times with the filtered water type. All samples were analysed in three-fold. The samples for measuring the hydrodynamic radius are sonicated before the measurement in order to break possible agglomerates.

3.2. Laboratory experiments

To gain insight in the possibilities of the SiDNAMag particle as hydrological tracer in river waters three things were investigated. Firstly, the differences or similarities in breakthrough behaviour and mass recovery of the SiDNAMag particle compared to NaCl and silica microparticles (subsection 3.2.2). Secondly, the influence of water quality on the SiDNAMag particle breakthrough behaviour (subsection 3.2.4). And thirdly, the possible interaction of SiDNAMag particles with sediments (subsection 3.2.3).

3.2.1. Open channel setup

For the laboratory experiments two identical PVC setups were build. PVC was chosen because it had no known interaction with the SiDNAMag particles. The setups were a 130 cm long and had a width of 6cm. The water height was 2.5 cm, so the volume was 1600 ml. The flow rate was 50 ml/min, sustaining a laminar flow in the setup. The flow rate was generated with a peristaltic pump (Watson-Marlow pumps, Falmouth, Cornwall). 7 cm from the inlet the water was mixed, to ensured that, despite the laminar flow, the tracer mass that entered the setup was mixed over the cross section perpendicular to the flow direction. Fluorescein sodium salt was added to the setup to visualise the mixing and transport pathway of injected tracer mass. Two mixing methods were investigated, (1) with a 2,5 cm long rotor at 210 rpm and (2) with two rows of air bubbles. Pulse-injection experiments of NaCl, with different mixing systems, were performed in duplicate to verify that the setup could produce reproducible results. Thus two experiments were performed in both setups and the outcomes were visually compared (in total four BTCs) to choose the best mixing method.

Tracer injection took place at the beginning of the setup through a tube connected to the pump. At the end of the setup water was detained because the hole of the outflow was much smaller than cross section of the entire setup. When water flowed out it was caught by a container at the other end. Figure 3.3 shows a schematisation of the setup.

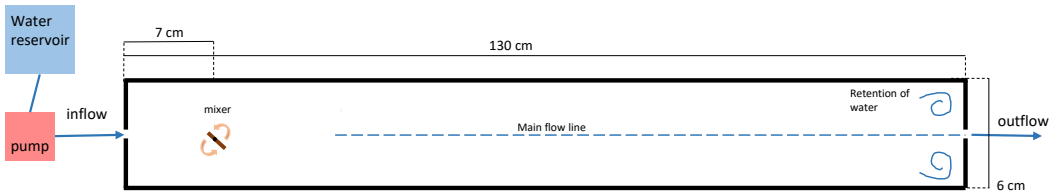

Figure 3.2 – A schematic representation of the laboratory setup for tracer injection experiments. On the left water from a reservoir was pumped into the setup with a flow rate of 50ml/min. The tracer was injected through the same pump. Then it got mixed over the entire cross-section by a rotor. Subsequently, the tracer flowed through the setup, until it got detained at the end and flowed out.

3.2.2. Injection experiments

Laboratory pulse injection experiments with NaCl, silica microparticles and SiDNAMag tracers were performed in the setup described in section 3.2.1. The aim was to gain insight in the breakthrough behaviour and mass recovery of SiDNAMag particles (research question 1). The breakthrough behaviour of SiDNAMag particles was compared to the NaCl tracer and silica microparticle tracer as reference tracers. Firstly, by comparing the shape of the BTC in terms of arrival of first tracer mass, peak time, peak concentration and when the values return to background concentration. The background value was defined as 0,1% of the injection concentration. Secondly, the dispersion coefficients were estimated for both NaCl and SiDNAMag tracers using the OTIS

software (section 3.4). The mass recovery for each experiment was calculated to quantify the possible sinks of tracer mass. Mass recovery was calculated by integrating the area underneath the BTC. During the experiments with SiDNAMag tracers all water was collected and DNA concentrations were measured.

For the injection experiments with SiDNAMag three natural water types were used in order to understand the possible influence of water quality. Tap water was used as reference, because it was assumed tap water was free of natural colloids and thus no interactions with the SiDNAMag particle were expected. More about the water quality can be found in section 3.2.4. For the experiments with NaCl and silica microparticles tap water was used.

Silica microparticles were used because the SiDNAMag tracers have a silica coating. Therefore it was assumed that the silica microparticles were a good proxy for the SiDNAMag particles. The silica particles had a size below 1000 nm. Analysing was carried out with a Lambda 365 UV/Vis Spectrophotometer (Perkin Elmer, Waltham, Massachusetts, USA) at a wavelength of 420 nm, which measures the optical density of a sample. A BTC of C/C_0 against time was created.

In all experiments the tracer mass was injected for 55 seconds. Then 30 second samples were taken at the outflow of the setup at given points in time, resulting in a BTC. In total the experiment took 160 minutes. The NaCl tracer samples were analysed with an EC meter (Multi 3620 IDS, Xylem Analytics Germany GmbH, Germany) and the SiDNAMag particles with the qPCR (section 3.3). Appendix A.1, A.2 and A.3 contain the full protocols for these experiments.

3.2.3. The influence of sediments

In order to perform field experiments it was important to understand the possible interactions of the SiDNAMag particle with river sediments (research question 2). Therefore, a layer of sediment was added to the setup. The used sediments are silica quartz sand with size range of 1200 - 1500 micron. Using these sediments was a simplification of reality but gives a first idea of the effect the presence of sediments could have on the SiDNAMag particle. Before using the sediments they were acid-washed with 10% of 96% concentrated nitric acid overnight ensure there were no metal oxides present on the sediments. The protocol can be found in appendix A.6. Per setup 210 gram of dry sediment was added. This results in a bottom layer with a width of about 4 cm, and height of 1 to 2 grains.

In the setup with sediments, the NaCl tracer and SiDNAMag tracer injection experiments described in 3.2.2 were repeated. The results of the experiments with and without channel-bottom sediments were compared to obtain an conclusion on the influence of them. The compression was in terms of breakthrough behaviour and mass recovery. The sediment layer changed the active layer of water in the experiment. To account for this it was important to compare the breakthrough behaviour of the SiDNAMag tracer experiments with channel-bottom sediments to the NaCl tracer injection experiments with channel-bottom sediments.

3.2.4. Water quality

Three natural water types were used in laboratory injection experiments in order to investigate the influence of water quality on the behaviour and mass loss of the SiDNAMag tracer. With the aim to determine whether the SiDNAMag tracer can be deployed and recovered in natural surface water environments. The three natural water types were collected from the river Meuse, the Strijbeekske brook, and the Merkske brook (see appendix B for exact locations). As control series tap water was used. The natural water was collected every two months and its quality was measured at the beginning and end of these months to monitor possible changes. Furthermore 1ml with 10mg Iodide was added per 10L water to gain a final of 1ppm Iodide in order to limit microorganism activities.

To understand what factor of the water quality could influence the behaviour of the SiDNAMag tracers during the injection experiments several parameters were measured: EC, pH, TOC, TSS, several anions and cations with the IC (Methrohm AG) and Iron and Aluminium with the ICP-MS (Alanlytik Jena, Jena, Germany).

3.3. SiDNAMag Sample analyses

qPCR was used to quantify the DNA concentrations of the samples from injection experiments. More details on the qPCR (Bio-Rad CFX96 Touch System (96 wells) instrument (CT052975)) can be found in appendix C.2. Prior to qPCR analysis, samples were magnetically separated twice (with racks from Bio-rad), washed and re-suspended before dissolving the silica-coating. With magnetic separation the used water type was replaced by Milli-Q water, with the goal to get rid of possible factors that can interfere with the qPCR measurement.

Appendix A.2 contains the full magnetic separation protocol. Subsection 3.3.1 describes the protocol to test the effectiveness of magnetic separation on replacing river waters and subsection 3.3.2 provides the protocol for investigating possible mass loss due to magnetic separation.

To convert the obtained Cq values to DNA concentrations a standard curve was prepared. Four 10-fold series diluted samples with concentrations ranging between D3 and D6 are analysed in twofold. All dilutions were prepared in Milli-Q water. On the x axis the dilution was plotted (-3, -4, -5, -6) and on the y axis Cq values are plotted. All samples were analysed at least twice and the Cq values were averaged. A straight line was fitted though the points and with the slope and intercept of this line Cq values can be converted in DNA concentration with formula3.1.

$$C = 10^{\frac{Cq-int}{slope}} \tag{3.1}$$

Where
C = the concentration of samples (mg/mL)
Cq = the threshold cycle
int = the intercept of the log-transformed standard curve
slope = slope of the log-transformed standard curve

For every experiment four qPCR runs are needed to analyse all samples. As quality control of these qPCR runs at least two sub-samples of the injection concentration were taken and were measured in each run. The Cq values of the same sub-sample over different runs can be compared to check the consistency of the qPCR. The injection concentration was a D4 solution which was prepared by diluting the original concentration (D0) 1000 times with Milli-Q water and then 10 times with the desired water type. After sub-samples from this injection concentration were taken they were magnetically separated twice.

3.3.1. The effectiveness of magnetic separation on replacing river water with Milli-Q water

Magnetic separation was performed to replace the river water in the sample with Milli-Q water. This was of importance since river water can contain qPCR inhibitors. To investigate if magnetic separation was achieving this goal, standard curves were prepared of SiDNAMAg particles that have been in Meuse, Merkske or Strijbeek water before being magnetically separated twice. The amplification efficiency and slope of the standard curve indicated if inhibition was occurring. Ideally the standard curve had an amplification of 100% and corresponding slope of the standard curve was -3.32.

The standard curves were prepared by diluting the initial concentration (D0) 1000 times with Milli-Q water (D3), and then 10 times with the desired water type (D4). Then three 10 fold dilutions where prepared (D5, D6, D7). Of all dilutions a 1ml sub-sample was taken and magnetically separated twice before being analysed with the qPCR. With magnetic separation the water type of the D4 sample gets replaced by Milli-Q water. For the full magnetic separation protocol see appendix A.4. For every water type two standard curves were prepared and the amplification efficiency was calculated with formula 3.2. Appendix C.2 provides information on how to prepare a standard curve. The samples were prepared in twofold to eliminate chance or experimental errors.

$$E = -1 + 10^{(\frac{-1}{slope})} \tag{3.2}$$

where:
Slope = the slope of the standard curve

3.3.2. The influence of magnetic separation on particle concentrations

To asses the possible influence of magnetic separation on the partcile concentration in a sample an experiment in which samples get magnetically separated multiple times was conducted. In the experiment samples undergone the process 1 up until 5 times before being analysed. A sample consisted of 1ml D4 solution in a 2ml Eppendorf vial. The D4 solution was prepared by diluting the original solution 1000 times with Milli-Q water and then 10 times with tap, Meuse, Merkske or Strijbeek water. Every sample was prepared in duplicate and analysed once. The Cq values of the duplicates were averaged before it was converted to DNA concentration. A series in Milli-Q water was included as reference. One sample of D4 solution in Milli-Q water was not

magnetically separated and served as initial concentration (C_0). The percentage of change compared to this sample was calculated to quantify the possible influence of magnetic separation on the particle concentrations.

3.4. Analysing the BTC with OTIS

The physical transport of NaCl and SiDNAMag particles in the injection experiments was estimated with OTIS41, a modified version of OTIS for specific use on laboratory scale. OTIS is a one-dimensional transport model that can account for transient storage [17]. It is suitable for the setup of this research because the setup mimics a main channel with a storage zone. The model was used to interpret the results of the experiments and assess the difference in dispersion coefficient (D) between NaCl and SiDNAMag. This section first describes the underlying theory of OTIS. Then the schematisation of the lab setup and parameter assumptions for the model will be discussed. Finally, a description is given of how the best OTIS fit was optimised from the measurement data.

Underlying theory of OTIS

OTIS is a mathematical simulation model that can reliably characterise the dominant physical processes in a stream and is one of the most commonly used surface water Transient Storage Models [51] [52]. The equation underlying the model is the advection-dispersion equation. This equation describes the rate of change in concentration with time in the downstream direction as a function of advection and dispersion. In OTIS four other terms can be added to this equation: transient storage, lateral inflow, first-order decay, and sorption [17]. In this research first-order decay and sorption were not used. This leads to equation 3.3 and 3.4

Main channel:

$$\frac{\delta C}{\delta t} = -\frac{Q}{A}\frac{\delta C}{\delta x} + \frac{1}{A}\frac{\delta}{\delta x}(AD\frac{\delta C}{\delta x}) + \frac{q_{LIN}}{A}(C_L - C) + \alpha(C_S - C) \tag{3.3}$$

Storage zone:

$$\frac{dC_s}{dt} = \alpha\frac{A}{A_S}(C - C_S) \tag{3.4}$$

Where:
A = *Main channel cross-sectional area*
A_S = *storage zone cross-sectional area*
C = *Main channel solute concentration*
C_S = *Storage zone solute concentration*
C_L = *lateral inflow solute concentration*
D = *dispersion coefficient*
Q = *volumetric flow rate*
q_{LIN} = *lateral inflow rate*
t = *time*
x = *distance*
α = *storage zone exchange coefficient*

The main limitation of a 1D representation of the setup is that homogeneous mixing over a cross-section is assumed and therefore, only longitudinal dispersion is taken into account. Besides, the system is divided in a series of stream segments. Each segment had a storage zone and main channel, two conceptual areas in which mass is conserved. The main channel is the section in which advection and dispersion are the dominant transport mechanisms and the storage zone contributes to transient storage. Each area is described by a time-variable mass balance equation.

Perception of the processes in the laboratory setup

The laboratory setup used for the tracer injection experiments is described in section 3.2.1. This section describes the perception of the processes taking place in the laboratory setup. The flow rate, measured at the inflow and outflow, was consist and therefore it is assumed the flow rate in the entire setup is homogeneous. At 7 cm form the inlet a rotor mixed the incoming tracer mass over the entire cross section of the channel. Thus it was assumed the tracer mass was completely mixed. It was presumed some tracer mass was detained by the rotor and released later. The influence of the rotor on the flow velocity was visualised with one injection experiment with florescent dye. This showed that the flow speed in the setup was influenced by the rotor in the first 35 cm. At the end of the setup the outlet is smaller than the whole cross sectional area of the channel, also resulting in a detaining of tracer mass (figure 3.3). Figure 3.3 also visualises the assumption that the main flow in the setup took place in the area between the inlet and outlet of the setup.

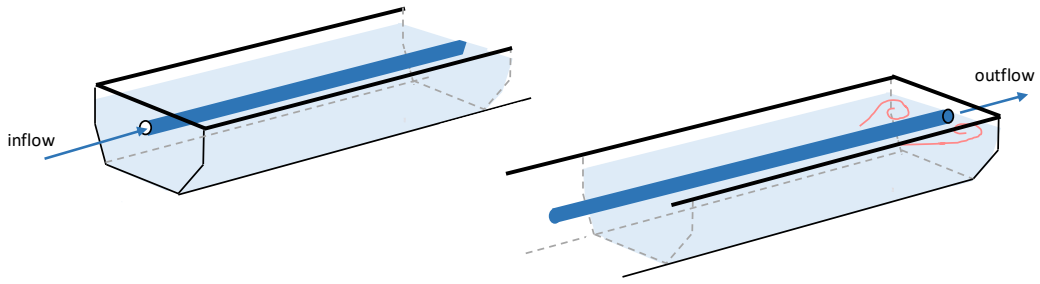

Figure 3.3 – A schematic representation the flow in the laboratory setup. The dark blue line is the main flow line, corresponding to the main channel. And the light blue is the storage zone area. Based on the assumption that the hole for the in and outflow are the same size, thus the main channel is in between these holes, with the size of these holes. The pink curls schematically indicate the detention of water at the end of the setup.

Conceptualisation of laboratory setup

The laboratory setup had a rotor in the beginning to enhance mixing, which subsequently also increased flow rate in the first 35 cm of the setup. Therefore, although there was no change in the dimensions of the channel, the OTIS model will consist of two reaches: 0 - 35 cm and 35 - 225 cm. However the flow rate in both reaches is assumed to be the same (Q.inp file). For both reaches the dispersion coefficient (D) and the storage zone exchange rate α were calibrated. It was assumed both of these values were influenced by the mixing, thus that D and α found in the second reach were more representative for SiDNAMag tracer transport in laminar flow conditions.

The main channel cross sectional area (A) was defined as the surface area of the circle through which water enters and exists the setup (diameter = 6mm), see figure 3.3. The storage zone cross sectional area A_s was assumed to be the cross section of the entire channel. To asses the influence of this choice a sensitivity analysis was performed on these parameters. In which A or A_s was changed with plus or minus 50% while all other parameters stayed the same. The model efficiency (formula 3.5) was calculated to assess the change in model performance.

Since the setup seems one big channel with no storage zones on the side, it may seem incorrect to model with and calibrate an α parameter. But, there are 3 reasons to include α in the calibration. (1) At the end of the setup water can only exit through a small hole. Therefore water was detained by the wall. This was storage the model needs to account for. (2) There are differences in flow velocity in the setup due to the mixing. However, the flow velocity in the entire setup was assumed to be the same in OTIS, since the inflow and outflow rate were the same. α can compensate for this simplification. (3) Mass could have been detained in the rotor area. In conclusion, α did not stand for an actual storage zone exchange rate, but it compensates for uncertainties in the setup that cannot be modelled and enhances model performance. Besides D and α, all other parameters were fixed in the calibration. For the used parameter settings see appendix E. It is assumed SiDNAMag particles do not undergo decay or sorption in the setup. Also NaCl is modelled as a conservative tracer. Therefore, These parameters are set to zero in the OTIS input file, for both tracers.

Because OTIS is a one-dimensional model it was not able to capture the 2 and 3D process in the laboratory setup of the SiDNAMag particles. Therefore assumptions around A, A_s, reach length etc were made. OTIS will be used to get an overall understanding about the difference in transport behaviour between SiDNAMag particles and NaCl, in terms of dispersion coefficient. A possible mismatch of the model fit compared to the measurement data can be discussed in terms of the missing physical processes taking place in the setup.

Fitting the measurement data

Every SiDNAMag injection experiment resulted in four BTCs. There were two setups which each provided one BTC, and every sample was analysed twice, leading to four BTCs. For fitting the measurement data with OTIS the four BTCs are combined to one graph, by averaging the Cq values and than translating the new Cq value to DNA concentration. When the best fit was found it was visualised against the four original BTCs. For NaCl one model fit per experiment was constructed. Besides plotting the data in a regular BTC also a cumulative BTC was modelled for the SiDNAMag tracer. A cumulative model fit provides a better representation of the big

picture, since it averages out small scale variations.

OTIS-P is a build-in package for parameter estimation which is frequently used to calibrate the parameters. However, OTIS-P was not able to do that for the experimental data of this research because of the model schematisation with two reaches. OTIS-P needs measurements points for both reaches and there were only measurements available for the second reach (at 130 cm). Therefore, the best fit of the BTC was was obtained by analysing four BTC characteristics. (1) the model efficiency was calculated with a formula from Hornberger, Mills and Herman (1992) ([53]). It was important to note that for the NaCl experiments only the data between minute 5 and 50 was used for calculating the efficiency, because this data had the same timestep, of 1 min. For SiDNAMag this was from min 1 - 35. (2) the timing of the peak, this gave important information about the average flow velocity of the tracer. (3) the height of the peak, which indicated the amount of tracer arriving with the average flow velocity. (4) the mass in the tail of the BTC, which gave information about the dispersion from main flow paths and storage along the way. The tail was defined as everything behind the peak. With a trial and error procedure the best fit was found. This best fit was visually checked against the cumulative BTC. The trial and error procedure was started with 200 fits with random values for D and (α) to check for possible parameter combinations that resulted in a good fit. The range of D was between 1E-5 till 20 and α between 0.0 and 100

Model efficiency:

$$E = (1 - \frac{sum(C_f^i - C_{obs}^i)^2}{sum(C_f^i - C_{mean})^2}) * 100\% \tag{3.5}$$

where

$$C_{mean} = sum(\frac{C_{obs}}{N}) \tag{3.6}$$

with
N = *number of observations*
C_f^i = *fitted concentrations at timestep i*
C_{obs}^i = *observed concentrations at timestep i*

4

Results

4.1. Description of the SiDNAMag particle

The zeta potential of the SiDNAMag particles is presented in table 4.1. Measured by a NanoSizer (Nano Series, Malvern Instrument Ltd., Worcestershire, United Kingdom). Similar zeta potential for the particles was found. With a slightly more negative value in Milli-Q water. The hydrodynamic radius was measured in all five water types but there was a poor quality report in the three river waters. Therefore these measurements will be repeated with the Lumisizer in NTNU. Tap water and Milli-Q water gave good results. The hydrodynamic radius got twice as big in tap water than it was in Milli-Q water.

Table 4.1 – Zeta potential and hydrodynamic radius for the SiDNAMag particles in different water types. The presented value is the average of three measurements presented with $\pm standarddeviation$

Water type	Zeta potential (mV)	Hydrodynamic radius (d.nm)
Meuse	-22.73 ±0.25	-
Merkske	-22.63 ±0.42	-
Strijbeek	-22.63 ±0.25	-
Tap	-21.67 ±0.15	1000.5
Milli-Q	-24.17 ±0.51	548.1

4.2. Laboratory open channel setup

To ensure the tracer was distributed over the entire cross-section of the channel two mixing methods were tested: air bubbles and a rotor mixing at 210 rpm. Figure 4.1 shows that the air bubble mixing resulted in more variation in the rising limb and peak of the BTC. Therefore rotor mixing was chosen to be the mixing method in further injection experiments.

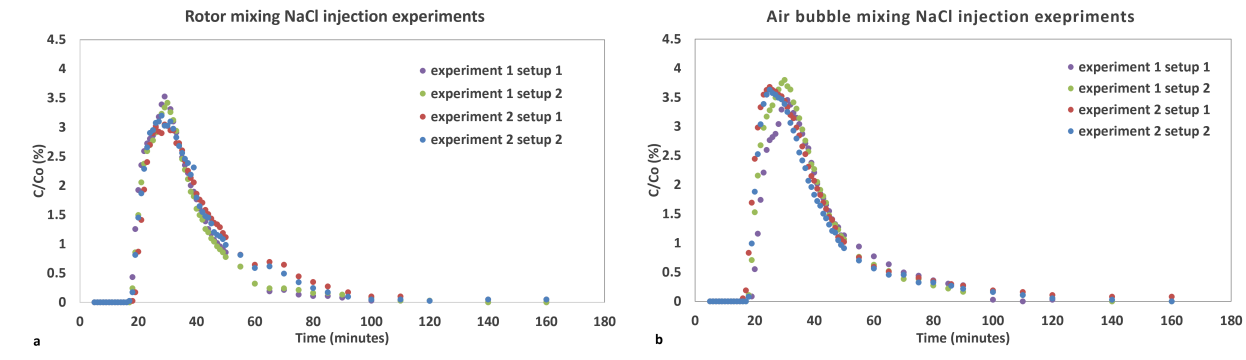

Figure 4.1 – NaCl injection experiments. figure a shows the results for rotor mixing at 210 rpm and figure b shows the results for the air bubble mixing method

4.3. Injection experiments in plain PVC gutter

In the laboratory setup without bottom-sediments experiments with three different tracers were performed: NaCl, SiDNAMag and Silica microparticles. This section presents the measured BTC, the OTIS fit and dispersion coefficient (D), transient storage exchange parameter (α) and the mass recovery per experiment.

4.3.1. NaCl lab experiments

Figure 4.1a shows the BTC of the NaCl injection experiments. NaCl experiments were performed twice in the two identical setups, generating four BTCs. The tracer arrived between 17 to 18 minutes, peaked at 29 min and returned to background concentrations at 110 minutes (table 4.2). Table 4.2 also shows the mass recovery for the NaCl tracer experiments was 100%. Overall, experimental setup generated reproducible results for the NaCl tracer, as the four BTCs show identical patterns.

Table 4.2 – Mass recovery, arrival time, peak time and end time for NaCl injection experiments. Two NaCl injection experiments were performed (experiment 1 and experiment 2). And every experiment was performed simultaneously in two setups (setup 1 and setup 2)

	Mass recovery (%)	**arrival time (min)**	**peak time (min**	**end time (min)**
Experiment 1 setup 1	108	18	29	100
Experiment 1 setup 2	101	18	30	110
Experiment 2 setup 1	101	17	29	120
Experiment 2 setup 2	97	17	28	100

Figure 4.2 shows the model fit through the measurement data of experiment 1 setup 1. The time of arrival, peak time and peak concentration were fitted well. The tail was underestimated by the model. This was also the case for model the fits of the other experiments, see appendix D.2.1. The values found for the model performance indicators are also presented in Appendix D.2.1, table D.6.

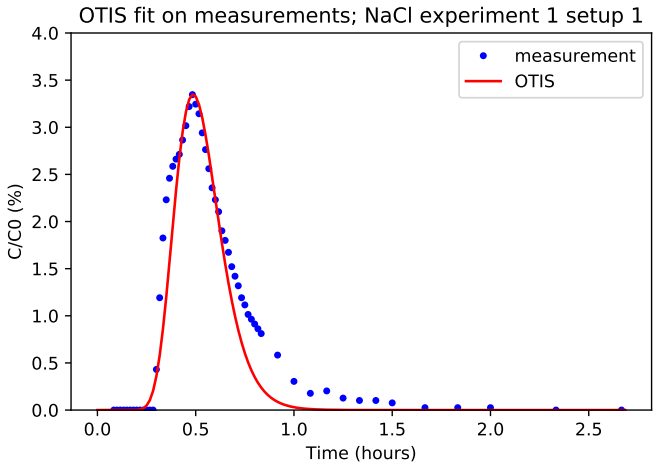

Figure 4.2 – 1D transient storage model fit for measurement data of NaCl injection experiment 1 setup 1. Using 1D advection-dispersion approximation with 1 transient storage.

Table 4.3 shows the calibrated values for D and α. Modelling the experimental BTC resulted in similar D and α for all experiments except experiment 2 setup 1 (table 4.3). The original best model fit for experiment 2 setup 1 had the following parameters: D1 = 0.01 E-3 m^2/s ; $\alpha 1$ = 6.29 /s; D2 = 3.20E-3 m^2/s ; $\alpha 2$ = 10.7 /s. In order to find one range of parameters for the experiments the parameters in reach one were fixed. The range in which they were fixed was provided by the other experiments, for D between 2.56E-3 m^2/s and 3.07E-3 m^2/s, and α between 6.82 /s and 11.9 /s. Then the parameters for the second reach were optimised. Resulting in a new parameter range. Table 4.3 shows the final D and α after reach 1 was fixed and optimal values were found for reach 2.

Table 4.3 – Results for D and α parameters of the NaCl injection experiments. '1' stands for reach one of the OTIS model and '2' stands for reach two of the OTIS model. Two NaCl injection experiments were performed (experiment 1 and experiment 2). And every experiment was performed simultaneously in two setups (setup 1 and setup 2)

	D 1 (m^2/s)	α 1 (/s)	D 2 (m^2/s)	α 2 (/s)
Experiment 1 setup 1	3.07 E-3	10.0	0.81 E-3	18.06
Experiment 1 setup 2	2.56 E-3	6.82	0.93 E-3	5.92
Experiment 2 setup 1	2.56 E-3	6.82	2.31 E-3	6.84
Experiment 2 setup 2	3.04 E-3	11.9	2.26 E-3	10.78
Range of parameters	**2.56 E-3 - 3.07 E-3**	**6.82 - 11.9**	**0.81 E-3 - 2.31 E-3**	**5.92 - 18.06**

4.3.2. SiDNAMag lab experiments

The injection experiments with SiDNAMag showed that the BTC of this tracer had a different than the BTC of the NaCl tracer (figure 4.5). Despite this difference with NaCl, the shape of the BTC of SiDNAMag was consistent, indicating the setup could generate reproducible results for particle tracers. SiDNAMag tracer particles arrived earlier, peaked earlier and higher and returned to background values quicker than NaCl tracers. Table 4.4 shows these times for the SiDNAMag tracer in minutes. On average SiDNAMag particles arrived 1.5 min earlier, peak 7.5 min earlier and went back to background values 50 min earlier.

Table 4.4 – Arrival, peak and end time of the BTCs of the SiDNAMag tracer.

	arrival time (min)	**peak time (min**	**end time (min)**
Meuse	15	21	60
Merkske	16	21	50
Strijbeek	16	21	60
Tap	17	23	60

For every experiment an average BTC was calculated from the Cq values of the four individual BTCs and the BTC was modelled using OTIS. Figure 4.3 and 4.4 show these results for Meuse water. The model results for the other water types can be found in appendix D.2.2. The BTCs of the SiDNAMag tracer showed more scatter than the NaCl tracer. Less scatter was observed in the rising limb of the SiDNAMag BTCs. When the modelled BTC was compared to the not averaged experimental data measurement points the efficiency of the fit decreased. The individual experimental results and the modelled BTC can be found in appendix D.2.2. This appendix also contains the cumulative fits and the values for the model performance criteria.

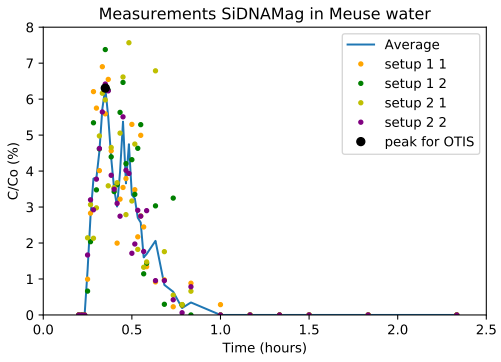

Figure 4.3 – Summary of the 4 individual SiDNAMag BTC measurements (dots) and the averaged BTC (line) in Meuse water

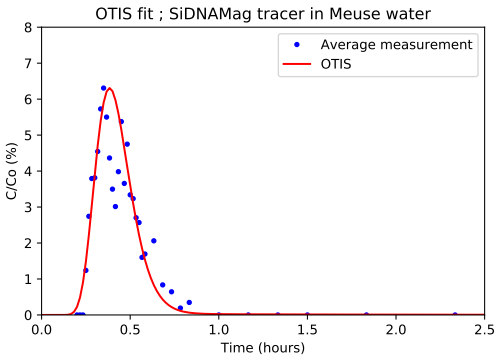

Figure 4.4 – Modelled BTC of SiDNAMag tracer in Meuse water (dots represent measured average of four experiments, see fig 4.3)

All experiments except for the one in Meuse water showed mass loss, see table 4.5 for the mass recovery. The percentage of mass recovery varied between different setups and measurements. The mass recovery of the average fit was lower than for the individual fits.

Table 4.5 – Mass recovery of the SiDNAMag experiments. 'Average' refers to the BTC calculated by averaging the four Cq values. mass recovery was calculated by integrating BTC over time. 1.1 and 1.2 are the first setup qPCR measurement 1 and 2. And 2.1 and 2.2 are the second setup, qPCR measurement 1 and 2.

	Mass recovery average BTC (%)	1.1 (%)	1.2 (%)	2.1 (%)	2.2 (%)
Meuse	97	106	121	123	98
Merkske	48	55	52	52	54
Strijbeek	42	52	52	36	54
Tap	59	60	68	76	72

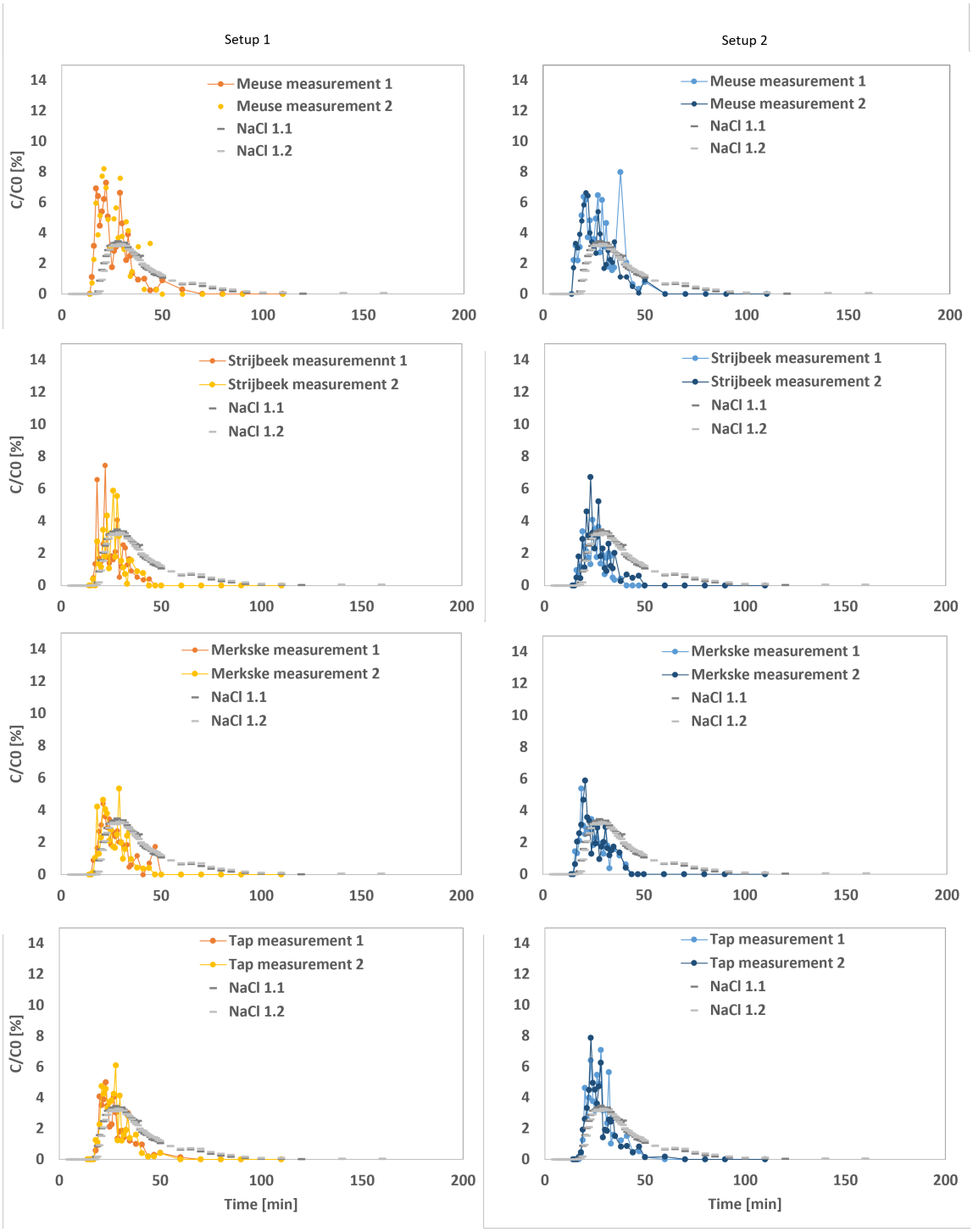

Figure 4.5 – SiDNAMag particle injection experiment in different natural water types. Performed in two setups. Per time-step two sub-samples were taken and analysed. The SiDNAMag measurements are compared to the BTC NaCl injection experiment.

The transport behaviour of the SiDNAMag particles was similar for every experiment, so there was no influence of the water type the experiment was performed in. The calibrated values for D and α are shown in table 4.6. The D and α are different from those found for the NaCl injection experiments. Indicating a change in transport behaviour of the two tracers. In reach 1 D was higher and α lower, and in reach 2 D was slightly lower and α was similar.

Table 4.6 – Transport parameters for the SiDNAMag tracer. Found with OTIS modelling based on the averaged BTC

	D 1 (m^2/s)	α 1 (/s)	D 2 (m^2/s)	α 2 (/s)
Meuse	20.0 E-3	0.01	0.88 E-3	10.7
Merkske	20.0 E-3	0.01	0.72 E-3	20.0
Strijbeek	20.0 E-3	0.01	0.69 E -3	7.70
Tap	19.4 E-3	0.11	0.34 E-3	5.00
Range of parameters	**19.4 E-3 - 20.0 E-3**	**0.01 - 0.11**	**0.34 E-3 - 0.88 E-3**	**5.00 - 20.00**

4.3.3. Silica microparticle lab experiments

The injection experiments with the silica microparticles showed the same shape in BTC as the SiDNAMag particles. Figure 4.6 shows the BTC of silica microparticles against NaCl. Just like the SiDNAMag tracers, the silica microparticles arrived, peaked and returned to background value earlier than the NaCl tracer (4.7). The experiment had no mass loss. The reason the measurements points were scattered was due to the late analysing of the samples, explained in appendix D.4.

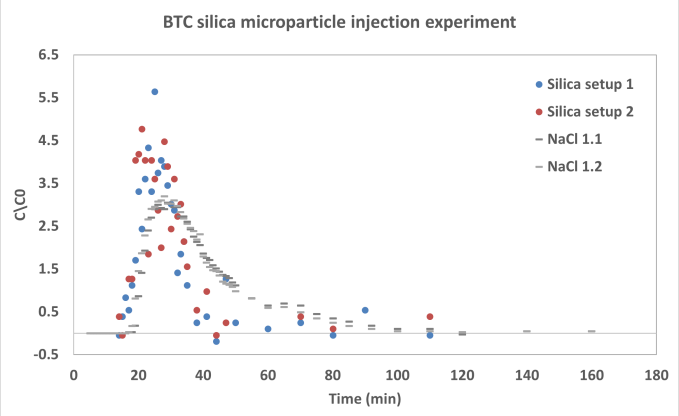

Figure 4.6 – BTC of the silica microparticle injection experiment against the NaCl BTC. Both experiments were performed in tap water.

Table 4.7 – Mass recovery, and arrival, peak and end time for silica microparticle injection experiments

	Arrival time (min)	**Peak time (min)**	**End time (min)**
Setup 1	15	25	44
Setup 2	14	21	44

4.4. Injection experiments with channel bottom-sediments

In the laboratory setup with bottom-sediments experiments with two different tracers were performed: NaCl and SiDNAMag. This section presents the measurement data in a BTC, the modelled BTC and found parameters and the mass recovery per experiment.

4.4.1. NaCl lab experiments - with channel bottom-sediments

Figure 4.7 shows the BTC of the NaCl experiments in the setup with and without channel bottom-sediments. The BTCs showed that the setup generated reproducible results for a solute tracer. It also showed that the BTC for NaCl changes slightly compared to the experiments in the setup without channel bottom-sediments. This was due to the volume the sediments occupied, creating a smaller active water layer. The average arrival time for both NaCl experiments was about the same, at 18 minutes. The peak time for the experiments with bottom-sediments compared to the experiments without bottom-sediments was 3 min earlier at 26 minutes and the tracer went back to background 27.5 min later at 135 minutes (table 4.8). Table 4.8 also

shows that the mass recovery for the NaCl tracer injection experiments was 100%. Indicating the addition of bottom-sediments was not influencing the mass recovery.

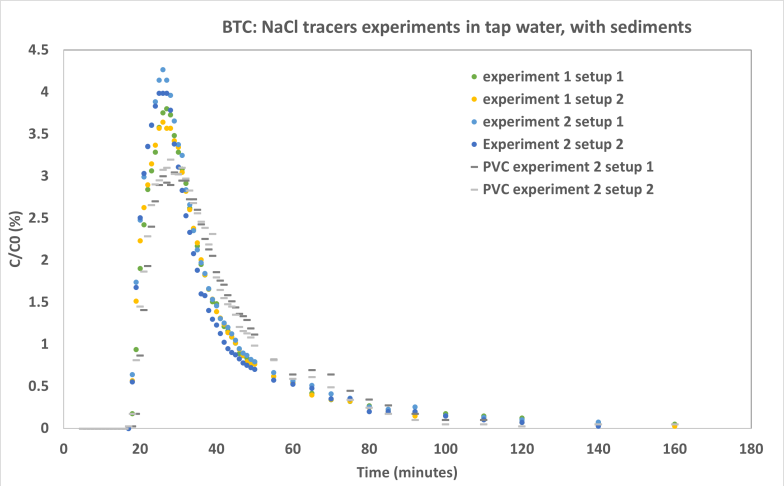

Figure 4.7 – BTC of two NaCl experiments in two setups with bottom-sediments, compared to NaCl experiments without bottom-sediments.

Table 4.8 – NaCl injection experiment mass recoveries in the setup with bottom-sediments. Two NaCl injection experiments were performed (experiment 1 and experiment 2). And every experiment was performed simultaneously in two setups (setup 1 and setup 2)

	Mass recovery (%)	**arrival time (min)**	**peak time (min**	**end time (min)**
Experiment 1 setup 1	97	18	27	140
Experiment 1 setup 2	95	18	26	120
Experiment 2 setup 1	104	17	26	140
Experiment 2 setup 2	94	18	25	140

Figure 4.8 shows the model fit for experiment 1 setup. The peak time and peak concentration were fitted well. The shape of the tail was less accurately represented. This was also the case for the modelled fits of the other NaCl experiments (appendix D.3.1). This appendix also shows the values found for the model performance parameters in table D.9.

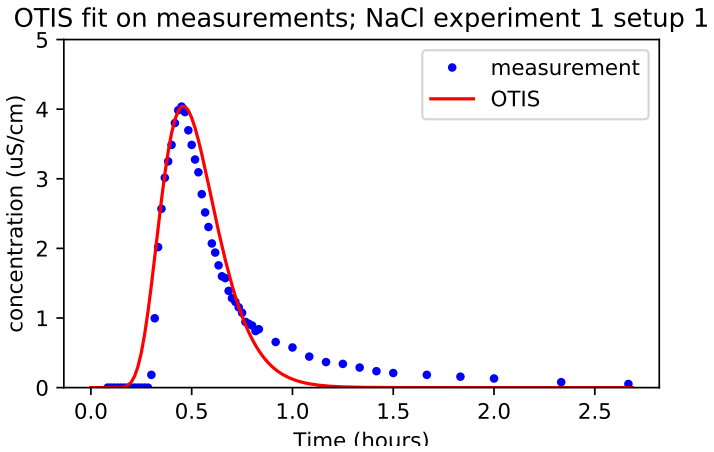

Figure 4.8 – Model results of NaCl tracer experiments with channel bottom-sediments experiment 1 setup 1. Using 1D advection-dispersion approximation with 1 transient storage.

Table 4.9 shows the values for D and α. When modelling the data all experiments had similar parameter values which were combined in one range. Furthermore, the range of D and α for the experiments with and without bottom-sediments was similar (table 4.3 and 4.9). Thus, the transport behaviour of the NaCl tracer stayed the same, despite the small visual change in the active flow layer in the setup.

Table 4.9 – parameters NaCl sediment injection experiments. Two NaCl injection experiments were performed (experiment 1 and experiment 2). And every experiment was performed simultaneously in two setups (setup 1 and setup 2)

	D 1 (m^2/s)	α 1 (/s)	D 2 (m^2/s)	α 2 (/s)
Experiment 1 setup 1	1.98 E-3	8.40	1.69 E-3	9.40
Experiment 1 setup 2	2.97 E-3	10.3	1.93 E-3	8.90
Experiment 2 setup 1	3.01 E-3	9.30	1.21 E-3	11.2
Experiment 2 setup 2	3.41 E-3	8.20	1.49 E-3	12.5
Range of parameters	**1.98 E-3 - 3.41 E-3**	**8.20 - 10.3**	**1.21 E-3 - 1.93 E-3**	**8.90 - 9.40**

4.4.2. SiDNAMag lab experiments - with bottom-sediments

The injection experiments with bottom-sediments showed visual differences for the SiDNAMag tracer compared to the experiments without bottom-sediments. This difference was similar to the visual difference observes in NaCl injection experiments with and without bottom-sediments. Figure 4.11 shows the BTC of SiDNAMAg experiments with bottom-sediments compared to NaCl experiments with bottom-sediments. Table 4.10 shows the time of arrival, peak and ending for the SiDNAMAg experiments with bottom-sediments. On average the particles arrived 3.25 minutes earlier, peaked 5.25 min earlier an went back to background concentration 95.5 minutes earlier than NaCl. It was noticeable the peak of the SiDNAMag particles in the experiments with bottom-sediments was higher than in the experiments without the bottom-sediments.

Table 4.10 – Time of arrival, peak, and end of the BTC of SiDNAMag experiments with bottom-sediments

	arrival time (min)	**peak time (min**	**end time (min)**
Meuse	14	19	41
Merkske	15	24	41
Strijbeek	13	19	38
Tap	16	21	38

For every experiment an average BTC was calculated from the Cq values of the individual experiments and an model fit was constructed for this average BTC. Figure 4.9 and 4.10 are representative for the outcomes of the experiments. The rest of the model fits can be found in appendix D.3.2. Again the data for SiDNAMag shows more scatter than the NaCl data, but in general the rising limb was quite clear. Furthermore, there seems to be more scatter in the data of the experiments with bottom-sediments than the ones without. When the model fit was compared to the original, not averaged, measurement points the efficiency of the fit decreases. The fit of the original measurement data can be found in appendix D.3.2. This appendix also contains the cumulative fits and the values for the model performance indicators.

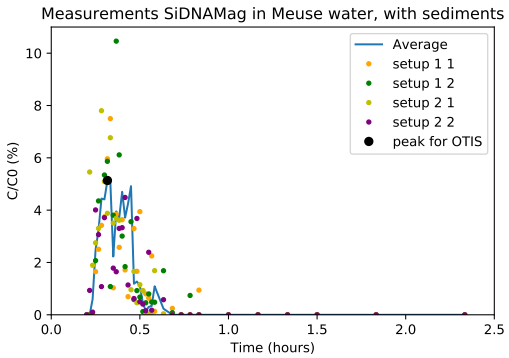

Figure 4.9 – Summary of the 4 individual SiDNAMag BTC measurements (dots) and the averaged BTC (line) in Meuse water

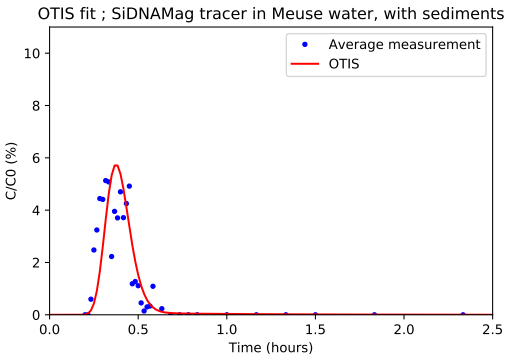

Figure 4.10 – Modelled BTC of SiDNAMag tracer in Meuse water (dots represent measured average of four experiments, figure 4.9).

Again mass losses were observed for the experiments with SiDNAMag particles. The experiment in Meuse and Strijbeek water had a full mass recovery in 3 of the 4 measurements. Also the experiment in tap water in setup 1 had a full mass recovery. Mass was found in the bottom-sediments after the experiment was finished, see table 4.12. Yet, the overall the mass recoveries of the SiDNAMag experiments with bottom-sediments were higher than the ones without bottom-sediments.

Mass recovery was calculated by integrating the BTC. To test if the amount of sampling points was

sufficient, and did not result in the observed mass losses, once a different procedure to calculate the mass recovery was performed. For this procedure all water that was not captured in the 30 second samples was captured in a big bucket. Then per sample and of the bucket the mass was calculated. This total amount of mass was summed up and divided by the injected mass of the experiment. This way of calculating the mass recovery also led to mass losses, as can be seen in table 4.11 (calculation 2).

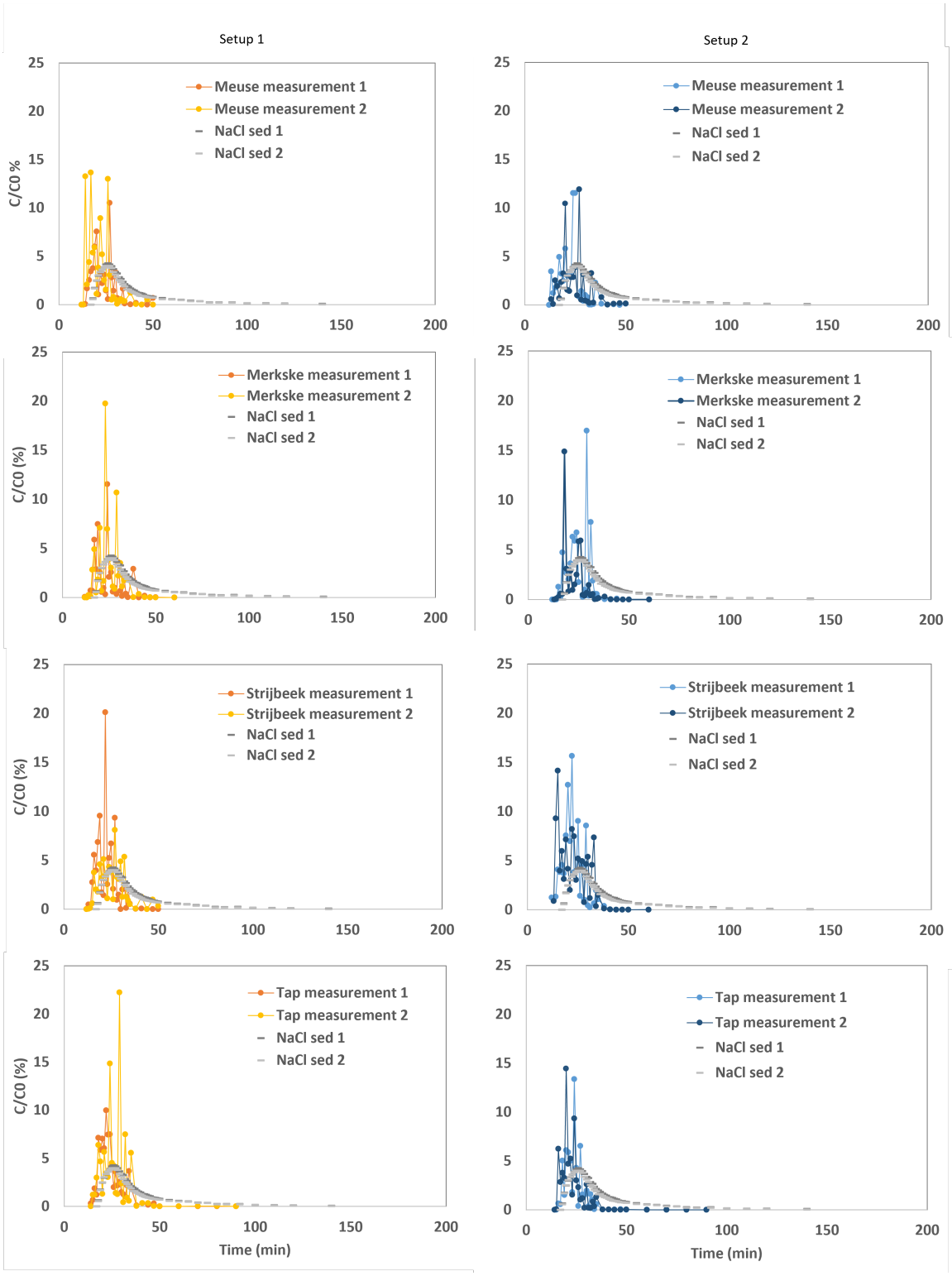

Figure 4.11 – SiDNAMag particle injection experiments in different natural water types with a layer of bottom-sediments. Performed in two setups. Per time-step two sub-samples were taken and analysed.

Table 4.11 – Mass recovery was calculated by integrating BTC over time. Calculation 2 refers to the mass recovery calculation based on mass per sample. 1.1 and 1.2 are the first setup qPCR measurement 1 and 2. And 2.1 and 2.2 are the second setup, qPCR measurement 1 and 2

	Mass recovery average BTC (%)	1.1 (%)	1.2 (%)	2.1 (%)	2.2 (%)
Meuse	62	72	103	115	100
calculation 2		50	74	84	72
Merkske	40	53	72	89	48
calculation 2		58	67	54	32
Strijbeek	82	91	74	120	131
calculation 2		69	53	71	77
Tap	63	91	105	59	69
calculation 2		57	61	66	72

Table 4.12 – The percentage of mass that was found in the bottom-sediments after the experiment was finished.

	Setup 1 (%)	**Setup 2 (%)**
Meuse	0.16	0.96
Merkske	8.64	4.01
Strijbeek	4.15	1.42
Tap	16.94	7.82

D and α show that the transport behaviour of the SiDNAMag particles was similar for all water types (table 4.13). The D and α were different from those found for the NaCl injection experiments, indicating a change in transport behaviour. In reach 1, D was higher and α lower, and in reach 2, D was lower and α similar. This was the same change observed between the SiDNAMag and NaCl experiments without bottom-sediments. Furthermore, range of transport parameters for the SiDNAMag tracer was the same with and without bottom-sediments, thus the bottom-sediments did not influence the transport behaviour of the particle.

Table 4.13 – Parameter values found with OTIS for SiDNAMAg injection experiments with bottom-sediments.

	D 1 (m^2/s)	α 1 (/s)	D 2 (m^2/s)	α 2 (/s)
Meuse	17.9E-3	0.01	0.43E-3	20.0
Merkske	20.0E-3	0.01	0.43E-3	8.40
Strijbeek	20.0E-3	0.01	0.49E-3	10.9
Tap	19.4E-3	0.11	0.34E-3	5.00
range of parameters	**17.9E-3 - 20.0E-3**	**0.01 - 0.11**	**0.34E-3 - 0.49E-3**	**5.00 - 20.0**

4.5. The influence of water quality on transport behaviour and mass recovery

For the tracer injection experiments with SiDNAMag particles three natural water types were used: Merkske water, Strijbeek water and Meuse water. One batch of water was collected in Januari and one in March. The experiments without bottom-sediments were all performed with the January water, and the experiments with bottom-sediments with the water collected in March. Table 4.14 shows the water quality parameters. It can be noted that there was a change of more than 10% for most parameters. Thus the water quality between the batches was different. See table B.3 for the perceptual differences. Despite the changes, Strijbeek and Merkske water were similar to each other and Meuse water was clearly different. Especially in TOC (lower), pH (higher), NO3 (lower), PO4 (presence of this ion), SO4 (lower) and K (lower).

One batch was used for two months, the change in water quality parameters over this period is presented in table B.1 and B.2. The difference between Meuse and Strijbeek & Merkske stayed clearly visible. For the batch of January the change was in TOC (lower), Cl (higher), No3 (lower) and K (higher). The batch of March had less changes, a clear change was in TSS, which got higher. Overall it was concluded the change in water quality was small enough for the purpose of the experiments. Since the purpose was to find out if a certain parameter influences the mass recovery of the SiDNAMag tracer. And the difference between Merkske & Strijbeek and Meuse stayed clearly visible.

Table 4.14 – Water quality batch January and March. Units are ppm for everything EC in uS/cm, and pH is unit less

	TOC	EC	pH	TSS	Cl	NO3	PO4	SO4	Na	NH4	K	Mg	Ca	Fe	Al
Batch January															
Meuse	6.043	371	7.93	10.40	24.08	22.19	1.20	28.33	18.28	0.00	4.37	5.09	50.84	1.62	0.61
Merkske	17.503	543	7.33	2.03	39.11	54.41	0.00	77.58	23.84	0.00	16.56	10.16	60.40	1.15	0.20
Strijbeek	17.027	491	7.08	1.97	33.28	69.52	0.00	74.38	21.70	0.00	14.79	7.39	48.22	1.42	0.27
Batch March															
Meuse	4.978	534	8.22	2.27	38.57	17.01	0.98	47.96	28.55	0.16	6.64	7.78	72.98	0.664	0.191
Merkske	21.100	450	7.53	1.57	33.25	40.55	0.00	58.03	22.29	0.24	18.75	8.91	46.84	1.501	0.400
Strijbeek	20.017	416	7.56	4.33	30.01	43.69	0.00	59.05	20.40	0.45	15.94	9.76	39.68	2.819	0.932
Tap	2.377	511	8.17	0.00	56.7	10.2	0.00	48.2	39.8	0.00	6.7	7.4	51.8		

There was no relation of the water quality and mass recovery of an injection experiment. All the experiments in Meuse water, except for setup 1 measurement 1 with bottom-sediments had 100% mass recovery. Also the experiment with Strijbeek water and bottom-sediments setup 1 measurement 1 and both measurements in setup 2 had 100% mass recovery. In the experiment with bottom-sediments and tap water setup 1 had a full mass recovery. The only consistent water quality parameter for all these experiments was a higher pH than the other water types. But pH of Merkske in the batch of March was very similar. Furthermore there was no effect of water quality on the breakthrough behaviour of the SiDNAMag tracer, since the dispersion coefficient and α have similar values for each experiment.

4.6. Reliability of qPCR results and preparatory procedures

This section discusses the reproducibility of the qPCR outcomes (subsection 4.6.1), the influence of magnetic separation sample concentrations (subsection 4.6.3) and the performance of magnetic separation on replacing river water with Milli-Q water (subsection 4.6.2).

4.6.1. The reproducibility of the qPCR outcomes

As quality control four sub-samples of the same injection concentration of every experiment were measured in different qPCR runs. Table 4.15 shows the results for the injection concentration of the Strijbeek experiment without bottom-sediments. Values for other experiments can be found in the appendix D.1. The biggest change of Cq within one sub-sample was 0.8 cycles (sub-sample 2), and the smallest change was 0.22 cycles (sub-sample 1). A variation of 1 Cq resulted in a variation in mass of about 50%, see table 4.16. The averaged Cq values of each sub-sample only showed a difference of 0.44 Cq while the maximum and minimum measured Cq differ 0.96 Cq. The averaged Cq value difference for the injection contraction in tap water was 0.3, in Merkske 0.42, in Meuse 0.48, see appendix D.1. Thus, to decrease the degree of uncertainty of the qPCR on the measurements it was better to analyse every sample multiple times and average the measurement replicates before converting Cq to DNA concentration. However, even after averaging replicate measurements the obtained DNA concentration had uncertainty of 29% (corresponding to the observed variation of 0.5 Cq). Important to note is that the analysed samples were of SiDNAMag particles suspended in natural waters.

Table 4.15 – four sub-samples were taken from the initial injection concentration of the injection experiment in Strijbeek water without bottom-sediments. They were measured in four different qPCR runs. This table presents the results. The average Cq value is presented with its standard deviation

	qPCR run 1	qPCR run 2	qPCR run 3	qPCR run 4	average Cq
sub-sample 1	12.21	12.31	12.37	12.15	12.26 ±0.10
sub-sample 2	13.05	12.81	12.25		12.70 ±0.41
sub-sample 3	12.70	12.64	12.09	12.65	12.52 ±0.29
sub-sample 4	12.47	12.34	12.69		12.50 ±0.18

Table 4.16 – Percentage of variation in mass for a change in Cq. Calculated with formula 3.1 and the the ideal slope of -3.32

Change in Cq value (Cq)	Change mass (%)
0.2	12.95
0.4	24.23
0.6	34.04
0.8	42.58
1	50.02
1.2	56.49

4.6.2. The influence of magnetic separation on particle concentrations

To asses the possible influence of magnetic separation on the particle concentration an experiment in which samples get magnetically separated multiple times was conducted (section 3.3.2). The outcomes in Milli-Q water show that there was no decline in sample concentration with repeated magnetic separation, since the mass stays around 100% for all samples besides the 3x magnetically separated one (figure 4.12a). This deviation is probably due to a pipetting error.

Figure 4.12b shows the outcomes for the magnetic separation experiment in the four different water types. Again there was no decline in particle concentration with repeated magnetic separation. But there was a clear variation between samples visible. This could be due to qPCR inhibitors present in the natural water types, which are not taken out by magnetic separation, like discussed in section 4.6.3. In conclusion the magnetic separation procedure did not influence the particle concentrations.

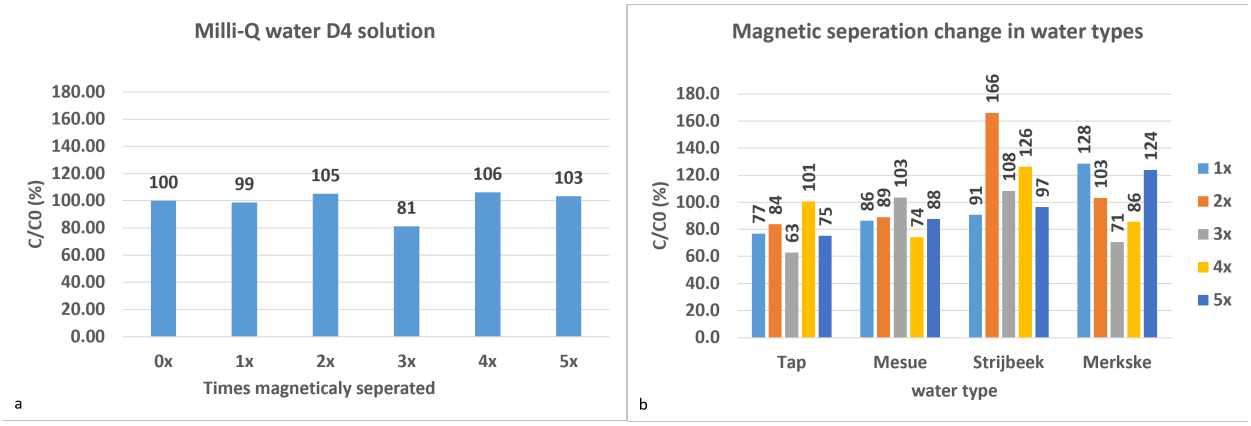

Figure 4.12 – Magnetic separation experiment with SiDNAMag particles. To obtain C/C_0 the 0x magnetically separated sample was used as original solution (D4). (a) Shows the control samples in Milli-Q water and (b) shows the samples that were dissolves in natural water types.

4.6.3. The effectiveness of magnetic separation on replacing river water with Milli-Q water

Table 4.17 shows Cq values, slope and intercept from standard curves prepared with SiDNAMag particles that have been in Meuse, Merkske or Strijbeek water before being magnetically separated twice and analysed. The ideal slope of such standard curves is 3.32, corresponding to an amplification efficiency of 100%. Conventionally an amplification efficiency of 80% till 120% is accepted. The standard curves do not meet these criteria. This indicated that the magnetic separation procedure was unable to replace all natural water with Milli-Q water, and, thus, qPCR inhibitors were left behind.

There was a variation in the Cq values of standard curves prepared in Milli-Q water. These variations only had a small influence on the slope since a higher Cq value in D4 also gave higher Cq values in D3 etc, see figure 4.13a. Figure 4.13b shows a bigger variation the Cq values of more diluted samples (D7) and less for less diluted samples (D4). The exact Cq values can be found in appendix D.1 (table D.5).

Table 4.17 – Cq values of stanrdard curves of particles that were suspended in river waters before being magnetically separated twice

	Meuse 1	Meuse 2	Merkske 1	Merkske 2	Strijbeek 1	Strijbeek 2
D4 (Cq)	13.90	13.67	14.33	15.09	14.91	13.70
D5 (Cq)	17.65	18.67	13.10	17.78	19.14	18.68
D6 (Cq)	23.60	25.64	23.51	21.95	22.26	23.62
D7 (Cq)	19.36	31.80	30.90	34.38	26.75	25.80
Slope	-2.2331	-6.1079	-6.0117	-6.0117	-3.86	-4.1228
Intercept	6.346	-11.124	11.817	-12.604	-0.4869	-2.2246
Amplification efficicncy (%)	180.41	45.79	46.67	44.94	81.48	74.80

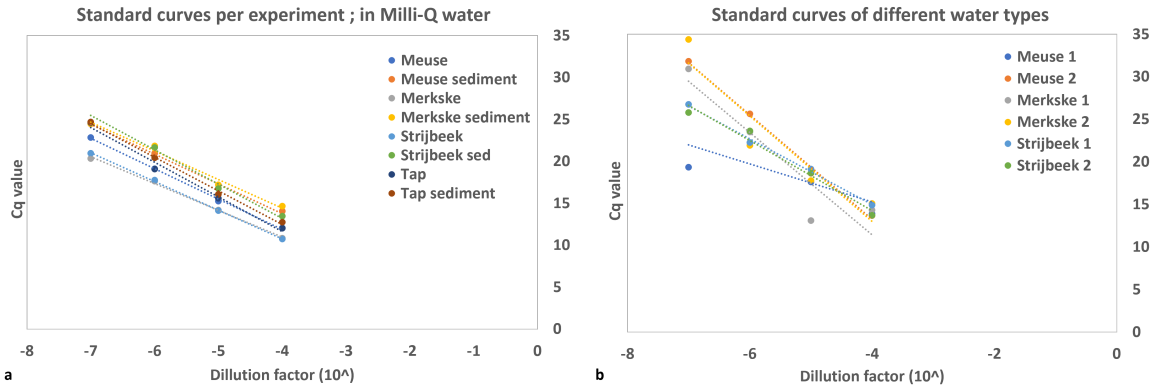

Figure 4.13 – (a) Standard curves of the SiDNAMag microparticle in Milli-Q water prepared for every injection experiment and (b) when the particle has been suspended in river water before being magnetically separated twice.

4.7. Sensitivity of conceptualisation of A and As

To assess the influence of the conceptualisation of the laboratory setup a sensitivity analysis was performed on the A and A_s parameters. The results show that a change in A_s had a clear influence on the modelled BTC (figure 4.14 and 4.15). The change was present in the height and timing of the BTC. A change in A had a smaller influence on the BTC (4.16 and 4.17). Table 4.18 shows the changes in model efficiency for a change of about 50% in A or A_s.

Furthermore, the assumption that A_s was the entire cross section of the channel, without subtracting the area calculated for A barely had an influence on the model fit (table 4.18). When one would change the assumption of A being the 6mm hole of the inflow/outflow of water and A_s being the entire cross section of the channel, to that A_s was small and A was the cross section of the entire channel then the model does not provide a decent fit at all (table 4.18).

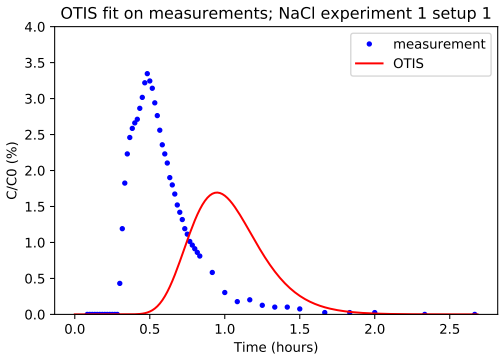

Figure 4.14 – BTC for As + 50%)

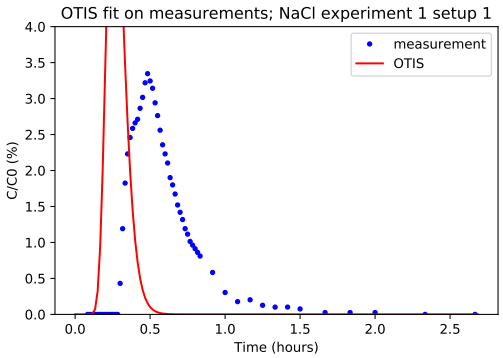

Figure 4.15 – BTC for As - 50%)

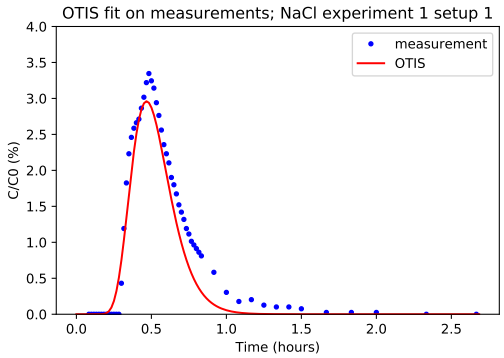

Figure 4.16 – BTC for A + 50%)

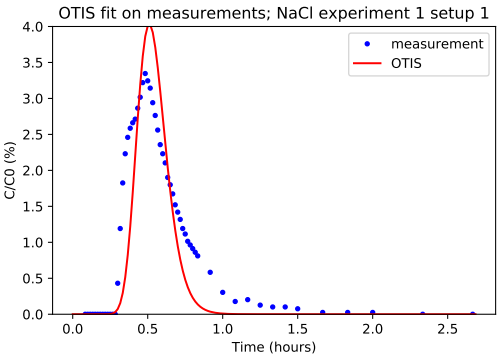

Figure 4.17 – BTC for A - 50%)

Table 4.18 – Outcomes for sensitivity analysis on the main channel cross sectional area (A) and storage zone cross sectional area (A_s).

change A	**Change As**	**Efficiency**	**change efficiency**
-	-	90.38	-
-	+50 %	-88.76	- 179.14
-	-50 %	-82.29	- 172.67
+50 %	-	90.73	0.35
-50 %	-	77.22	-13.16
-	As - A	90.88	0.5
= As	1 E-5	-284.08	-374.46

5

Discussion

5.1. Uncertainties related to the qPCR

5.1.1. Consistency in qPCR results

As quality control for the qPCR measurements, the injection concentration of every experiment is measured multiple times, as described in section 4.6. Within all samples and measurements, a difference of 0.96 Cq was found. But after averaging Cq values of replicate measurements, the difference between samples decreased to 0.5 Cq. Thus, the results show that averaging the Cq of the measurements increases the reproducibility of the results. This finding is supported by the findings of Mikutis et al. (2018), who suggest analysing samples five times instead of two [54]. Thus in future research, the number of replicate measurements can be increased to decrease the scatter in the measurement values..

Moreover, Mikutis et al. (2018) state that colloids in the presence of other substances might not have a uniform distribution when suspended [54]. Therefore, they suggest sonicating and vortexing samples ahead of pipetting. Figure 5.1 shows that improving the mixing protocol as well as measuring in 5 replicates improves the data. In this research the experimental samples were only vortexed, which could have been an insufficient mixing protocol. Thus, future research can investigate adding sonification to the protocol to decrease the scatter in the measurement values.

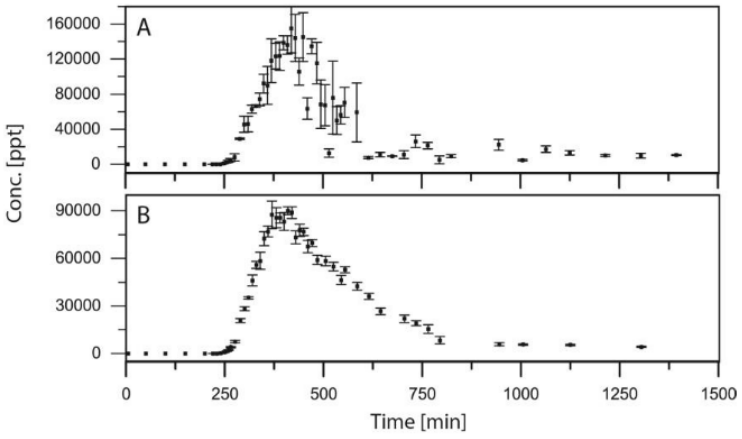

Figure 5.1 – Results of Mikutis et al. (2018) with silica-encapsulated DNA-based tracers. (A) A BTC analyzed directly from the sample tubes. (B) A BTC after vortexing and sonicating the sample as well as measuring in five replicates instead of two [54]

5.1.2. The presence of qPCR inhibitors

It is well known that surface waters contain a diverse range of qPCR inhibitors (e.g. humic acids, fats, heavy metals), which can cause problems when the sample is being processed with the qPCR [55] [56] [57]. This

research aimed to eliminate qPCR inhibitors by performing magnetic separation on each sample. This procedure purifies the samples by replacing the natural water in the sample with Milli-Q water. However, standard curves of samples prepared in surface waters, which have been magnetically separated twice, compared to standard curves prepared in Milli-Q water showed a decrease in amplification efficiency. This indicates the presence of qPCR inhibitors (section 4.6.3) and thus, magnetic separation performed insufficient for eliminating qPCR inhibition. This finding was supported with the magnetic separation experiment, where samples that were prepared in river water showed scatter in the measurements compared to the samples prepared in Milli-Q water (section 4.6.2). Moreover, the magnetic separation experiment (section 4.6.2) showed no improvement in measured values when magnetic separation was repeated more times. Two possible explanations for the presence of qPCR inhibitors in the sample after magnetic separation are (1) the inhibitors attached to the silica shell of the particle or (2) the inhibitors were attracted by the magnet in the magnetic separation process, and therefore not being pipetted out of the sample. In conclusion, magnetic separation proved to be insufficient in eliminating qPCR inhibitors and, therefore, this research was able to detect the presence of DNA but not able to accurately quantify DNA concentrations with the qPCR.

Quantifying the effect of the qPCR inhibitors on the measurement data was outside the scope of this research. However, quantification would improve the interpretation of the experimental data. Gibson et al. (2012) developed a standardised method for measuring inhibition [55] which could be used in future research. This method uses a commercially available standard RNA control and then defines inhibition by the change in the Cq of the standard RNA control when added to the sample concentrate. Furthermore, they suggest that dilution of the samples with nuclease-free water could mitigate the effect of inhibitors. Although this option would improve the quality of the results, it complicates the possibility of sample up-concentration by magnetic separation since it dilutes the samples. A second option to quantify the effect of qPCR inhibitors is to perform an experiment in Milli-Q water. The difference between this experiment and experiments in the other water types is the inhibition of the qPCR.

The standard curves prepared in natural waters all have a different slope. This suggests that the influence of water quality inhibitors on the qPCR is inconsistent, and thus inhibition is causing unpredictable changes in Cq values. The arbitrarily of the inhibition was confirmed by the observation that the BTC with the most mass loss was not generated by the standard curve performing the worst. Additionally, the created standard curves in natural waters show that there was a bigger variation in Cq values of more diluted samples, see figure 4.13. Therefore the influence of water quality could be more profound in the tail of the BTC where the lowest concentrations were. Kittila et al. (2019) conclude that measurement variations for samples with low particle concentrations occur due to the redistribution of DNA particles [58]. Therefore, the concentrations of the samples with two magnitudes could create better-performing standard curves in natural waters. Also, the effect of improving the mixing protocol could be examined.

This research assumed tap water to be a reference water type. However, the magnetic separation experiment (section 4.6.2) showed similar chaos in the data samples prepared in tap water to the data of samples prepared in the natural waters. Thus also tap water contains inhibitors that influence the qPCR. Thus, tap water can not serve as a reference water type compared to the river waters.

In conclusion, it is very likely the measurements of all samples of experiments performed in river water were influenced by inhibition in qPCR analysing, even after magnetic separation. Therefore, this research was able to detect the presence of DNA but not able to accurately quantify DNA concentrations with the qPCR.

5.2. The limitations of the laboratory setup

For the injection experiments, two identical laboratory setups were created. Small variations were visible in the data produced by setup 1 and 2. But the dispersion coefficients found for the NaCl, Silica microparticles and SiDNAMag tracers were identical for both setups. Therefore, the small visible variations were neglectable and setup 1 and 2 were identical. At the beginning of the setup, the tracer mass was being mixed. For this influence to be neglectable the setup needed to be longer than the mixing length of each tracer. The reproducibility of the results with the different tracers indicated that the setup was indeed long enough to overcome the influence of the rotor mixing for solutes as well as colloids.

The model fit created through the NaCl measurements underestimated the tail of the BTC. NaCl is a conventional tracer, known to accurately represent the movement of water in rivers. Therefore, the one-dimensional advection-dispersion model should be able to model the measurements data without a

mismatch. The observed mismatch of the model fit and the experimental data can have two reasons, (1) the design of the laboratory setup cannot be represented with the model or (2) the physical processes in the setup are inaccurately conceptualised. The main uncertainties concerning the design of the setup are the rotor mixing, which is disturbing the flow in the first 35cm of the setup, and, the small outlet of water at the end of the setup, which results in the detention of water. When considering the conceptualisation of the setup the assumptions with the biggest uncertainty were the division of the setup in two reaches and the definition of A and A_s. Furthermore, OTIS is a one-dimensional model, and thereby not able to capture two- and three-dimensional processes, present in the laboratory setup. Thus, it could be possible that there is a representation of physical processes is missing, resulting in the mismatch. In conclusion, the mismatch could be due to the design of the laboratory setup, and/or the representation of the physical processes. The mismatch of the model fit against the measurement data is a bit different for each experiment. But the calibrated dispersion coefficients were similar for each experiment. Therefore, the mismatch was not influencing the goal to gain an overall understanding of the difference in transport behaviour between SiDNAMag particles and NaCl.

5.3. The assumptions made for OTIS

For the conceptualisation of the laboratory setup it was assumed that the setup consisted of two reaches. With the influence of the mixing still present in the first reach, but not the second one. This mixing was generating a higher flow rate in the first reach than in the second one. But, in the one-dimensional advection-dispersion model there was only one value for the flow rate for the entire setup. To obtain a good model fit through the measurement data the dispersion coefficient (D) and α were calibrated. To compensate for simplification of the flow rate in the setup the values for D and α were probably influenced. When interpreting the obtained values for D and α it is important to realise they are representative for laminar flow conditions in the second reach but, it is more complicated to know what D and α in the first reach represent.

The conceptualisation of the setup with two reaches meant the model was over-dimensioned, which could lead to equifinality in the calibrated parameters. This research did not perform a test to check for this. However, for every dataset the calibration was started by generating 200 plots with random values for the two α and two D parameters. From these random plots ranges of parameters were defined. These ranges were narrowed until one value for each parameter was found, that produced the best model fit on the experimental data. While modelling all the BTCS only once a different set of parameters was found that fitted equality well (NaCl experiment 2 setup 1, without bottom-sediments). This suggested that there were not many different parameter combinations giving rise to the same outcomes. However, to prove that a Monte Carlo test should be performed.

In the one-dimensional advection-dispersion model the main channel cross-sectional area (A) and the storage zone cross-sectional area (A_s) were schematised. To asses the influence of the assumptions made for this schematisation a sensitivity analysis was performed. This showed that the schematisation of A and A_s influences the shape of the modelled BTC a lot. Thus, the found values for D and/or α would change when modelling the experimental data with a different schematisation for A and A_s. Furthermore, the cross-sectional area of A is very small (diameter = 6mm), resulting in a small area of advective and dispersive transport. But, upon entering the setup the tracer mass is mixed over the entire cross-section. Thus, the calibrated α in reach 1 had to compensate for this instantaneous presence of mass in the storage zone. Therefore, the α in reach 1 is not representative of the flow in the setup.

Literature on solute and colloids transport behaviour in groundwater, and some literature on surface waters, suggest that colloids tend to travel in faster flow lines and disperse less, compared to solutes. This raises the question if the length of the first reach should be the same when modelling colloids and solutes. The length was defined by performing an injection experiment with a fluorescent dye, thus length was accurate for solutes. If indeed colloids travel faster in surface water environments the length of reach one should be longer when modelling the data from injection experiments with the SiDNAMag tracer. However, the movement of the SiDNAMag tracer in the setup could not be visualised in this study. Therefore it is unknown if the length of reach 1 was sufficient to overcome the influence of mixing for the SiDNMag particles.

Thus, different assumptions made for the schematisation of the laboratory injection experiment could give different values for D and α. However, this is not influencing the outcomes of this research, since the aim of the research was to identify similarities and differences in breakthrough behaviour of SiDNAMag and NaCl. Therefore, the importance was that there is a difference, not the exact values of this difference since the exact values will also differ in other experimental environments. Furthermore, the change between SiDNAMag and

NaCl is also seen in shape BTC itself, indicating that the observed difference in D and α between the reaches was indeed correct.

5.4. Mass recovery of injection experiments

The NaCl tracer and silica microparticle tracer injection experiments showed full mass recovery, however, the SiDNAMag tracer injection experiments had mass recoveries ranging between 36% and 131%. The literature on SiDNAMag tracers of section 2.2 showed that previous experiments also observe incomplete mass recoveries. The literature on encapsulated DNA tracers attributed the mass loss to sorption to suspended particles or sediment storage. Several reasons for the observed mass loss will be discussed in this section.

Firstly the question raised if the mass loss could result from the way of calculating it or an insufficient sample interval during the experiment. Therefore, the mass recovery for this tracer is calculated in two ways. With the integration of the BTC from the measurement data and through collecting all the water used in one experiment and calculating the mass found in this water. Both ways showed that there is mass loss. Therefore it was concluded the mass loss was not occurring due to the calculation method or the sampling interval for creating the BTC.

Secondly, it was investigated if mass loss was happening inside or outside the laboratory setup. Hereto, a silica microparticle tracer experiment was performed, since it was a particle like SiDNAMag but with a different analysing technique. The results show that silica microparticles have the same BTC characteristics as SiDNAMag but without mass loss. This indicated that mass was lost outside of the experimental setup, and thus in the sample analysing procedure. This is supported by the findings of F. Zhang (2022) that showed no particle settling during the experimental period of 2 hours took place [59].

After the experiment was finished sub-samples are taken and magnetic separation of these sub-samples took place. The magnetic separation experiment (section 4.6, figure 4.12) showed that magnetic separation had no influence on SiDNAMag tracer mass loss. However, one sample showed mass was loss due to a pipetting error. This error could also occur when analysing the samples of the BTC, therefore pipetting errors could lead mass loss or gain in the experiments. More importantly, this experiment showed magnetic separation to be insufficient in eliminating the presence of qPCR inhibitors in the samples. This finding is supported by the deviation the standard curves made in the natural water types showed compared to standard curves in Milli-Q water. Therefore, it is likely DNA quantification of each sample is influenced by inhibition, which is likely the main cause behind the mass loss.

Another argument that the mass loss is occurring due to the analysing procedure is that there are big variations in mass recovery within BTCs constructed of sub-samples taken from the same sample. From every sample of one experiment in one setup two sub-samples are taken and analysed. The most considerable observed difference in mass recovery between these two sub-samples is 41% (Setup 2 of the Merkske experiments with bottom-sediments). This difference could be due to the way samples were taken. It is less likely it is due to the way samples were taken since the samples for the standard curves in Milli-Q water are taken in the same way, and these perform well. However, mass loss could also result from an insufficient mixing protocol and measurement of too few sample replicates (section 5.1.1). Improving the mixing protocol by adding sonification and increasing the measurement of each sample from 2 to 5 times, can decrease the measurements variations. And thereby resulting in more accurate mass recoveries.

In conclusion, mass losses originated in the sample analysing procedure. It is very likely all the values of samples of experiments in river water were influenced by qPCR inhibitors. Furthermore, insufficient mixing, limited replicate measurements and, pipetting errors could explain a part of the observed mass loss. At present, due to the many uncertainties around the incomplete mass recovery of the SiDNAMag particle in tracer injection experiments, it is impossible to calculate an accurate mass recovery for SiDNAMag tracers.

5.4.1. The influence of bottom-sediments

On average, bottom-sediments reduced the mass loss for SiDNAMag tracers. But, mass of the SiDNAMag tracer was found in the bottom-sediments after the experiments finished. SiDNAMAg tracer mass captured in the sediment is mostly < 10 % and did not explain the high mass loss of the experiments. The variation in mass found was 0.16% up until 16.94% of the injection concentration and can not be explained. Furthermore, it is unclear why the mass recovery of experiments was higher when bottom-sediments are present. A possible explanation is that there is an unknown influence of PVC on the SiDNAMag particle since the experiments with bottom-sediments have a smaller surface area of PVC.

Per injection experiment four BTCs were constructed and their mass recovery was calculated. The variation in outcomes of mass recovery was bigger for the experiments where bottom-sediments were present than for the experiments where it was not. Furthermore, the scatter in the measurement values also increased for the experiments where the bottom-sediments were present. This indicates that the presents of bottom-sediments brings more variation to the outcomes of the experiments.

5.4.2. The influence of water quality

Strijbeek and Merkske water had very similar values for the water quality parameters. Meuse water was a clearly different natural water type, which was more similar to tap water. Meuse and tap water have in common that they have a lower TOC, higher pH, lower NO3, lower SO4 and lower K concentration compared to Strijbeek and Merkske. However, only Meuse water had a mass recovery of 100% in 7 of the 8 BTCs (not in the experiment with bottom-sediments, setup 1, measurement 1). Experiments with tap water had a full mass recovery in only 2 BTCs (experiment with bottom-sediments, setup 1, both measurements). The main difference in the water types was that tap water had a higher Cl and Na concentration than Meuse water. The experiment with bottom-sediments and Strijbeek water showed a full mass recovery in 3 of the 4 BTCs. The only consistent parameter between the experiments with full mass recovery was a pH of about 8. But, the Merkske water of March has a pH in a similar range and showed incomplete mass recovery. Thus no conclusion can be drawn on which water quality parameter was influencing the mass recovery of the experiments.

In the experiments tap water is used as a reference water type. No change in water quality is expected, and therefore it is not measured. However, the mass recovery in tap water is inconsistent, which could be to an unknown change in tap water. However, for the experiment in tap water with bottom-sediments the same water was used in setup 1 and 2, yet the mass recovery in setup 1 is 100% while it is 65% in setup 2. Therefore, the reason for the incomplete mass recovery is not related to the water quality in which the experiments took place.

5.5. Breakthrough behaviour of the SiDNAMag tracer

In the first reach of the setup, the flow rate was faster than in the second reach, but in OTIS this was all modelled at the same flow rate. Presumably, this was compensated in the value of D, which was found to be higher in reach 1 than reach 2 for every experiment. For the SiDNAMag experiments, the change in D was more than one magnitude, while for NaCl it stayed in the same range. This indicated the SiDNAMag tracer was moving faster through the first reach than the NaCl tracer. This was supported by the low value of α (0.01 - 0.11 /s) found for the SiDNAMag tracer in the first reach, indicating there was barely any exchange with the storage zone, thus the tracer was mainly moving in the fast flow line of the model.

The underlying equation for the one-dimensional advection-dispersion model (OTIS) is equation 3.3. For modelling the experimental data the D and α in this equation were calibrated. Literature on solute and colloids transport behaviour in groundwater, and some literature in surface water experiments, suggest that colloids tend to travel in faster flow lines and disperse less, compared to solutes. Therefore it would be logical if the advective part of the advection-dispersion equation would change when modelling colloids instead of solutes. Since advection stands for the movement of the tracer with the water flow, and this 'water flow' is faster for colloids than solutes. However, this was not changed when modelling the BTCs of SiDNAMag and NaCl. Literature on modelling solutes and colloids in surface waters do not present a method to deal with this difference.

To gain an understanding of the physical processes of the tracers the experimental data was modelled with a one-dimensional advection-dispersion model. The model fit was made through the average of the data of the four BTC generated with one experiment. The model efficiency of the OTIS fit through the average BTC was better than when the modelled BTC was compared to the four original BTCs. Moreover, the mass recovery of the averaged BTC was always lower than the mass recovery of the original BTCs. These two observations indicate that combining the four BTC into one could be incorrect. This could be due to a small time shift between the setups. But, even the replicate measurements of one setup show a lot of variation, indicating the way samples were analysed gave rise to variations in the BTC and not a time-shift between the setups. Section 5.1.1 and 5.1.2 confirm the uncertainties in the analysing procedure. Therefore, lower mass recovery of the average BTC and the decrease in model efficiency of the modelled BTC when it is compared to the original BTC instead of the average one, could be explained by measurement variations resulting from the analysing procedure.

The literature review on solutes and colloids (section 2.3) mentioned a known difference in the transport behaviour of solutes and colloids in groundwater studies. Whereby the colloids tend to travel in the faster flow paths and diffuse less. The finding matched the findings of this research, the SiDNAMag particle was moving faster than the NaCl solute. Surface water studies were less existing and less consistent in their findings. McClusky et al. (2021) support the difference between solutes and colloids in surface water that was found in this research [38]. Additionally, the silica microparticle was demonstrating the same breakthrough behaviour as the SiDNAMag particle, confirming the conclusion that there was indeed a difference between solutes and colloids in the laboratory setup.

However, there were some important differences in the findings from the literature and this thesis. First of all the examples in literature are field experiments. Thus the literature talks about much larger scales than the laboratory experiments of this thesis. Furthermore, the flow rate of the laboratory setup of this thesis much smaller (5E-5 m3/min) than the flow rate of the rivers discussed in the literature. Therefore, a field experiment should be performed to verify the findings of this research on field-scale.

Despite, the occurrence of mass losses between 50% and 0% the shape of the BTC stayed the same. Also, the transport parameters D and α stayed in the same range for all experiments. Therefore the mass losses occurring when processing each sample were small enough not to influence the overall transport behaviour. This indicated that although the tracer experiences mass loss it is still able to provide information on advective and dispersive transport.

The BTC of SiDNAMag tracers showed more scattered data points than the BTC of NaCl tracers. One explanation for this could be that solutes and colloids responded differently to mixing with the rotor. Furthermore, particles and solutes could have a different response when they hit into the wall at the end of the setup. A second explanation could be that the randomness was linked to the sample analysis with the qPCR (section 5.1). Which discusses qPCR measurements are influenced by inhibition in sample quantification. Furthermore, it is suggested the mixing and analysing protocol is insufficient. It could also be inherent to the qPCR since the qPCR only measured full cycles and the decimals of a cycle number are determined with a fitted mathematical equation. A small deviation here could lead to a big variation when converting the Cq value to linear scale, since a small change in logarithmic scale leads to a big change on linear scale. Although the BTCs of SiDNAMag tracers show more scatter, the experiments gave reproducible results, visually and in terms of D and α. Thus the influence per sample is small enough to not influence the outcomes in breakthrough behaviour of the SiDNAMag particle.

In conclusion, the data of the tracer injection experiments showed that BTCs of SiDNAMag tracers arrived, peaked and ended earlier than NaCl tracers. This observation was consistent overall experiments performed. Furthermore, the found dispersion coefficient (D) and storage zone exchange rate (α) of SiDNAMag and NaCl were different, confirming the change in observed breakthrough behaviour. Thus SiDNAMag particles moved faster through the setup than NaCl solutes. These observations are not influenced by the observed mass losses or scatter of the BTCs.

5.5.1. The influence of bottom-sediments

A predominant observation was the change in the shape of the BTC of the NaCl injection experiments with and without bottom-sediments. This change originated from the smaller active flow area in the setup when the bottom-sediments were present. A similar change was observed for the SiDNAMag tracer experiments. This mainly resulted in a clear higher peak in the tracer breakthrough in the experiments with bottom-sediments. Specifically for the SiDNAMag particle, it can be noticed there is more scatter in the data points when the bottom-sediments are present. However, the increased scatter did not influence the general breakthrough behaviour of the SiDNAMag tracer since the Dispersion coefficient found with OTIS was consistent for the experiments with and without bottom-sediments.

5.5.2. The influence of water quality

Although this research suggests that the scatter observed in the measurement values is mainly arising from sample analysis, it could also be the influence of water quality on the transport behaviour. However, BTCs of SiDNAMag tracers in three natural water types had the same shape, and when modelling the data it shows the tracer had the same dispersion coefficient in all water types. Therefore no relationship was found between the water quality and breakthrough behaviour of the SiDNAMag particle.

6

Conclusions and recommendations

6.1. Conclusion

The main question of this research was: *What is the transport behaviour of SiDNAMag tracers compared to a conventional solute tracer and what is its potential as a tracer in surface water hydrology?*

The laboratory experiments performed in this thesis show that SiDNAMag particles have a reproducible, but different transport behaviour than NaCl solutes. The SiDNAMag particles arrive, peak and return to background concentrations earlier than NaCl solutes. Furthermore, the interpretation of the data with a 1D advection and dispersion model showed that the dispersion coefficient for SiDNAMag was lower (0.34E-3 m^2/s – 0.88E-3 m^2/s) than that of NaCl (0.81E-3 m^2/s – 2.31E-3 m^2/s). Literature on solutes and colloids in the aquatic environment supports the possible difference in the transport behaviour of solutes and colloids. No relationship of transport behaviour with water quality or sediments was found.

The mass recoveries for SiDNAMag experiments were between 36% and 131%, which could be partly explained by the bottom-sediments which detained between 0.16% and 16.94% of the SiDNAMag mass during the experiments. No relationship was found between the three natural water types and the observed mass losses. Additionally, the silica microparticle injection experiment showed the same BTC characteristics for silica microparticles as SiDNAMag though without mass loss, indicating mass loss occurred in the lab analysis. the main issues related to the lab analysis are (1) the presence of inhibitors on the qPCR measurements. (2) The possible pipetting errors in the magnetic separation procedure. (3) The magnification of small errors in the logarithmic detection scale of the qPCR when being translated to DNA concentration and, (4) a possibility of insufficient sample mixing. Due to the uncertainties in the lab analysis, no accurate mass recovery for the SiDNAMag tracer could be calculated. Furthermore, the observed scatter in the measurement data could be explained by the uncertainties in lab analysis as well as possible differences in transport behaviour of solutes and colloids. Despite the scatter the experimental results for transport behaviour are reproducible, indicating the factors causing the scatter did not influence the transport behaviour of the SiDNAMag tracer.

Thus the laboratory study this thesis presents showed that the SiDNAMag tracer can be used to identify the transport behaviour of colloids. Thereby SiDNAMag can be a valuable tool to gain information on the movement of microparticles, like microplastics and pathogens, in the natural environment. The next step towards achieving this goal is performing a field experiment, for which upscaling of the SiDNAMag tracer production is required. Several other considerations are:

- The detection limit of the tracer. This research showed that the more diluted the tracer gets in river waters the more random values the qPCR produces. Therefore the tracer should not get more diluted than D6 values ($10^{-6} mg/ml$). However, with magnetic separation up-concentration of a sample is possible. This is a time-consuming process.
- At the moment no field experiment was conducted due to the number of particles needed. Which was estimated to be 325 batches of 0.24 mg/l (prepared by NTNU) to get a good Cq value (D5 a D6) at 100 meters downstream. Without taking into account up-concentration. see appendix F for the full calculation.
- There was mass found in the bottom-sediments in the laboratory experiment. Therefore it is expected that in field experiments also mass will be lost due to the presence of bank and bottom-sediments.

6.2. Recommendations

I would recommend three next steps for future studies. First, I would recommend performing a field experiment to find out if the observations in the laboratory are the same in the field, and to examine the tracers performance at larger scales. Secondly, to improve the quality of the results I suggest adding sonification to the analysing protocol to investigate its influence on measurement reproducibility. Furthermore, I strongly suggest to keep on analysing each sample at least two times and average Cq values and more if the laboratory capacity allows. To limit variations and get more reproducible results. Thirdly, to quantify the influence of the inhibition on the qPCR measurement, I would either conduct a SiDNAMag tracer injection experiment in Milli-Q water in the same setup, when the variation between the BTC in Milli-Q water to the BTCs in the four other water types will quantify the variation. Or use the method described by Gibson et al (2012) [55]. Quantification of the inhibition could give a better understanding of the differences in transport behaviour of solutes and colloids.

A

Protocols

A.1. NaCl injection experiment

For 1 experiment in duplicate (2 setups)

1. make 200ml NaCl solution of 2000ppm in tap water. (400 mg NaCl). And devide this over 2 50 ml tubes and weigh them.
2. fill the setups with water (1600 ml)
3. fill the setups with sediments (210 gram, per setup) so that the bottom is covered with a layer of 1 to 2 grains.
4. Check that the outflow rate of both pumps is 50 ml/min. If it is, connect the pumps to the setup.
5. Wait 30 minutes for the flow to stabilise in the setup. Check if the flow is stable by measuring the outflow, it should be 50 ml/min.
6. Inject the 2000ppm NaCl solution for 55 seconds via the tube of the pump. And press start on a stopwatch to measure the time of the experiment
7. Weigh the injection tube again, to gain the total injected amount of tracer.
8. Take half a minute samples according to the schema in table A.1. In 50 ml Eppendorf tubes.
9. With an EC meter (Multi 3620 IDS, Xylem Analytics Germany GmbH, Germany) measure the electrical conductivity of the sample in µS/cm and store the data

Table A.1 – Sampling interval for NaCl injection experiment

time	**sampeling interval**	**number of samples**
10 to 50 min	1 minute	40
55 to 90 min	5 minute	8
100 to 120 min	10 minute	3
140 to 160 min	20 minute	2

A.2. SiDNAMag injection experiment

Magnetic separation is performed to seperate the SiDNAMag particles from the water they are in and put them in MilliQ water.

For 1 experiment, performed in 2 setups.

1. make 140ml SiDNAMag solution that is 4 times 10 fold diluted from the original solution (D4) by first making a D3 solution in miliQ water and then diluting it into D4 with the water type you will use in the experiment. Then divide this over two 50 ml tubes and weigh them.

2. fill the setups with water (1600 ml)
3. fill the setups with sediments (210 gram per setup) so that the bottom is covered with a layer of 1 to 2 grains.
4. Check that the outflow rate of both pumps is 50 ml/min. If it is, connect the pumps to the setup.
5. Wait 30 minutes for the flow to stabilise in the setup. Check if the flow is stable by measuring the outflow, it should be 50 ml/min.
6. Inject the SiDNAMag solution for 55 seconds via the tube of the pump. And press start on a stopwatch to measure the time of the experiment
7. Weigh the injection tube again, to gain the total injected amount of tracer.
8. Take half a minute samples according to the schema in table A.1.
9. After the last sample is taken take 3 1ml samples in the gutter to check if particles are left behind. One in the rotor area, middle and end. Take the samples as close to the bottom of the setup as possible. Put the samples in a 2ml Eppendorf vial.
10. if the experiment contains sediments: Empty the channel from the water, and add 400 ml Milli-Q water. Remove this water and the sediments and mix for 5 munutes. Then take a sub-sample of 1 ml in an Eppendorf vial.
11. Vortex the 25 ml samples 1 minute at 3000rpm before taking a 1 ml sub-sample in a 2ml Eppendorf vial. Take 2 sub-samples per sample.
12. Perform magnetic separation on all sub-samples, for the protocol see section A.4.
13. Analyse the samples in the qPCR

A.3. Silica injection experiments

The protocol for the experiment is the same as for NaCl (section A.1), but with the silica suspension described below. Analysing is done with a Lambda 365 UV/Vis Spectrophotometer (Perkin Elmer, Waltham, Massachusetts, USA) at a wavelength of 420 nm, which measures the optical density of a sample. a BTC of optical density against time is created

Silica suspension

The silica suspension used in the experiments is made as follows from silica powder, which is purchased from Sigma-Aldrich (Germany, product number: 85356).These particles have a particle size of 0.2 - 0.7 mm. In order to get to a particle size of less than 1000 nm the protocol from F. Zhang [59] is used:

- Mill 15g silica particles in a mortar with a pestle for 30mins;
- Put the milled silica and 1L Milli-Q water in a 1 litre plastic bottle and shake well;
- Let the silica solution settle for for 24hrs;
- Take the supernatant (between the water surface and 4.8 cm depth) of the silica solution.

A.4. Magnetic separation

For magnetic separation racks from Bio-rad are used.

Protocol

1. Put on gloves
2. Disinfect the area you will work with bleach
3. put the vials with caps open in the magnetic separation rack for 30 min. Make sure the vials are covered with a box during this 30 min to limit contamination.
4. From each vial: Take out 850 ul with a 1ml clean filter pipette point
5. Add 850 ml of MiliQ water with a clean filter pipette point

6. Vortex the vials for 1 minute with 3000 rpm
7. Centrifuge the vials for 1 second on 1500rpm
8. Repeat step 3 till 5

A.5. Magnetic separation experiment

The goal is to quantify mass loss upon repeated magnetic separation in 2 ml Eppendorf vials in different water types: Tap, Meuse, Merkske and, Strijbeek.

Per water type samples will be separated 1, 2, 3, 4, or 5 times and analysed for the occurrence of mass loss. This will be done in duplicated. As control series demi-water will be included. In the SiDNAMag injection experiments a D4 solution was the initial injection concentration, thus for this experiment we will use D4. Table A.2 gives an overview of the vials that are analysed at the end.

Protocol

1. Put on gloves
2. Disinfect the area you will work with bleach
3. Make 12 ml D4 solution in tap/Merkske/Meuse/Strijbeek/ (so you have 4 different solutions in the end, all 12 ml) + 16 ml D4 solution in Demi water
4. Vortex all the solutions for 1 minute at 3000rpm
5. Per water type label 10 vials. With water type and number of time it will be magnetically separated (1x till 5x).
6. Put 1ml of the solution in 2ml vials. So you will have 50 vials (10 per water type)
7. From the left over 6 ml of D0 in demi water, put 1 ml in 4 2ml vials. Store as these will not be magnetically separated so we know the initial concentration before magnetic separation took place. (in total: 54 vials)
8. Open the lid and put the vials in the magnetic separation racks for 30 minutes. Open the lid
9. From each vial: Take out 850 ul with a pipet
10. Add 850 ml of MiliQ water
11. Store the once separated vial (2 per water type)
12. Vortex all other vials (in total 52-5x2-2=40) for 1 minute at 3000rpm
13. Centrifuge these vials for 1 second on 3000rpm
14. Repeat step 8-13 for the vials that are left.
15. Then the vials need to be analysed with the qPCR

Table A.2 – Vials for analysing in the magnetic separation experiment

# magnatic seperation	0	1	2	3	4	5
Tap water		2 vials	2 vials	2 vials	2 vials	2 vials
Merkske water		2 vials	2 vials	2 vials	2 vials	2 vials
Meuse water		2 vials	2 vials	2 vials	2 vials	2 vials
Strijbeek water		2 vials	2 vials	2 vials	2 vials	2 vials
Demi water	4 vials	2 vials	2 vials	2 vials	2 vials	2 vials

A.6. Washing the sediments

The sediments used in the injection experiments where cleaned with the following protocol in order to remove metal oxides.

1. Weigh the amount of sands (silica quartz sand, from Sibelco) with size range of 1200 micron - 1500 micron.
2. Wash the above-mentioned sands with tap water until the water turns clean
3. Soak the Sands in nitric acid in 10% v/v, dilute from the 69% concentrated HNO3, overnight (12 hour)
4. Wash the sand with deionized (DI) water until the pH of sand-washed water goes back to pH of DI water.
5. Oven dry the sands at 80 °C overnight (12 hrs)
6. Retrieve the acid-washed sands and make it homogeneous for later use.

B

Water types

In the experiments of this thesis three natural water types are used. This chapter explains where this water is collected and its water quality.When the water was collected 1ml with 10mg Iodide was added per 10L water to gain a final of 1ppm Iodide in order to limit microorganism activities.

B.1. Collecting water

Water was collected at 3 locations:

- Meuse = 51.718261, 4.890969
- Merkske = 51.415870, 4.846792
- Strijbeek = 51.498938, 4.783012

Water was collected in plastic bottles of 10 litre and upon arrival at TU Delft stored at 4 degrees Celsius.

B.2. Water quality

Water was collected 2 times. Once on 6-01-2021 secondly on 16-03-2021.

Water January 2021

Table B.1 – Changes in water quality batch January

	TOC (mg/l)	EC	pH	Cl	NO3	PO4	SO4	Na	NH4	K	Mg	Ca
Meuse	6.043	371	7.93	24.08	22.19	1.20	28.33	18.28	0.00	4.37	5.09	50.84
change (%)	-25.36	4.13	-0.17	27.16	-26.35	-16.71	7.26	3.25	0	126.20	4.88	1.20
Merkske	17.503	543	7.33	39.11	54.41	0.00	77.58	23.84	0.00	16.56	10.16	60.40
change (%)	-12.56	3.56	3.27	21.14	-14.68	0.00	2.46	1.89	0.00	52.56	7.69	-2.11
Strijbeek	17.027	491	7.08	33.28	69.52	0.00	74.38	21.70	0.00	14.79	7.39	48.22
change (%)	-8.61	11.19	3.44	54.06	-26.26	0.00	2.44	2.73	0.00	126.24	63.43	1.67

Water March 2021

Table B.2 – Changes in water quality batch March

	TOC (mg/l)	EC	pH	TSS (mg)	Cl	NO3	PO4	SO4	Na	NH4	K	Mg	Ca
Meuse	4.978	534	8.22	2.27	38.57	17.01	0.98	47.96	28.55	0.16	6.64	7.78	72.98
change (%)	-15.11	0.69	-0.41	33.82	2.60	7.91	-21.67	-0.34	-1.37	5.77	4.82	-4.28	-1.77
Merkske	21.100	450	7.53	1.57	33.25	40.55	0.00	58.03	22.29	0.24	18.75	8.91	46.84
change (%)	-9.67	0.44	1.15	61.70	3.02	4.29	-	-0.23	-1.30	-100.00	5.03	-2.54	-2.63
Strijbeek	20.017	416	7.56	4.33	30.01	43.69	0.00	59.05	20.40	0.45	15.94	9.76	39.68
change (%)	-8.38	0.24	-3.04	67.69	1.74	3.78	-	-0.31	-1.79	-32.07	1.13	-2.03	-2.46

Change between water collected in January and March

Table B.3 – Changes between January and March

	TOC (mg/l)	EC	pH	TSS (mg)	Cl	NO3	PO4	SO4	Na	NH4	K	Mg	Ca	Fe	Al
Meuse	6.043	371	7.93	10.40	24.08	22.19	1.20	28.33	18.28	0.00	4.37	5.09	50.84	1.62	0.61
change (%)	-17.61	43.72	3.70	-78.21	60.17	-23.36	-18.79	69.26	56.16	-	52.02	52.76	43.55	-58.99	-68.77
Merkske	17.503	543	7.33	2.03	39.11	54.41	0.00	77.58	23.84	0.00	16.56	10.16	60.40	1.15	0.20
change (%)	20.55	-17.18	2.77	-22.95	-14.99	-25.47	0.00	-25.20	-6.50	-	13.27	-12.25	-22.45	30.05	95.62
Strijbeek	17.027	491	7.08	1.97	33.28	69.52	0.00	74.38	21.70	0.00	14.79	7.39	48.22	1.42	0.27
change (%)	17.56	-15.40	6.73	120.34	-9.80	-37.15	0.00	-20.62	-5.99	-	7.79	32.14	-17.71	98.55	248.73

C

SiDNAMag microparticle

C.1. DNA and primer sequences

Table C.1 shows the DNA and primer sequences for the SiDNAMag tracer.

Table C.1 – Information on the DNA strands in the SiDNAMag particle produced by NTNU.

NTNU particle name	M5
DNA strand name	GM05-S2
DNA sequence	TTCGGACAATCCTTTCCATATTACGCTCTGAAGGCTACTACTCCTTCTTATTAACTGGGTCTCGTTT
DNA reverse sequence	AAACGAGACCCAGTTAATAAGAAGGAGTAGTAGCCTTCAGAGCGTAATATGGAAAGGATTGTCCGAA
Forward primer	5'–CGG ACA ATC CTT TCC ATA–3'
reverse primer	5'–ACG AGA CCC AGT TAA TAA G–3'

C.2. qPCR analysis

To quantify DNA concentrations of the samples from the injection experiments, Quantitative Polymerase Chain Reaction (qPCR) will be used. This method is able to distinguish between the different synthetic DNA strands that are inside the SiDNA particles. qPCR is a widely used method for DNA detection in molecular microbiology and biomedical research and it has a theoretical detection limit down to one DNA molecule. [14]

In qPCR fluorescence dye is bound to DNA in different thermal cycles. These cycles consist of repeated heating and cooling of the reaction, which results in DNA melting and enzymatic replication of the DNA. In every cycle the amount of DNA is doubled. The amount of DNA is monitored at the end of each cycle by determining the fluorescence, generating an amplification profile, which is a graph of the fluorescence as a function of the cycle number (Quantification cycle; Cq), figure C.1. This graph contains a threshold line indicating when the fluorescence level reaches above the background value. The cycle at which the sample reaches this level is called the threshold Cq [60].

A standard curve is created by determining the Cq values for several serial-diluted samples with known concentrations. With this curve the Cq of a sample with unknown concentration can be converted into a DNA concentration. To the standard curve a No Template Control (NTC) is added. The NTC has as purpose to check for pollution during the qPCR procedure. Furthermore it assesses the importance of random amplification and the formation of primer-dimers. Since SYBR Green is used, an non-specific dsDNA-binding dye, any non-specific product can make false positive results. [61]. With the standard curve the efficiency of the qPCR run is calculated, which indicates how well the qPCR is performing in amplifying the DNA each cycle. A reason for poor qPCR efficiency could be bad primer design or inappropriate melting temperatures. Ideally the number of DNA strands of the target sequence should double during each cycle, giving an efficiency f 100%. The formula for calculating the efficiency is:

$$E = -1 + 10^{(\frac{-1}{slope})}$$

. Slope = the slope of the standard curve.

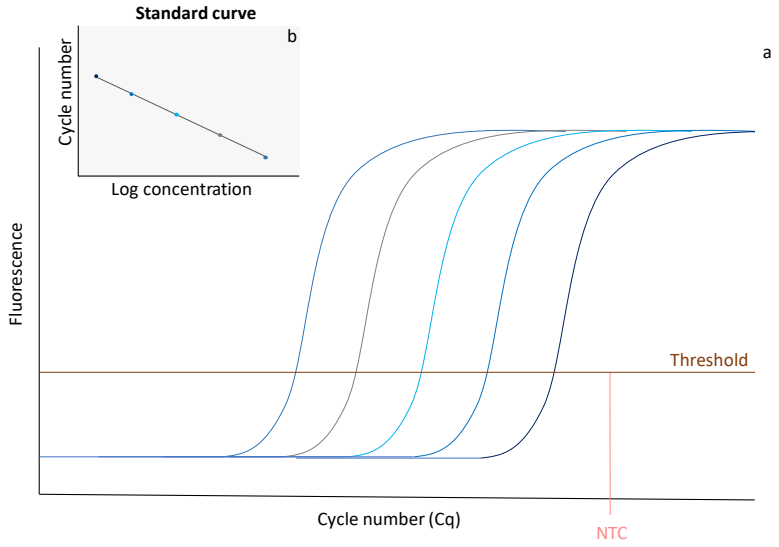

Figure C.1 – a) Schematisation of an amplification profile of five serial-diluted samples. Where the amplification line intersects the threshold line the threshold of fluorescence is reached. On the x-axis the Cq value will be determined. If the Cq value is above the NTC value the sample does not contain any DNA. b) standard curve of the five samples.

To every run a NTC was added to check for pollution during the process of preparing for PCR analysis and to assess the occurrence of random amplification. Random amplification of NTCs took place at a Cq around 35. In order to distinguish positive samples from negative ones the lowest reliable detection threshold cycle was determined at 30. Therefore all samples with a Cq values above 30 were considered to have no DNA. This corresponds to a dilution bigger than D7. To check the functioning of the qPCR the amplification efficiency was calculated for each run.

qPCR mixture

Before the qPCR can analyse the samples the silica coating must be dissolved. This is done with a Buffered Oxide Etch (BOE) solution (HF/NH4F, a buffered HF solution, 2.3 g of NH4FHF (Sigma Aldrich) and 1.9 g of NH4F (J.T.Baker)).

qPCR was conducted on Bio-Rad CFX96 Touch System (96 wells) instrument (CT052975) with SYBR green master mix. The final mixture of 20 µL per qPCR well consisted of:

- 10 µL KAPA SYBR FAST qPCR Master Mix (2X) Universal(Kapa Biosystem);
- 1 µL 10 µM Forward Primer;
- 1 µL 10 µM Reverse Primer;
- 3 µL qPCR water;
- 5 µL DNA template.

The qPCR cycles are: 6 min and 40 s at 95°C, followed by 42 cycles of a three-step thermal profile (20 s at 95°C, 40 s at 58°C, 35 s at 72°C) [62].

D

Results experiments

D.1. qPCR sample analysis

Table D.1 – Cq values for the injection conentration of the experiment in Tap water.

	qPCR run 1	qPCR run 2	qPCR run 3	qPCR run 4	average Cq
sub-sample 1	12.52	12.3		12.17	12.33
sub-sample 2	12.08		12.49	12.2	12.26
sub-sample 3		12.15	12.22		12.19
sub-sample 4	12.1	12.15		11.83	12.03
sub-sample 5	12.09		12.19	12.32	12.20
sub-sample 6		11.96	12.6		12.28

Table D.2 – Cq values for the injection conentration of the experiment in Meuse water.

	qPCR run 1	qPCR run 2	qPCR run 3	qPCR run 4	average Cq
sub-sample 1	12.09	12.05		11.98	12.04
sub-sample 2	12.59		12.48	12.45	12.51
sub-sample 3		12.44	12.6		12.52
sub-sample 4	12.36	12.24		12.24	12.28
sub-sample 5	12.54		12.08	11.94	12.19
sub-sample 6		11.91	12.55		12.23

Table D.3 – Cq values for the injection conentration of the experiment in Merkske water.

	qPCR run 1	qPCR run 2	qPCR run 3	qPCR run 4	average Cq
sub-sample 1	11.63	12.18			11.91
sub-sample 2	12.14	11.83			11.98
sub-sample 3	11.27	11.85			11.56
sub-sample 4	11.75	12.15			11.95

Table D.4 – Cq values for the injection conentration of the experiment in Strijbeek water.

	qPCR run 1	qPCR run 2	qPCR run 3	qPCR run 4	average Cq
sub-sample 1	12.21	12.31	12.37	12.15	12.26
sub-sample 2	13.05	12.81	12.25		12.70
sub-sample 3	12.70	12.64	12.09	12.65	12.52
sub-sample 4	12.47	12.34	12.69		12.50

Table D.5 – Cq values for standard curves in milli-Q water. Per performed injection experiment with SiDNAMag one standard curve is made. The header of the column shows to which experiment the standard curve belongs. The presented Cq values are an average of at least two measurements.

	Meuse	Meuse sed	Merkske	Merkske sed	Strijbeek	Strijbeek sed	Tap	Tap sed
D3 (Cq)		10.81	7.48					9.42
D4 (Cq)	12.04	14.05	10.82	14.65	10.74	13.46	12.02	12.74
D5 (Cq)	15.24	16.78	14.20	17.20	14.11	16.75	15.69	16.07
D6 (Cq)	19.11	20.97	17.64	21.84	17.75	21.65	19.07	20.43
D7 (Cq)	22.84	24.48	20.32	24.49	20.96		24.64	24.68
D8 (Cq)		33.86	29.39				25.88	
Slope	-3.628	-3.427	-3.2511	-3.4154	-3.433	-4.0965	-3.5226	-3.8196
Intercept	-2.6472	0.2824	-2.1639	0.7575	-2.9907	-3.1966	-2.0204	-2.429
Amplification efficiency (%)	88.64	95.794	103.04	96.24	95.56	75.43	92.25	82.73

D.2. Injection experiments

D.2.1. NaCl injection experiment

This appendix presents the results for the NaCl injection experiments performed in the laboratory setup. Two experiments have been performed in two identical setups, creating four BTCs. All BTCs are fitted with OTIS based on a multi parameter analysis. The criteria and if these are met are presented in tabel D.6. Figure D.1, D.2, D.3 and D.4.

Table D.6 – Model performance indicators for NaCl injection experiments

	Peak time (h)	Peak time OTIS (h)	Peak value (ppm)	Peak value OTIS (ppm)	Mass tail (%)	Mass tail OTIS (%)	Model efficiency
Exp 1 setup 1	0.483	0.484	333.606	333.638	70.47	60.66	90.38
Exp 1 setup 2	0.5	0.5	330.418	330.572	63.64	56.8	96.0
Exp 2 setup 1	0.483	0.487	319.598	319.665	76.18	63.58	82.67
Exp 2 setup 2	0.467	0.467	321.211	321.482	72.52	62.22	88.6

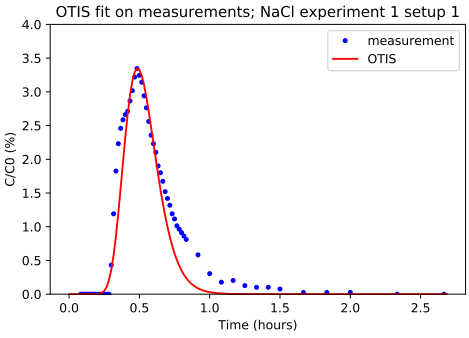

Figure D.1

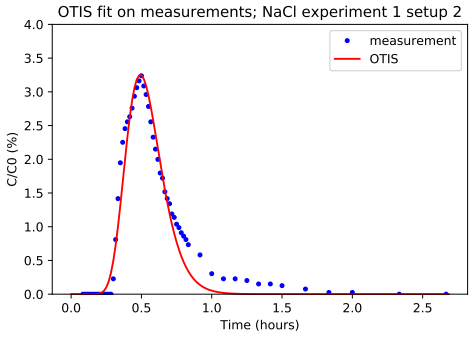

Figure D.2

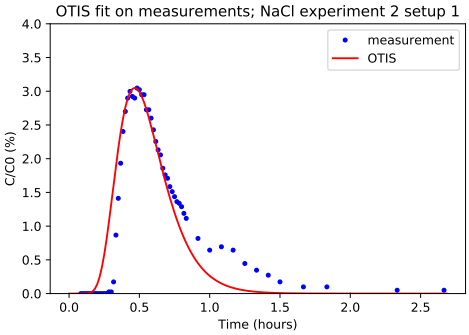

Figure D.3

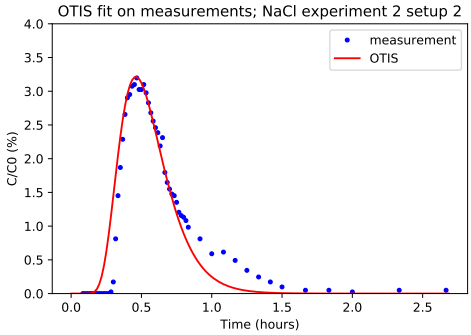

Figure D.4

D.2.2. SiDNAMag injection experiment

This appendix presents the measurement data and averaged BTC for SiDNAMag tracer injection experiments. Furthermore the OTIS fit through the average BTC is visualised. Fitting parameters can be found in table D.7.

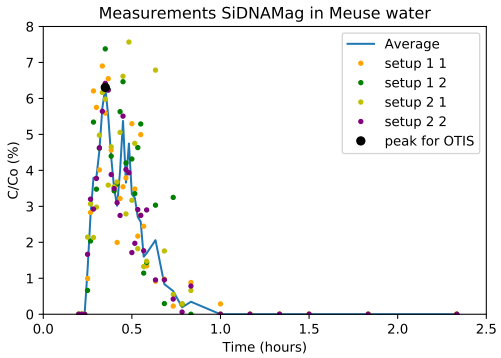

Figure D.5

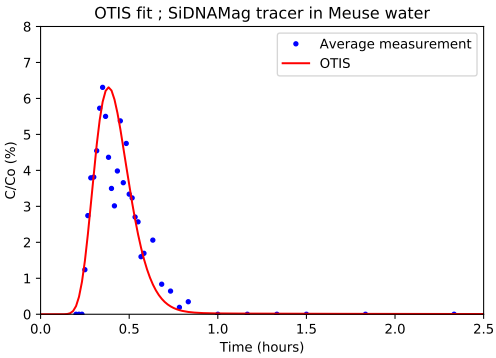

Figure D.6

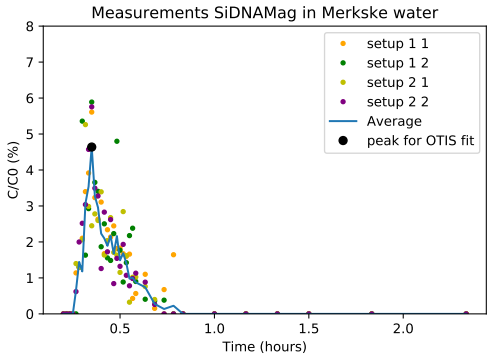

Figure D.7

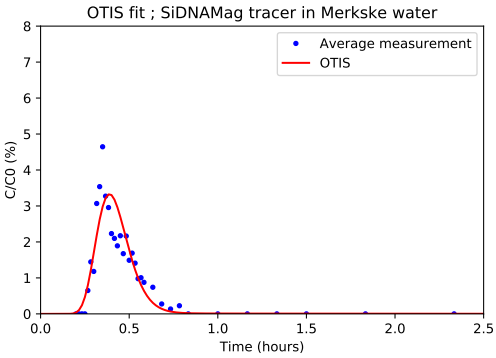

Figure D.8

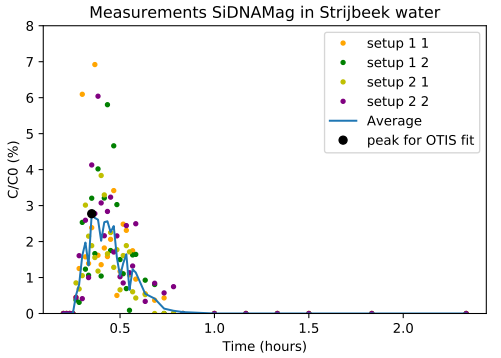

Figure D.9

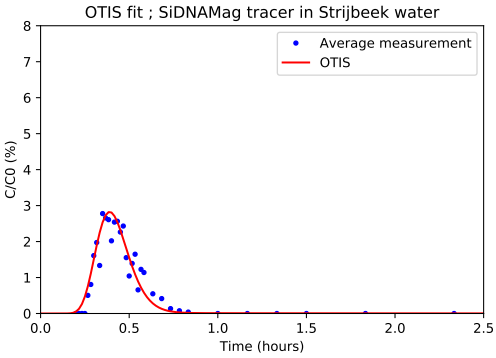

Figure D.10

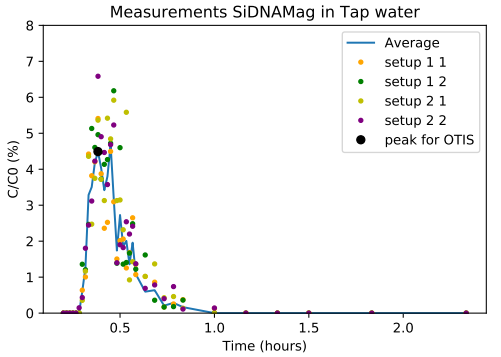

Figure D.11

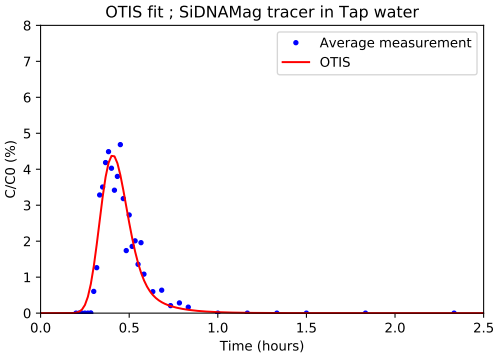

Figure D.12

Table D.7 – Model performance indicators for SiDNAMag injection experiments, for average fit

	Peak time (h)	Peak time OTIS (h)	Peak value (ppm)	Peak value OTIS (ppm)	Mass tail (%)	Mass tail OTIS (%)
Meuse	0.35	0.384	4.83 E-6	4.83 E-6	70.69	60.07
Merkske	0.35	0.384	2.27 E-6	1.63 E-6	34.88	29.41
Strijbeek	0.35	0.384	8.7 E-7	8.8 E-7	33.77	25.68
Tap	0.383	0.4	4.61 E-6	4.49 E-6	43.25	37.29

The OTIS fit visualised against the original measurement data. Table D.8 presents the model efficiency of OTIS against the data points. Figure D.13, D.14, D.15 and D.16.

Table D.8 – Model efficiency for all watertypes. For average values and seperate measurements.

	Model Efficiencey average fit	E 1.1	E 1.2	E 2.1	E 2.2
Meuse	74.1	11.28	-0.03	48.11	57.73
Merkske	66.05	47.42	-45.02	35.46	18.50
Strijbeek	82.35	-167.39	-63.63	42.02	-25.13
Tap	86.88	62.23	53.41	35.41	65.71

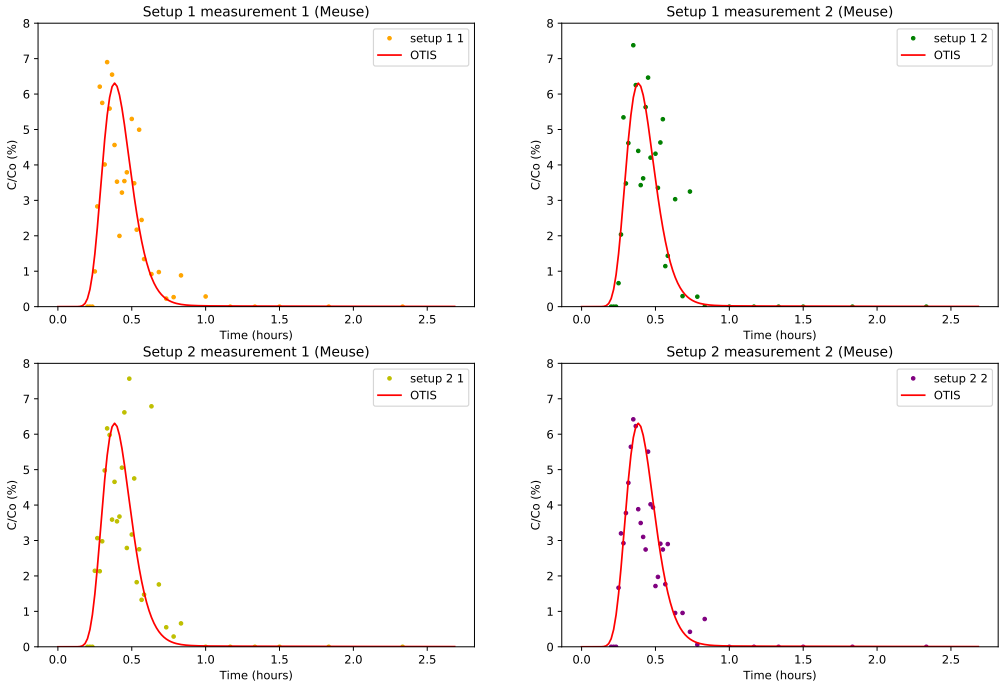

Figure D.13 – OTIS fit through the measured data points of the BTCs of the Meuse water injection experiment with SiDNAMag

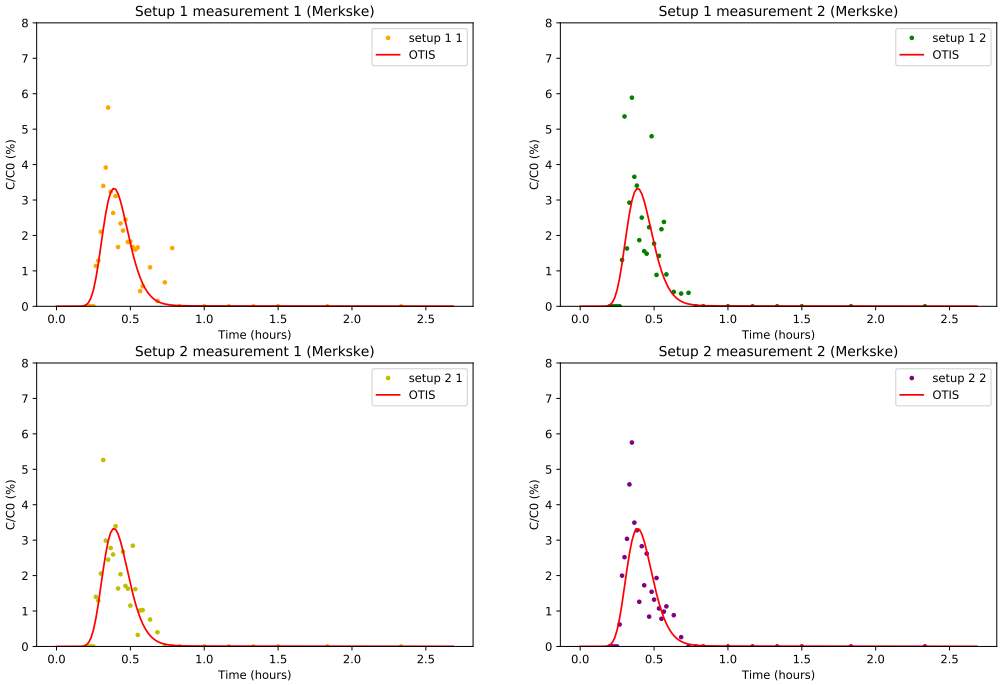

Figure D.14 – OTIS fit through the measured data points of the BTCs of the Merkske water injection experiment with SiDNAMag

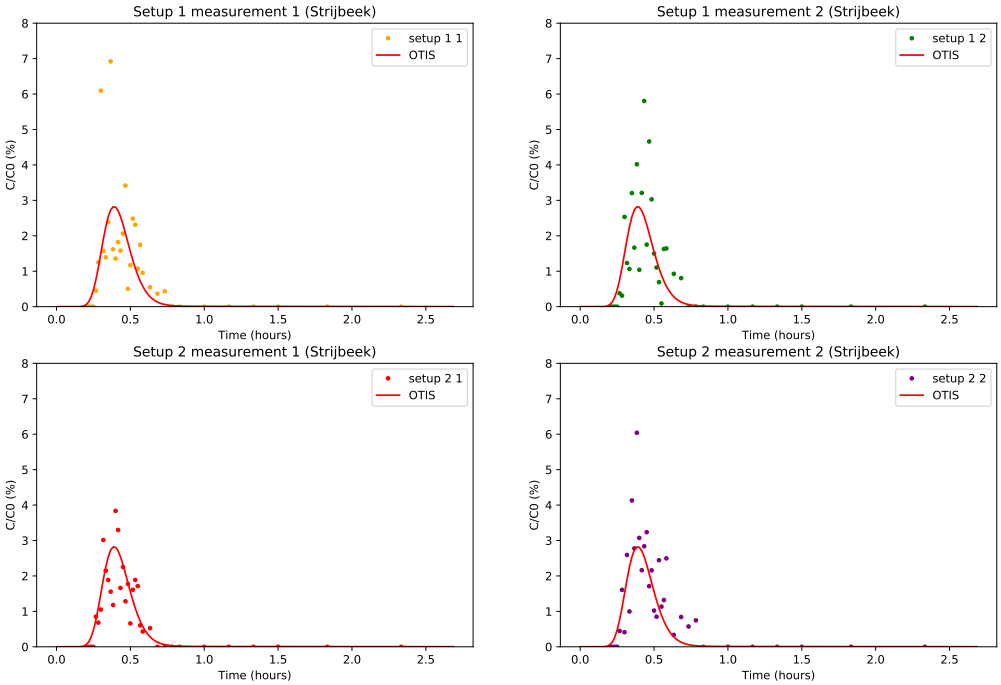

Figure D.15 – OTIS fit through the measured data points of the BTCs of the Strijbeek water injection experiment with SiDNAMag

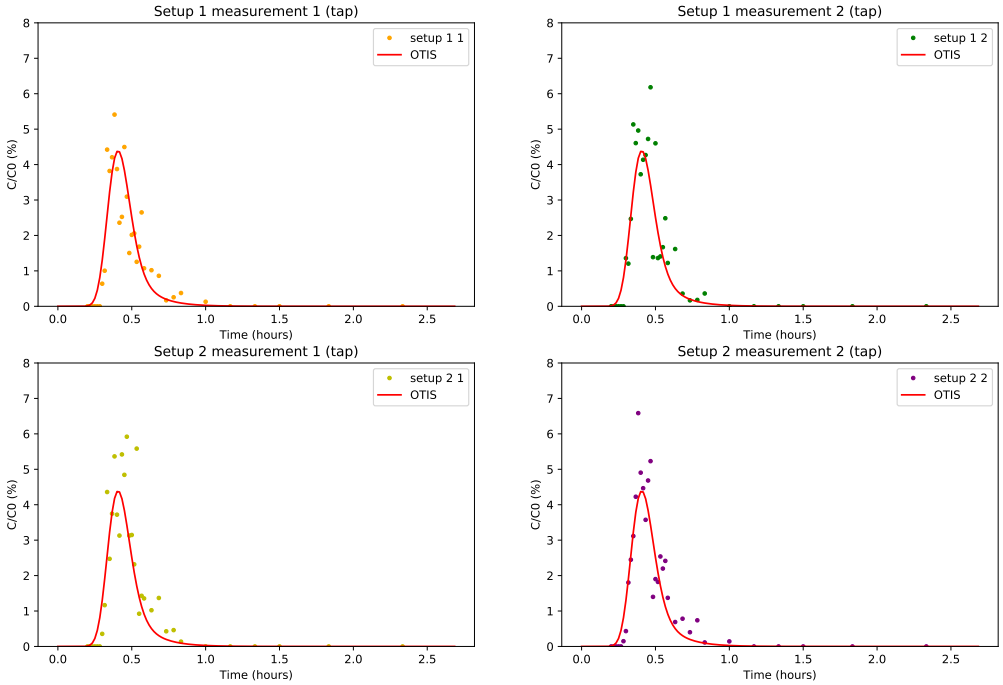

Figure D.16 – OTIS fit through the measured data points of the BTCs of the Tap water injection experiment with SiDNAMag

The figures below show the cumulative fit for each watertype.

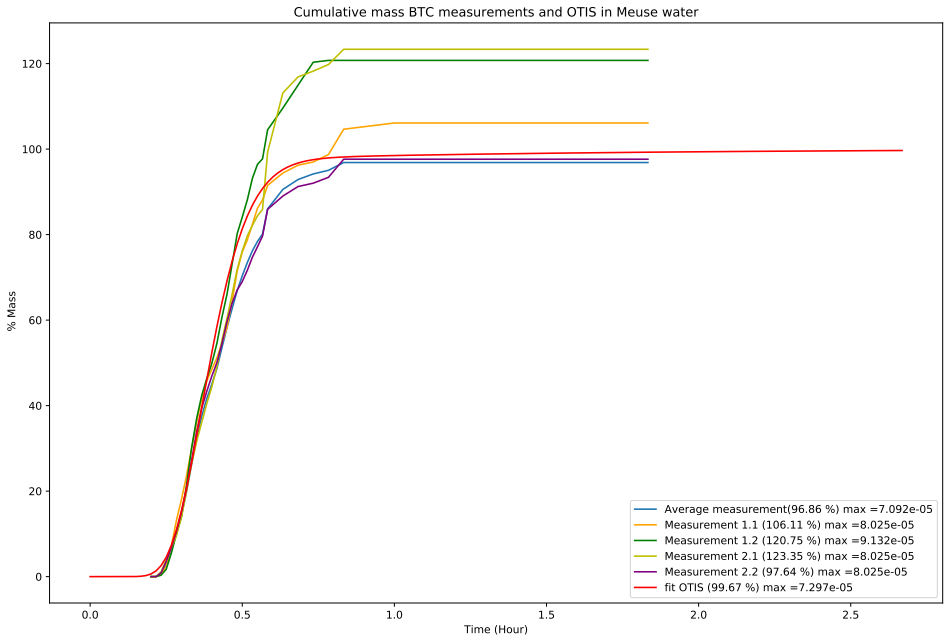

Figure D.17 – Cumulative BTC for the SiDNAMag injection experiment in Meuse water

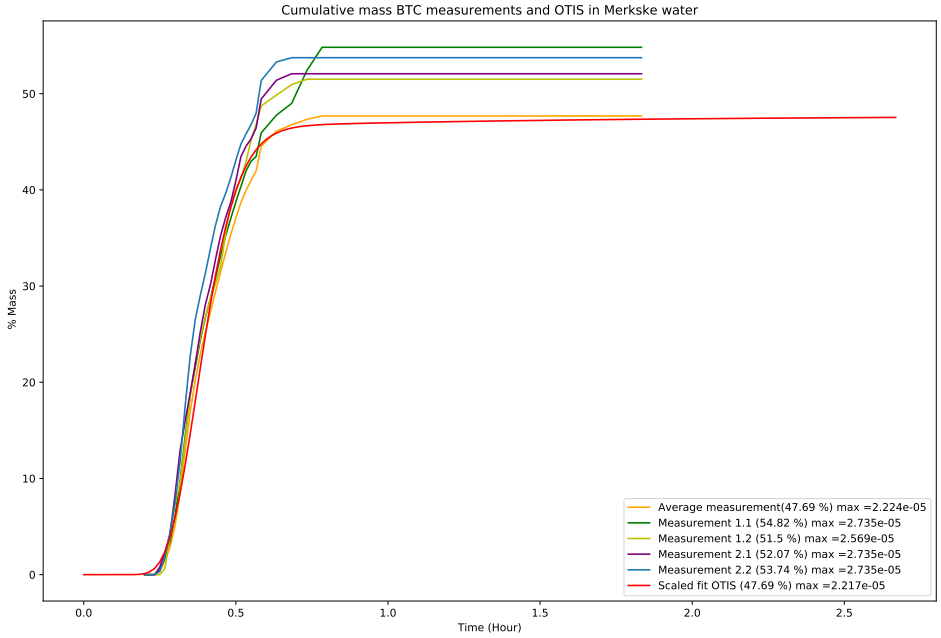

Figure D.18 – Cumulative BTC for the SiDNAMag injection experiment in Merkske water

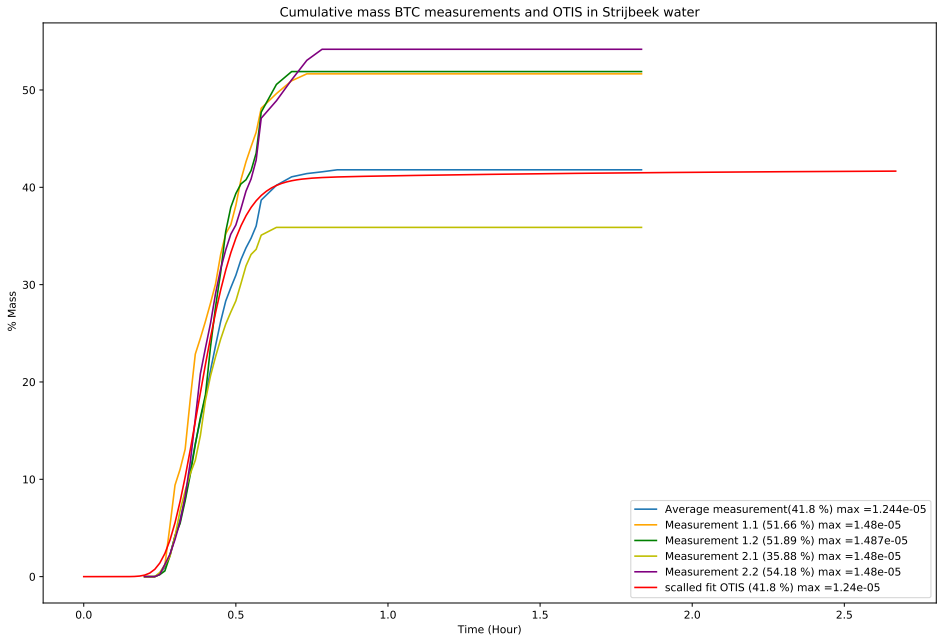

Figure D.19 – Cumulative BTC for the SiDNAMag injection experiment in Strijbeek water

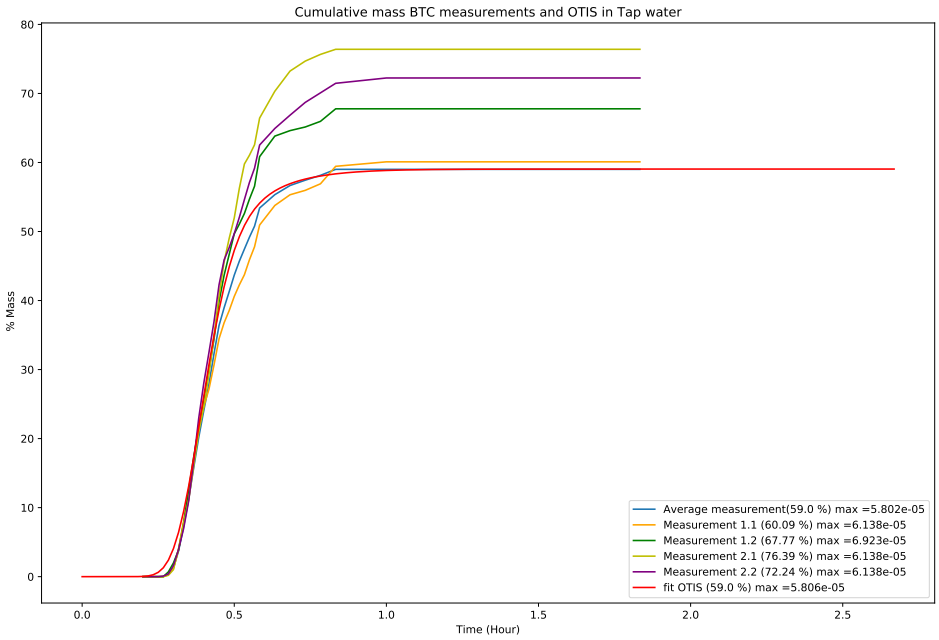

Figure D.20 – Cumulative BTC for the SiDNAMag injection experiment in tap water

D.3. Injection experiment with channel bottom-sediments

D.3.1. Nacl injection experiment with sediments

This appendix presents the results for the NaCl injection experiments performed in the laboratory setup with bottom-sediments. Two experiments have been performed in two identical setups, creating four BTCs. All BTCs are fitted with OTIS based on a multi parameter analysis. The criteria and if these are met are presented in tabel D.9. Figure D.21, D.22, D.23 and D.24.

Table D.9 – Model performance indicators for NaCl sediment injection experiments.

	Peak time (h)	Peak time OTIS (h)	Peak value (ppm)	Peak value OTIS (ppm)	Mass tail (%)	Mass tail OTIS (%)	Model efficiency (%)
Exp 1 setup 1	0.45	0.45	330.419	330.474	71.87	63.87	91.56
Exp 1 setup 2	0.433	0.434	328.516	328.558	72.28	64.22	89.97
Exp 2 setup 1	0.433	0.45	349.798	349.787	77.56	60.94	94.13
Exp 2 setup 2	0.417	0.434	339.746	339.834	71.67	63.91	90.29

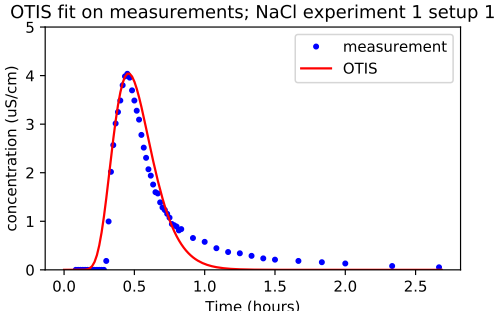

Figure D.21

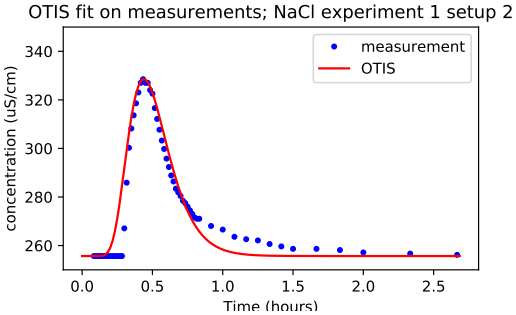

Figure D.22

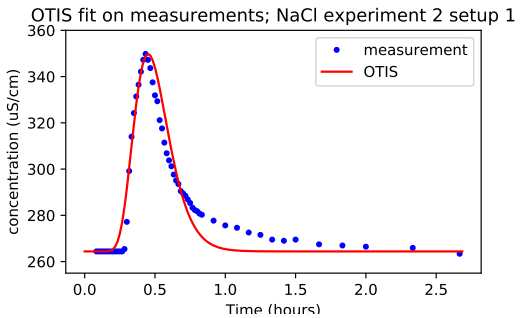

Figure D.23

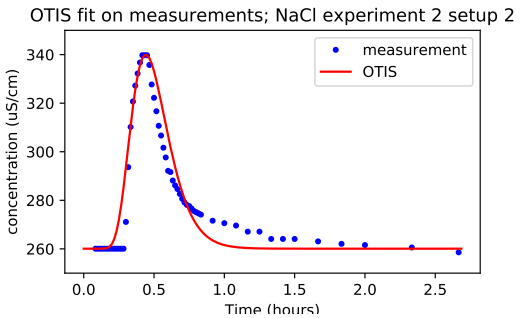

Figure D.24

D.3.2. SiDNAMag injection experiment with sediments

This appendix presents the measurement data and averaged BTC for SiDNAMag tracer injection experiments. Furthermore the OTIS fit on the average BTC is visualised. Fitting parameters can be found in table D.10.

Table D.10 – Model performance indicators for SiDNAMag sediment injection experiments.

	Peak time (h)	Peak time OTIS (h)	Peak value (ppm)	Peak value OTIS (ppm)	Mass tail (%)	Mass tail OTIS (%)
Meuse	0.317	0.367	4.07E-06	4.53E-06	43.98	63.05
Merkske	0.4	0.367	5.05E-6	4.32E-6	18.71	24.64
Strijbeek	0.317	0.367	6.35E-6	4.94E-6	56.52	49.93
Tap	0.35	0.384	4.57E-6	3.81E-6	40.4	59.35

Table D.11 – Model efficiency SiDNAMag sediment injection experiments.

	Model Efficiency average fit (%)	E 1.1	E 1.2	E 2.1	E 2.2
Meuse	49.22	-76.49	-446.31	-722.44	-311.11
Merkske	34.44	-99.91	-231.98	-1184.7	-464.9
Strijbeek	39.2	-133.2	3.84	-146.59	-305.83
Tap	38.49	-54.74	-506.2	-45.51	-298.07

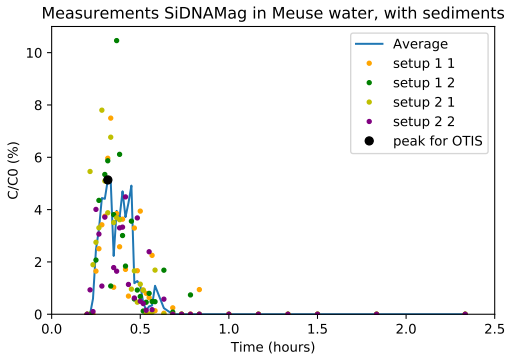

Figure D.25

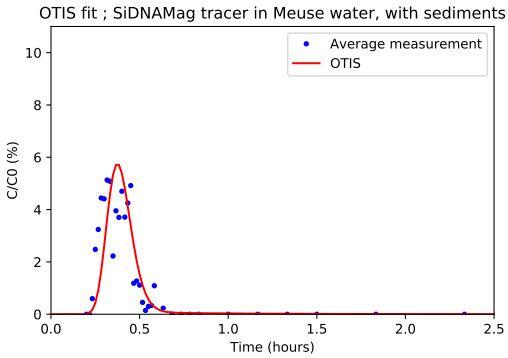

Figure D.26

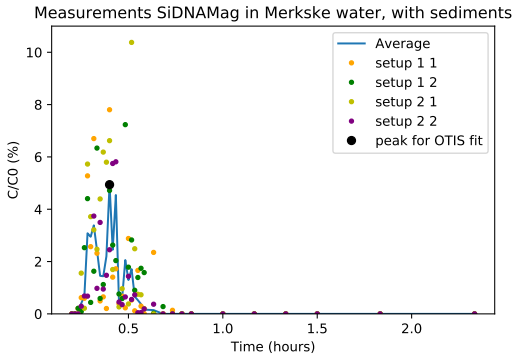

Figure D.27

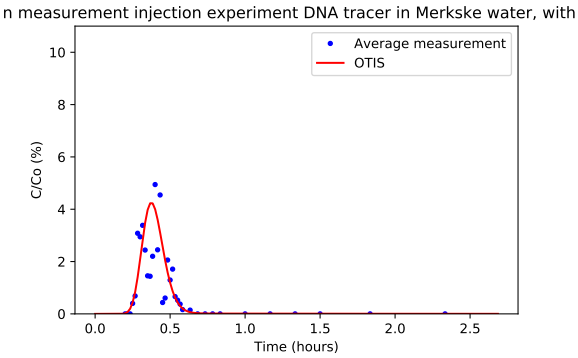

Figure D.28

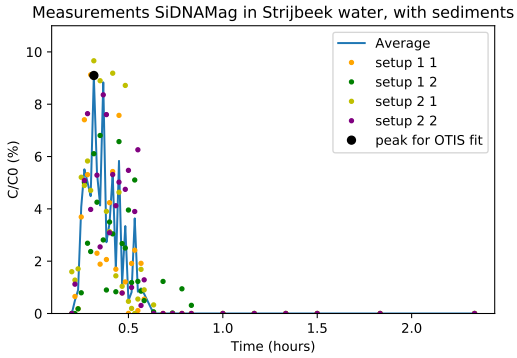

Figure D.29

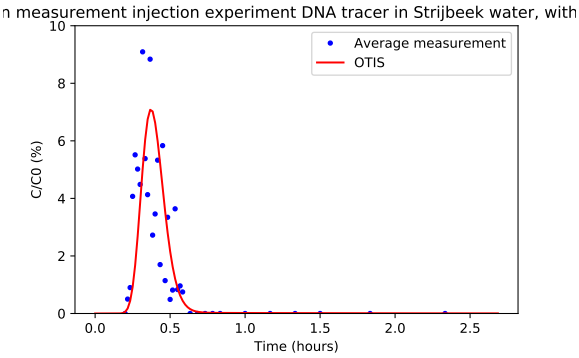

Figure D.30

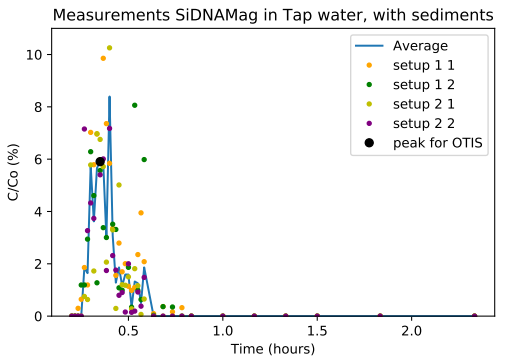

Figure D.31

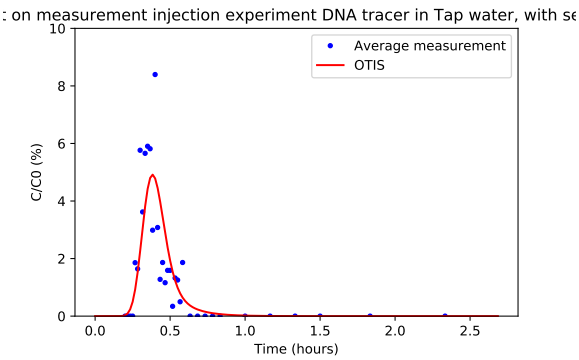

Figure D.32

The OTIS fit visualised against the original measurement data. Table D.11 presents the model efficiency of OTIS against the data points. Figure D.33, D.34, D.35 and D.36.

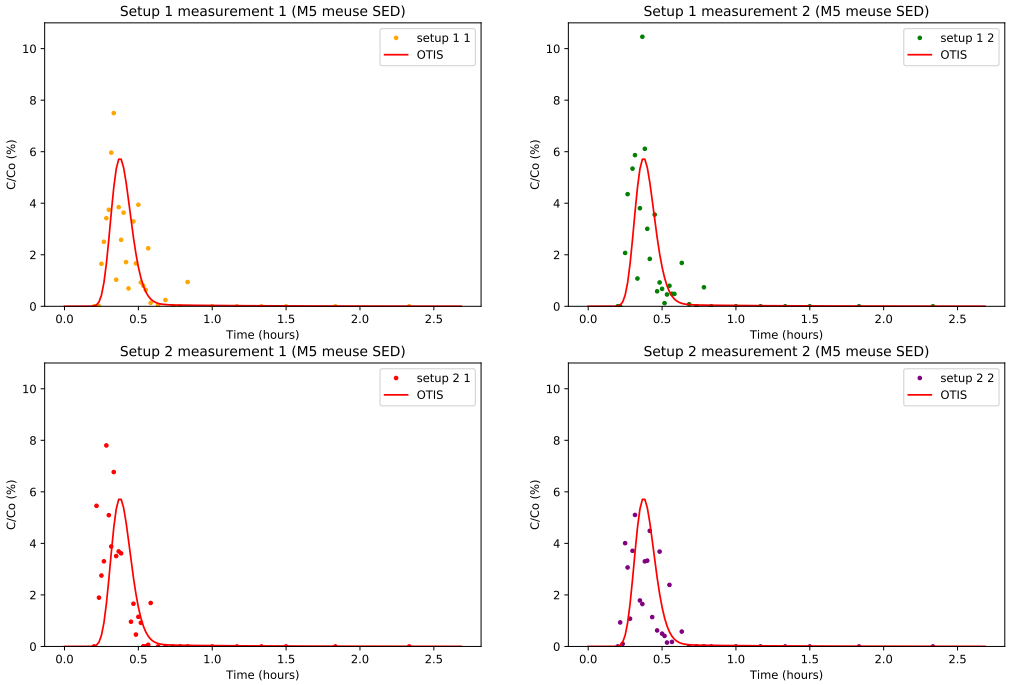

Figure D.33 – OTIS fit through the measured data points of the BTCs of the Meuse water injection experiment with SiDNAMag

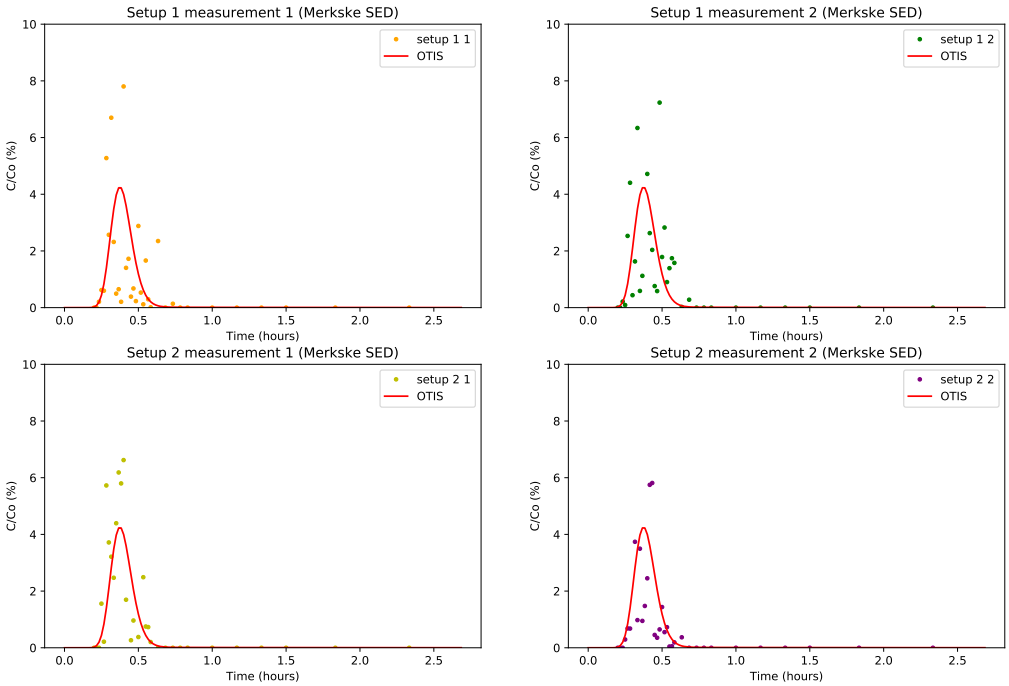

Figure D.34 – OTIS fit through the measured data points of the BTCs of the Merkske water injection experiment with SiDNAMag

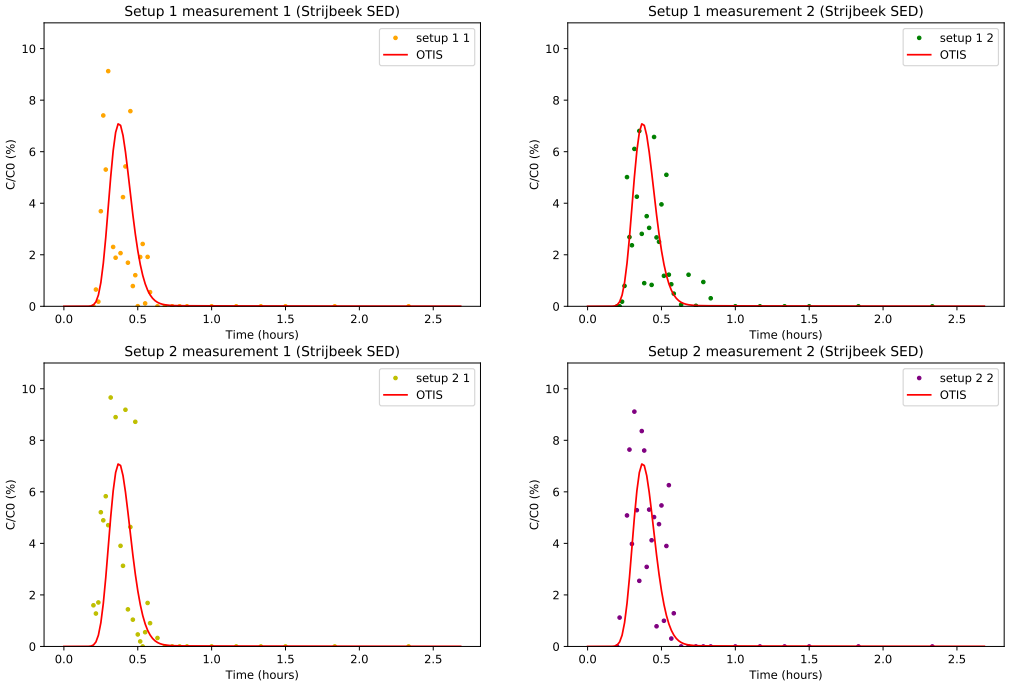

Figure D.35 – OTIS fit through the measured data points of the BTCs of the Strijbeek water injection experiment with SiDNAMag

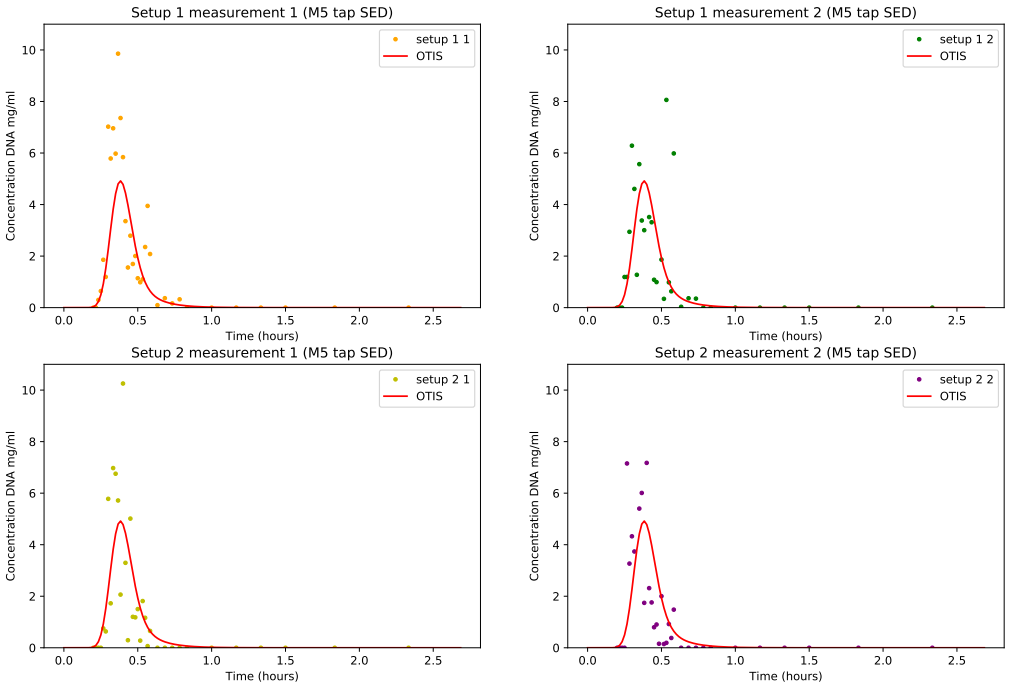

Figure D.36 – OTIS fit through the measured data points of the BTCs of the tap water injection experiment with SiDNAMag

The figures below show the cumulative fit for each watertype.

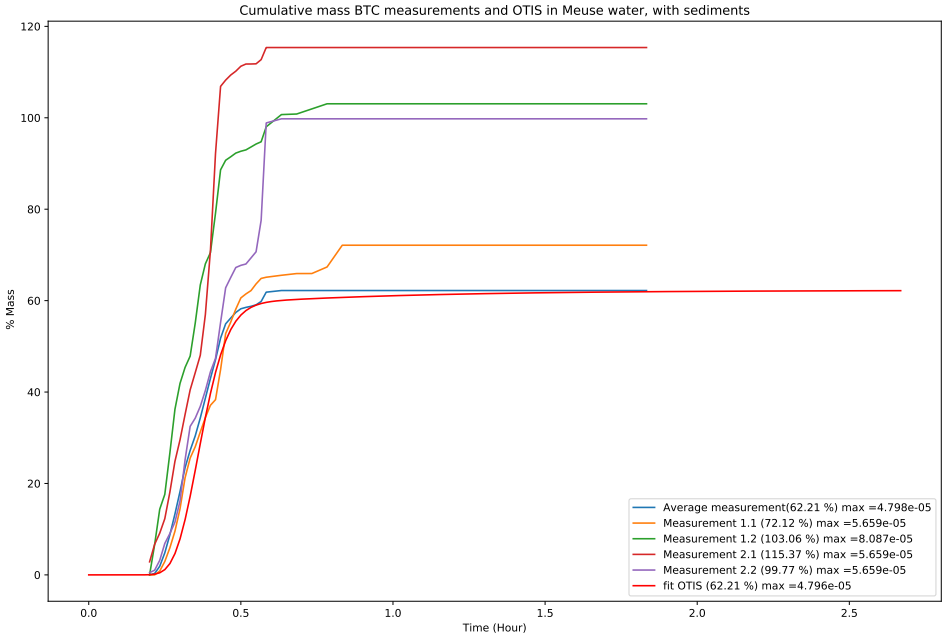

Figure D.37 – Cumulative BTC for the SiDNAMag injection experiment in Meuse water

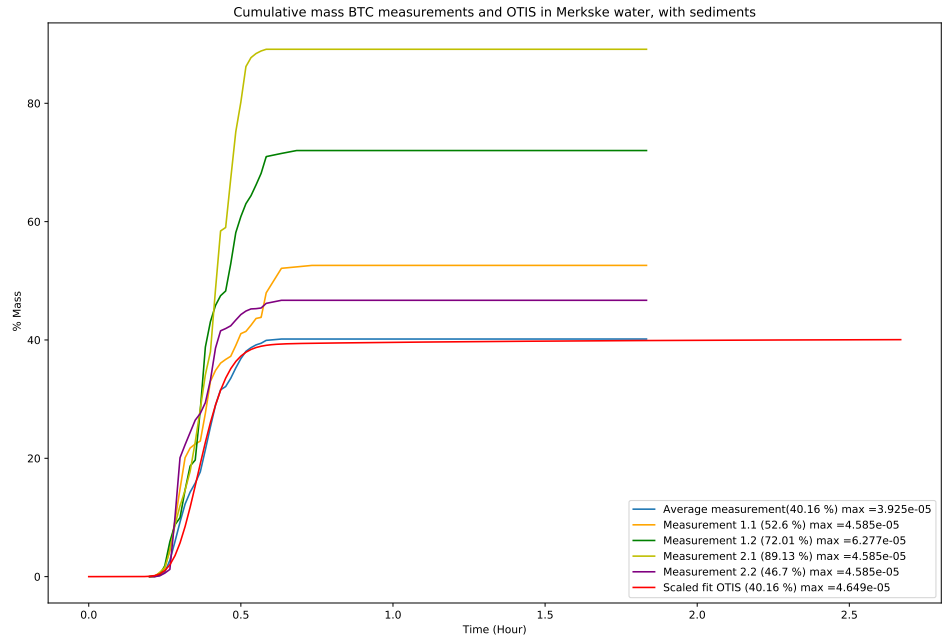

Figure D.38 – Cumulative BTC for the SiDNAMag injection experiment in Merkske water

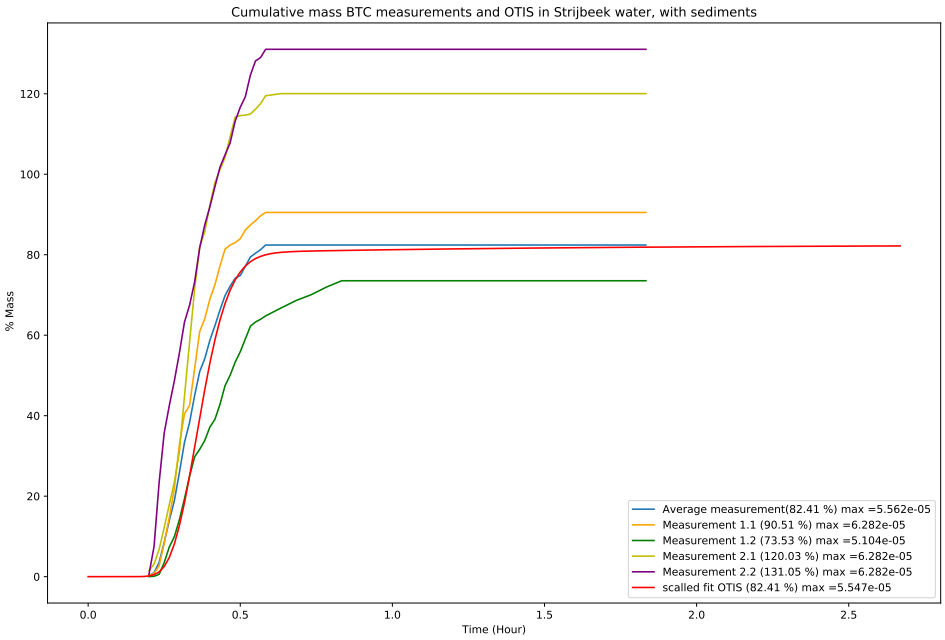

Figure D.39 – Cumulative BTC for the SiDNAMag injection experiment in Strijbeek water

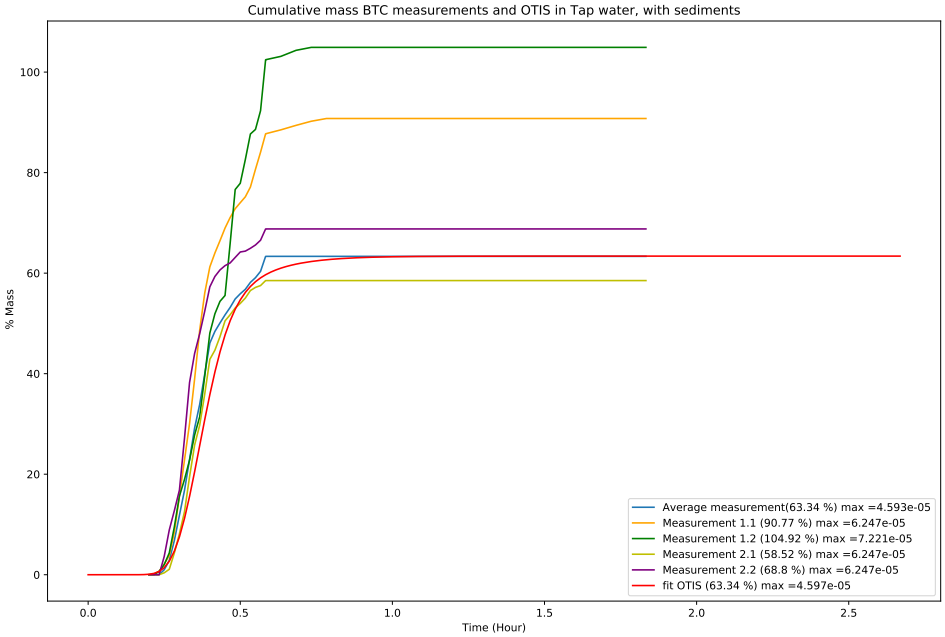

Figure D.40 – Cumulative BTC for the SiDNAMag injection experiment in tap water

D.4. Silica injection experiment

The mass recovery of the silica experiments was 77% for setup 1 and 50% for setup 2. However, there was no mass loss in the experiment. The mass low was due to the fact that the samples were analysed 5 days after the experiment was performed. This resulted in a decline in optical density. This decline was measured with a silica batch experiment in tap water, discussed in subsection D.4.1. The batch experiments showed that the

mass loss in the samples over five days is about 50%. Therefore the mass recovery of the experiment would be 100% of the samples were analysed on day 1.

This decline in optical density which varies per sample is also the reason for the scattered data points in the BTC, figure 4.6

D.4.1. Batch experiment silica

The goal of this experiment is to find out if the measured silica concentration in tap water in a sample changes over time.

Samples with 3 different percentages of silica suspension in tap water are prepared. The first one is 6% , which is a C/C_0 value above the BTC peak. Secondly, 3% which is below the peak and, 1% is a value representing concentrations in the in the rising and falling limb. All samples will be prepared in duplicate. For each day there will be a new sample tubes (but containing the same solution as the samples of the days before). There are new samples for each day so the samples stay undisturbed until analysed. As control there will be one tube per day with the original (D0) solution in MiliQ water.

Making the samples:
First put on gloves

- 6% = 3.6 ml silica suspension + 56.4 ml tap water
- 3% = 1.8 ml silica suspension + 58.2 ml tap water
- 1% = 0.6 ml silica suspension + 59.4 ml tap water
- Vortex the solutions for 1 minute at 3000 rpm
- Per solution, put 5ml in 10 15ml tubes. (2 per day, 5 days)
- Fill 5 tubes with 5 ml D0 silica suspension

On day 0, 3, 4, 5, and 6 two samples from each solution, 1 sample in demi water and, 2 background samples are analysed. The following protecol is used

Protocol:

1. Take the samples that belong to this day (7 samples per day)
2. Vortex the sample 10 seconds at 3000rpm
3. Analyse with the spectrophotometer
4. Analyse again with the spectrophotometer (to get duplicate)
5. Continue to the next sample and repeat step 2-4
6. Measure the zeta potential and hydrodynamic radius for the 2 6% samples

Results:
The results of the experiment show that the Do solution of silica particles in Milli-Q water stays the same. But that the concentration of particles in tap water changes over days. Furthermore the Zeta potential and Hydrodynamic radius also show a change, indication hetero-aggregation is taking place within the sample. This explains the measured mass loss in optical density values.

Table D.12 – Optical density loss of silica microparticle over 5 days in different dilutions

	% mass lost in OD
decrease mass over 5 days 6%	48.6
decrease mass over 5 days 3%	48.9
decrease mass over 5 days 1%	55.3
average	50.9

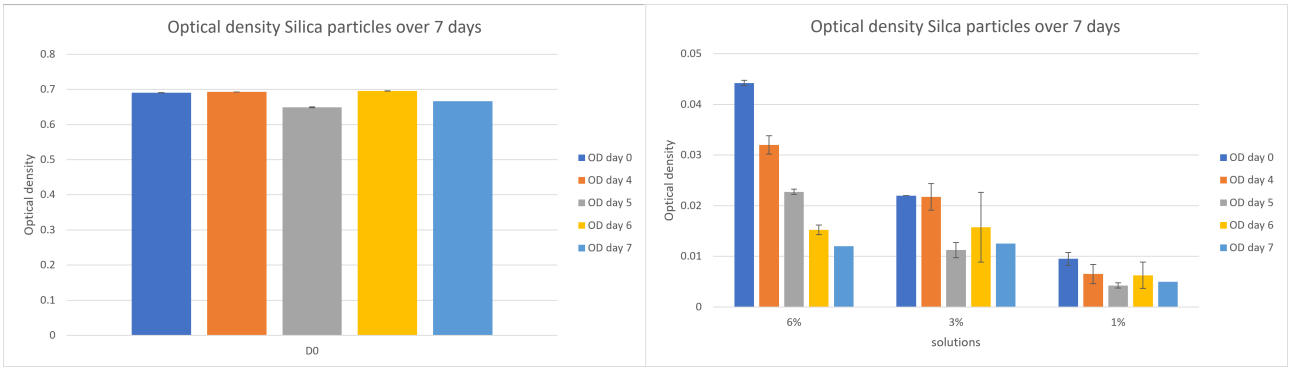

Figure D.41 – Silica microparticle experiment in tap water over 7 days. The graphs show the averages of two measurements. With a D0 solution in Milli-Q water as control series and the other solutions are made in tap water.

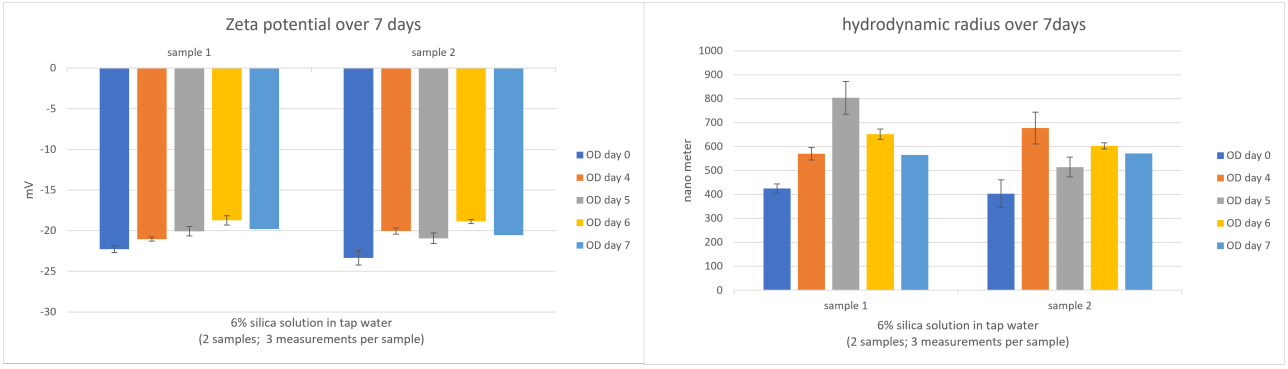

Figure D.42 – Zeta potential and hydrodynamic radius of the 6% solution of silica microparticles in tap water, over 7 days.

E

OTIS

Table E.2 and E.1 provide the input values for the OTIS modelling for NaCl, SiDNAMag and Silica microparticles experiments with and without sediments. A short explanation for some parameter chooses is given below.

The tracer arrived in the channel after 20 sec of injection then it was mixed instantaneously with the rotor. Therefore the start of injection in the USTIME parameter is at 20 seconds. In OTIS the tracer is injected for 1 minute while in the real experiments this was only 55 sec. Therefore injection concentration of OTIS is recalculated so that the mass stayed the same (USBC). By multiplying the injection concentration with the injected volume, dividing it by the flow rate and multiplying it by 1 minute minus the background concentration. OTIS can not account for background concentration in storage zone, thus background must be 0 when modelling. Therefore when plotting the graphs background must be added to the values. The rotor gave the water a local acceleration which was not present anymore after 35 cm. Therefore the first reach is 35 cm and the second one the remaining 95 of the channel.

For the experiments without sediments the volume of water was 1600 ml water and with added sediments the volume became 1450 ml. This change effected the storage zone cross sectional area.

Although the setup is only a 130 cm, the second reach is 2*(130-35) cm to have no influence of the downstream boundary condition. The print location of the data is 130 cm.

Table E.1 – OTIS parameters for the Q.INP file

	no sediments	**with sediments**
QSTEP (hour)	0.00	0.00
Qstart ($m^3/second$)	8.33e-7	8.33e-7
QLATIN	0.00	0.00
QLATOUT	0.00	0.00
AREA (m^2)	2.8274E-5	2.8274E-5

Table E.2 – OTIS parameters for the PARAMS.inp file.

	no sediments	**with sediments**
PSTEP	0.0167	0.0167
TSTEP (hour)	0.00278	0.00278
TSTAT (hour)	0.00000	0.00000
TFINAL (hour)	2.6667	2.6667
XSTART (m)	0.0	0.0
DSBOUND (L/sec)/CU	0.0	0.0
NREACH	2	2
Nseg	350 1900	350 1900
RCHLEN (m)	0.35 1.90	0.35 1.90
DIPS (m^2/s)	guess guess	guess guess
AREA2 (m^2)	0.00123 0.00123	0.00115 0.00115
ALPHA (/s)	guess guess	guess guess
NSOLUTE	1	1
NPRINT	1	1
IOPT	0	0
PRINTLOC	1.3	1.3
NBOUND	3	3
IBOUND	1	1
USTIME (hour)	0.0 0.00556 0.02224	0.0 0.00556 0.02224
USBC (ppm NaCl or mg/ml DNA)	0 (injection value) 0	0 (injection value) 0

F

Field experiment

For a field experiment with a peak in range D5 D6 at 100 meters downstream we need 325 batches of NTNU. This is calculated as follows:

- Using fieldwork data from Foppen et al (2010) in the Merkske. At a distance of 100 meters the peak arrived after 360 sec and by then 59.76 m^3 water was passed
- In the lab the amount of water passed when the tracer arrived = 21 min * 50 ml/min = 1.05E-3m^3
- thus the amount of water increased with a factor 5.69e4
- In the lab we use D4 (concentration) = 3e-5 mg/ml* We inject 46 ml, thus the injected DNA mass is 1.38e-3 mg
- If we scale the injected mass with the increase of water volume (from lab to field) we need 78.5 mg tracer
- NTNU sends D0 = 0.3 mg/ml * 0.8 ml = 0.24 mg per batch
- Thus we need 325 batches of NTNU to get a BTC of the same quality as in the lab.

* 3e-5 mg/ml is the D4 calculation of Ahmed. Where the D0 = 0.75 mg/ml of DNA, of which 40% will be encapsulated. Our D4 concentration measurement in the experiments is about 7e-5 mg/ml. So same order of magnitude.

Bibliography

[1] Liao, R.; Yang, P.; Wu, W.; Luo, D.; Yang, D. A DNA Tracer System for Hydrological Environment Investigations. *Environmental Science and Technology* **2018**, *52*, 1695–1703.

[2] Sabir, I. H.; Haldorsen, S.; Torgersen, J.; Aleström, P. DNA tracers with information capacity and high detection sensitivity tested in groundwater studies. *Hydrogeology Journal* **1999**, *7*, 264–272.

[3] Sharma, A. N.; Luo, D.; Walter, M. T. Hydrological tracers using nanobiotechnology: Proof of concept. *Environmental Science and Technology* **2012**, *46*, 8928–8936.

[4] Sabir, I. H.; Haldorsen, S.; Torgersen, J.; Aleström, P.; Gaut, S.; Colleuille, H.; Pedersen, T. S.; Kitterød, N. O. Synthetic DNA tracers: Examples of their application in water related studies. *IAHS-AISH Publication* **2000**, 159–165.

[5] Leibundgut, C.; Maloszewski, P.; Külls, C. *Tracers in Hydrology*; 2009; pp 1–415.

[6] Runkel, R. Using OTIS to Model Solute Transport in Streams and Rivers. *U.S. Geological Survey Fact Sheet FS–138–99* **2000**, 4.

[7] Leibundgut, C.; Seibert, J. Tracer Hydrology. *Treatise on Water Science* **2011**, *2*, 215–236.

[8] Olsen, J.; Seierstad, I.; Vinther, B.; Johnsen, S.; Heinemeier, J. Memory effect in deuterium analysis by continuous flow isotope ratio measurement. *International Journal of Mass Spectrometry* **2006**, *254*, 44–52.

[9] Tang, Y.; Bogaard Thomas, A.; Jan-Willem, F.; Bahareh, K. Understanding surface water using DNA-tagged nanoparticle. *Eguga* **2018**, *20*, 5561.

[10] Kianfar, B.; Bogaard, T.; Foppen, J. W. Environmental factors affecting the transport of DNA-tagged particle tracers in saturated porous media. *Geophysical Research Abstracts* **2018**, *20*, 16963.

[11] Behrens, H. et al. Toxicological and ecotoxicological assessment of water tracers. *Hydrogeology Journal* **2001**, *9*, 321–325.

[12] Field, M. S. Assessing Aquatic Ecotoxicological Risks Associated with Fluorescent Dyes Used for Water-Tracing Studies Assessing Aquatic Ecotoxicological Risks Associated with Fluorescent Dyes Used for Water-Tracing Studies. **2014**,

[13] Foppen, J. W.; Orup, C.; Adell, R.; Poulalion, V.; Uhlenbrook, S. Using multiple artificial DNA tracers in hydrology. *Hydrological Processes* **2011**, *25*, 3101–3106.

[14] Pang, L.; Robson, B.; Farkas, K.; McGill, E.; Varsani, A.; Gillot, L.; Li, J.; Abraham, P. Tracking effluent discharges in undisturbed stony soil and alluvial gravel aquifer using synthetic DNA tracers. *Science of the Total Environment* **2017**, *592*, 144–152.

[15] Puddu, M.; Paunescu, D.; Stark, W. J.; Grass, R. N. Magnetically recoverable, thermostable, hydrophobic DNA/silica encapsulates and their application as invisible oil tags. *ACS Nano* **2014**, *8*, 2677–2685.

[16] Dahlke, H. E.; Williamson, A. G.; Georgakakos, C.; Leung, S.; Sharma, A. N.; Lyon, S. W.; Walter, M. T. Using concurrent DNA tracer injections to infer glacial flow pathways. *Hydrological Processes* **2015**, *29*, 5257–5274.

[17] Runkel, R. L. One-dimensional transport with inflow and storage (otis): a solute transport model for streams and rivers. *Water-Resources Investigations Report 98-4018* **1998**, 0–80.

[18] Baker, M. A.; Webster, J. R. *Methods in Stream Ecology: Third Edition*; Elsevier Inc., 2017; Vol. 2; pp 129–145.

[19] Sangelerat, G. Chapter 2 - General Theory. *The Penetrometer and Soil Exploration* **1972**, *1*, 93–119.

[20] Sokáč, M. Determination of the longitudinal dispersion coefficient in lowland streams with occurrence of dead zones. *10th International Conference on Environmental Engineering, ICEE 2017* **2017**, 27–28.

[21] Grass, R. N.; Schälchli, J.; Paunescu, D.; Soellner, J. O.; Kaegi, R.; Stark, W. J. Tracking Trace Amounts of Submicrometer Silica Particles in Wastewaters and Activated Sludge Using Silica-Encapsulated DNA Barcodes. *Environmental Science and Technology Letters* **2014**, *1*, 484–489.

[22] Paunescu, D.; Puddu, M.; Soellner, J. O.; Stoessel, P. R.; Grass, R. N. Reversible DNA encapsulation in silica to produce ROS-resistant and heat-resistant synthetic DNA 'fossils'. *Nature Protocols* **2013**, *8*, 2440–2448.

[23] Pang, L.; Abeysekera, G.; Hanning, K.; Premaratne, A.; Robson, B.; Abraham, P.; Sutton, R.; Hanson, C.; Hadfield, J.; Heiligenthal, L.; Stone, D.; McBeth, K.; Billington, C. Water tracking in surface water, groundwater and soils using free and alginate-chitosan encapsulated synthetic DNA tracers. *Water Research* **2020**, *184*, 116192.

[24] Alestrom, P. Novel method for chemical labelling of objects. *International Patent Application No. PCT/IB95/01144 and publication No. WO 96/17954, World Intellectual Property Organization (WIPO)* **1995**,

[25] Foppen, J. W.; Seopa, J.; Bakobie, N.; Bogaard, T. Development of a methodology for the application of synthetic DNA in stream tracer injection experiments. *Water Resources Research* **2013**, *49*, 5369–5380.

[26] Zhang, W.; Tang, X.; Weisbrod, N.; Guan, Z. A review of colloid transport in fractured rocks. *Journal of Mountain Science* **2012**, *9*, 770–787.

[27] Luhmann, A. J.; Covington, M. D.; Alexander, S. C.; Chai, S. Y.; Schwartz, B. F.; Groten, J. T.; Alexander, E. C. Comparing conservative and nonconservative tracers in karst and using them to estimate flow path geometry. *Journal of Hydrology* **2012**, *448-449*, 201–211.

[28] Goeppert, N.; Goldscheider, N. Improved understanding of particle transport in karst groundwater using natural sediments as tracers. *Water Research* **2019**, *166*, 115045.

[29] Goldscheider, N.; Meiman, J.; Pronk, M.; Smart, C. Tracer tests in karst hydrogeology and speleology. *International Journal of Speleology* **2008**, *37*, 27–40.

[30] Auckenthaler, A.; Raso, G.; Huggenberger, P. Particle transport in a karst aquifer: Natural and artificial tracer experiments with bacteria, bacteriophages and microspheres. *Water Science and Technology* **2002**, *46*, 131–138.

[31] Göppert, N.; Goldscheider, N. Solute and colloid transport in karst conduits under low- and high-flow conditions. *Ground Water* **2008**, *46*, 61–68.

[32] Bales, R. C.; Gerba, C. P.; Grondin, G. H.; Jensen, S. L. Bacteriophage transport in sandy soil and fractured tuff. *Applied Environmental Microbiology* **1989**, *55*, 2061–2067.

[33] Keller, A. A.; Sirivithayapakorn, S.; Chrysikopoulos, C. V. Early breakthrough of colloids and bacteriophage MS2 in a water- saturated sand column. *Water resources research* **2004**, *40*.

[34] Chrysikopoulos, C. V.; Syngouna, V. I. Effect of gravity on colloid transport through water-saturated columns packed with glass beads: Modeling and experiments. *Environmental Science and Technology* **2014**, *48(12)*, 6850–6813.

[35] Powelson, D. K.; Gerba, C. P.; Yahya, M. T. Virus transport and removal in wastewater during aquifer recharge. *Water Resources* **1993**, *27*, 583 – 590.

[36] Zhang, P.; Johnson, W. P.; Piana, M.; Fuller, C.; Naftz, D. L. Potential artifacts in interpretation of differential breakthrough of colloids and dissolved tracers in the context of transport in a zero-valent iron permeable reactive barrier. *Ground Water* **2001**, *39(6)*, 831–840.

[37] Chrysikopoulos, C. V.; Sim, Y. One-dimensional virus transport in homogeneous porous media with time-dependent distribution coefficient. *Journal of Hydrology* **1996**, *185*, 199–219.

[38] Mccluskey, J.; Flores, M. E.; Hinojosa, J.; Jafarzadeh, A.; Moghadam, S. V.; Phan, D. C.; Green, R. T.; Kapoor, V. Tracking Water with Synthetic DNA Tracers Using Droplet Digital PCR. *ACS ES&T Water* **2021**,

[39] P. Rossi, K. K. I. M. M. A., N. Dorfliger Bacteriophages as surface and groud water tracers. *Hydrology and Earth system Sciences* **1998**, *2*, 101 – 110.

[40] Molnar, I. L.; Johnson, W. P.; Gerhard, J. I.; Willson, C. S.; O'Carroll, D. M. Predicting colloid transport through saturated porous media: A critical review. *Water Resources Research* **2015**, 6804–6845.

[41] Chrysikopoulos, C.; Katzourakis, V. Colloid particle size-dependent dispersivity. *Water Resources Research* **2015**, *51*, 4668–4683.

[42] Markus, A. A.; Parsons, J. R.; Roex, E. W.; de Voogt, P.; Laane, R. W. Modelling the transport of engineered metallic nanoparticles in the river Rhine. *Water Research* **2016**, *91*, 214–224.

[43] Quik, J. T.; de Klein, J. J.; Koelmans, A. A. Spatially explicit fate modelling of nanomaterials in natural waters. *Water Research* **2015**, *80*, 200–208.

[44] Jamieson, R.; Joy, D. M.; Lee, H.; Kostaschuk, R.; Gordon, R. Transport and deposition of sediment-associated Escherichia coli in natural streams. *Water Research* **2005**, *39*, 2665–2675.

[45] Hendren, C. O.; Lowry, M.; Grieger, K. D.; Money, E. S.; Johnston, J. M.; Wiesner, M. R.; Beaulieu, S. M. Modeling approaches for characterizing and evaluating environmental exposure to engineered nanomaterials in support of risk-based decision making. *Environmental Science and Technology* **2013**, *47*, 1190–1205.

[46] Petersen, E. J.; Zhang, L.; Mattison, N. T.; O'Carroll, D. M.; Whelton, A. J.; Uddin, N.; Nguyen, T.; Huang, Q.; Henry, T. B.; Holbrook, R. D.; Chen, K. L. Potential release pathways, environmental fate, and ecological risks of carbon nanotubes. *Environmental Science and Technology* **2011**, *45*, 9837–9856.

[47] Drewry, J. J.; Newham, L. T.; Greene, R. S.; Jakeman, A. J.; Croke, B. F. A review of nitrogen and phosphorus export to waterways: Context for catchment modelling. *Marine and Freshwater Research* **2006**, *57*, 757–774.

[48] Gottschalk, F.; Sun, T.; Nowack, B. Environmental concentrations of engineered nanomaterials: Review of modeling and analytical studies. *Environmental Pollution* **2013**, *181*, 287–300.

[49] Merritt, W.; Letcher, R.; Jakeman, A. A review of erosion and sediment transport models. *Environmental Modelling and software* **2003**,

[50] Sharma, A.; Foppen, J. W.; Banerjee, A.; Bachhar, N.; Bandyopadhyay, S. Magnetic Nanoparticles to Unique DNA Tracers-Effect of Functionalization on Physico-Chemical Properties. **2020**, 1–21.

[51] Choi, J.; Harvey, J. W.; Conklin, M. H. Characterizing multiple timescales of stream and storage zone interaction that affect solute fate and transport in streams. *Water Resources Research* **2000**, *36*, 1511–1518.

[52] Femeena, P. V.; Chaubey, I.; Aubeneau, A.; McMillan, S.; Wagner, P. D.; Fohrer, N. Simple regression models can act as calibration-substitute to approximate transient storage parameters in streams. *Advances in Water Resources* **2019**, *123*, 201–209.

[53] Hornberger, G.; Mills, A.; Herman, J. Bacterial transport in porous media: evaluation of a model using laboratory observations. *Water Resources Research* **1992**, *28*, 915–938.

[54] Mikutis, G.; Deuber, C. A.; Schmid, L.; Kittilä, A.; Lobsiger, N.; Puddu, M.; Asgeirsson, D. O.; Grass, R. N.; Saar, M. O.; Stark, W. J. Silica-Encapsulated DNA-Based Tracers for Aquifer Characterization. *Environmental Science and Technology* **2018**, *52*, 12142–12152.

[55] Gibson, K.; Schwab, K.; Spencer, S.; Borchardt, M. Measuring and mitigating inhibition during quantitative real time PCR analysis of viral nucleic acid extracts from large-volume environmental water samples. *Water research* **2012**, *46*, 4281–91.

[56] Sidstedt, M.; Jansson, L.; Nilsson, E.; Noppa, L.; Forsman, M.; Rådström, P.; Hedman, J. Humic substances cause fluorescence inhibition in real-time polymerase chain reaction. *Analytical Biochemistry* **2015**, *487*, 30–37.

[57] Wilson, I. Inhibition and Facilitation of Nucleic Acid Amplification. *Applied and Environmental Microbiology* **1997**, *63*, 3741–3751.

[58] Kittilä, A.; Jalali, M. R.; Evans, K. F.; Willmann, M.; Saar, M. O.; Kong, X. Z. Field Comparison of DNA-Labeled Nanoparticle and Solute Tracer Transport in a Fractured Crystalline Rock. *Water Resources Research* **2019**, *55*, 6577–6595.

[59] Zhang, F. Settling and aggregation of colloidal silica and engineered DNA tagged silica-iron particles in surface water. **2022**,

[60] Bustin, A.; Nolan, T. Analysis of mRNA Expression by Real-time PCR. *Polymerase Chain Reaction: Theory and Technology* **2019**,

[61] Tajadini, M.; Panjehpour, M.; Javanmard, S. H. Comparison of SYBR Green and TaqMan methods in quantitative real-time polymerase chain reaction analysis of four adenosine receptor subtypes. **2014**,

[62] Tang, Y.; Foppen, J.; Bogaard, T. Transport of silica encapsulated DNA microparticles in controlled instantaneous injection open channel experiments. *paper under review* **2021**,